

EXTENDED BURNUP EVALUATION

FRAMATOME ANP

Lynchburg, VA

TOPICAL REPORT BAW-10186NP-A, Rev. 2

June 2003

EXTENDED BURNUP EVALUATION

KEY WORDS: UO₂ Fuel
Fuel Rods
Fuel Assembly
Fuel Burnup
Extended Burnup
Pressurized Water Reactor
Fuel Performance



UNITED STATES
NUCLEAR REGULATORY COMMISSION
WASHINGTON, D.C. 20555-0001

June 18, 2003

Mr. James F. Mallay
Director, Regulatory Affairs
Framatome ANP
3315 Old Forest Road
Lynchburg, VA 24501

**SUBJECT: SAFETY EVALUATION OF FRAMATOME ANP TOPICAL REPORT
BAW-10186P-A, REVISION 1, SUPPLEMENT 1, "EXTENDED BURNUP
EVALUATION" (TAC NOS. MB3650 AND MB7548)**

Dear Mr. Mallay:

By letter dated November 19, 2001, Framatome ANP submitted Supplement 1 to BAW-10186P-A, Revision 1, "Extended Burnup Evaluation," for review by the NRC staff. Framatome ANP has two fuel designs, Mark-B and Mark-BW, for Babcock & Wilcox-designed and Westinghouse-designed pressurized water reactors (PWRs), respectively. The staff previously approved both Mark-B and Mark-BW fuel designs to peak rod average burnup limits of 62,000 and 60,000 MWd/MTU, respectively, as described in the approved Topical Report (TR) BAW-10186P-A, Revision 1, "Extended Burnup Evaluation." At that time, Framatome ANP requested a burnup limit of 60,000 MWd/MTU for Mark-BW fuel rods due to the limited irradiation data available. Supplement 1 requests an extension of Framatome ANP's Mark-BW fuel design with an advanced cladding material M5 to the burnup limit of 62,000 MWd/MTU. The justification for this extension of the Mark-BW fuel burnup limit to 62,000 Mwd/MTU is based on the similarity to the Mark-B product and the additional data now available regarding the Mark-BW fuel. In addition, Framatome ANP has committed to performing additional post irradiation examinations of high burnup fuel. Data will be acquired on lead test assemblies and full batches of fuel. The results of these examinations will be presented to the NRC during the fuel vendor fuel performance review meetings.

The staff has completed its review of the subject TR and finds it is acceptable for referencing in licensing applications to the extent specified and under the limitations delineated in the report and in the associated safety evaluation (SE). The enclosed SE defines the basis for acceptance of the report.

Pursuant to 10 CFR 2.790, we have determined that the SE does not contain proprietary information. However, we will delay placing the SE in the public document room for a period of 10 working days from the date of this letter to provide you with the opportunity to comment on the proprietary aspects only. If you believe that any information in the enclosure is proprietary, please identify such information line by line and define the basis pursuant to the criteria of 10 CFR 2.790.

We do not intend to repeat our review of the matters described in the subject report, and found acceptable, when the report appears as a reference in license applications, except to ensure that the material presented applies to the specific plant involved. Our acceptance applies only to matters approved in the report.

In accordance with the guidance provided on the NRC website, we request that Framatome publish an accepted version of this TR within three months of receipt of this letter. The accepted version shall incorporate this letter and the enclosed SE between the title page and the abstract. It must be well indexed such that information is readily located. Also, it must contain in appendices historical review information, such as questions and accepted responses, and original report pages that were replaced. The accepted version shall include a "-A" (designated accepted) following the report identification symbol.

Should our criteria or regulations change so that our conclusions as to the acceptability of the report are invalidated, Framatome and/or the applicants referencing the TR will be expected to revise and resubmit their respective documentation, or submit justification for the continued applicability of the TR without revision of their respective documentation.

Sincerely,



Herbert N. Berkow, Director
Project Directorate IV
Division of Licensing Project Management
Office of Nuclear Reactor Regulation

Project No. 693

Enclosure: Safety Evaluation



UNITED STATES
NUCLEAR REGULATORY COMMISSION
WASHINGTON, D.C. 20585-0001

- SAFETY EVALUATION BY THE OFFICE OF NUCLEAR REACTOR REGULATION

TOPICAL REPORT BAW-10186P-A, REVISION 1, SUPPLEMENT 1,

"EXTENDED BURNUP EVALUATION"

FRAMATOME ANP

PROJECT NO. 693

1.0 INTRODUCTION

On November 19, 2001, Framatome ANP submitted Supplement 1 to Topical Report (TR) BAW-10186P-A, Revision 1, "Extended Burnup Evaluation," for NRC staff review and approval. Supplement 1 provides justification for extension of the burnup limit for the Mark-BW fuel design with an advanced cladding material M5 to 62,000 MWd/MTU. Previously, Framatome ANP requested an approved burnup limit of 60,000 MWd/MTU for Mark-BW fuel rods due to the limited irradiation data available. As part of this submittal, Framatome ANP provided more irradiation data and updated models.

Framatome ANP has two fuel designs, Mark-B and Mark-BW, for Babcock & Wilcox-designed and Westinghouse-designed pressurized water reactors (PWRs), respectively. These fuel designs are mainly for reload licensing applications of PWRs. TR BAW-10229-A, "Mark-B11 Fuel Assembly Design Topical Report," describes the recently approved Mark-B fuel design. The staff previously approved the Mark-BW fuel design in TR BAW-10172P-A, "Mark-BW Mechanical Design Report." The staff approved both Mark-B and Mark-BW fuel designs to peak rod average burnup limits of 62,000 and 60,000 MWd/MTU, respectively, as described in the TR BAW-10186P-A, Revision 1, "Extended Burnup Evaluation."

The staff approved the advanced cladding material M5 for fuel designs in TR BAW-10227P-A, "Evaluation of Advanced Cladding and Structural Material (M5) in PWR Reactor Fuel." Unlike Zircaloy, M5 is a zirconium-based material with nominally 1 percent niobium added. The staff also approved using M5 as cladding and other structural components for both Mark-B and Mark-BW fuel designs. The staff approved the same burnup limits of 62,000 and 60,000 MWd/MTU, as described previously, for Mark-B and Mark-BW fuel designs, respectively, with the M5 cladding material.

Framatome ANP will redesign the Mark-BW fuel with the advanced cladding material M5, rather than the conventional Zircaloy-4, for reload licensing applications. The fuel assembly structural materials like guide tubes, spacer grids, etc., may be either Zircaloy-4 or M5. Previously, the staff approved the Mark-BW fuel design to a burnup limit of 60,000 MWd/MTU rather than

62,000 MWd/MTU because Framatome ANP did not provide sufficient data to support the higher limit. Framatome ANP has obtained additional high burnup data. Based on the additional data and the similarity to the Mark-B fuel design, Framatome ANP requests to extend the burnup limit for Mark-BW fuel design with the M5 cladding material to 62,000 MWd/MTU.

2.0 REGULATORY EVALUATION

The acceptance criteria are based on Section 4.2, "Fuel Design System," of the Standard Review Plan (SRP). These criteria include three parts: (1) design bases – describes specified acceptable fuel design limits (SAFDLs) as depicted in General Design Criterion (GDC) 10 to 10 CFR Part 50, Appendix A, (2) design evaluation – demonstrates that the design bases are met, and (3) testing, inspection, and surveillance plans – shows that there are adequate monitoring and surveillance of irradiated fuel. For this review, the staff focused mainly on those areas where it determined that the data were insufficient in the previous review and could have impacts in the fuel performance of Mark-BW fuel design. These areas included, but were not limited to: fuel rod and assembly growth, oxidation, control rod drop time, and post-irradiation examination (PIE).

3.0 TECHNICAL EVALUATION

3.1 High Burnup Data

Framatome ANP recently expanded the Mark-BW fuel performance data base. Framatome ANP has a comprehensive PIE program that collects lead test assembly (LTA) irradiation data in high burnup regimes from various plants including Catawba, McGuire, North Anna, and Oconee. Framatome ANP provided a list of plants with completed PIEs. The PIE involves poolside and hotcell examinations of Mark-B and Mark-BW fuel rods with either Zircaloy-4 or M5 cladding. Framatome ANP has also committed to continue collecting data as described below. Based on the additional PIE data and the Framatome ANP commitment, the staff concludes that Framatome ANP has provided adequate high burnup data to support the peak rod average burnup limit of 62,000 MWd/MTU.

3.2 Fuel Rod and Assembly Axial Growth

Fuel rods tend to grow and close the lower clearance with the bottom nozzle earlier than the upper clearance with the top nozzle. The loss of these clearances will cause fuel bowing. All bowing phenomena will lead to thermal and hydraulic penalties during reactor operations. The Framatome ANP design basis for rod axial growth is that adequate clearance be maintained between fuel rod ends and top and bottom nozzles to accommodate the difference in the growth of fuel rods and fuel assembly. The clearance between the fuel rod top ends and the top nozzle is called the shoulder gap. A shoulder gap closure model estimates the time of the clearance disappearance, thereby commencing fuel rod bowing. Similarly, for assembly growth, Framatome ANP requires that sufficient axial clearance between core plates and bottom and top nozzles be maintained for fuel assembly irradiation growth during the assembly lifetime. Assembly growth is a result of guide thimble growth. Similarly, excessive assembly growth to close axial clearances between core plates and top and bottom nozzles will cause the assembly to bow.

Framatome ANP updated the shoulder gap closure model including Zircaloy-4 growth data to support the extension of the burnup limit to 62,000 MWd/MTU. The new model is conservative because it is based on the maximum shoulder gap closure for those assemblies measured during PIEs. The result showed that the Framatome ANP fuel designs of existing Zircaloy-4 cladding have adequate clearances to support the new burnup limit of 62,000 MWd/MTU. According to the information in TR BAW-10227P-A, the M5 fuel rods have shown consistently lower growth rates than the Zircaloy-4 fuel rods. Therefore, Framatome ANP concluded that the new shoulder gap closure model is also conservative for the M5 clad fuel rods for the extension of the burnup limit to 62,000 MWd/MTU. Based on the irradiation performance and the staff's review of the use of M5 in TR BAW-10227P-A, the staff agrees with the Framatome ANP assessment.

Framatome ANP also updated the fuel assembly growth model. Framatome ANP plotted the Zircaloy-4 and M5 thimble growth curves separately due to the material dependence. The result showed that the clearances between core plates and the top and bottom nozzles are adequately maintained for Zircaloy-4 to support a burnup limit of 62,000 MWd/MTU. The updated growth model showed that the M5 thimble growth is consistently below the Zircaloy-4 thimble growth. Thus, the M5 thimble tubes have enough clearances with regard to the assembly growth to a burnup limit of 62,000 MWd/MTU. Based on the irradiation performance and the staff review of the use of M5 in TR BAW-10227P-A, the staff agrees with the Framatome ANP conclusion.

Therefore, based on the acceptable data and previous irradiation performance, the staff concludes that the performance of fuel rod growth and assembly growth is acceptable for Mark-BW fuel design to the peak rod average burnup limit of 62,000 MWd/MTU.

3.3 Oxidation and Crud

SRP Section 4.2 identifies cladding oxidation and crud buildup as potential fuel damage mechanisms in the design bases. Cladding oxidation (corrosion) usually results in crud buildup. The SRP does not establish specific limits on cladding oxidation and crud, but specifies that their effects be accounted for in the thermal and mechanical analyses. Recent PIE data demonstrated that extensive corrosion could occur and result in premature fuel failures. In order to maintain adequate fuel cladding ductility at high burnups, the total amount of oxidation or corrosion should be limited during normal operations, including anticipated operational occurrences. The staff has strongly recommended that fuel vendors and licensees establish a corrosion limit to prevent further degradation of fuel rods. Framatome ANP adopted a corrosion thickness limit of 100 microns in TR BAW-10186P-A, Revision 1. The staff also concluded in TR BAW-10227P-A that the same corrosion limit was applicable for the M5 cladding.

Framatome ANP has generated more corrosion data of M5 cladding for the burnup regime greater than 60,000 MWd/MTU. The result demonstrated that the M5 corrosion trend starts leveling off and does not increase significantly as Zircaloy-4 does in the high burnup regime. This behavior confirms that M5 cladding has a quality of lower sensitivity to oxidation kinetics for various irradiation conditions. Thus, the M5 cladding has a greater margin to the 100 microns limit than the Zircaloy-4 cladding. Because crud formation is partially due to clad oxidation, the M5 cladding will have less crud buildup with other crud buildup factors remaining

the same. Therefore, overall, the M5 cladding will perform better than the Zircaloy-4 cladding with respect to corrosion and crud.

Based on the new corrosion data, the staff concludes that the Mark-BW fuel rods with M5 cladding have acceptable performance of corrosion and crud buildup for the peak rod average burnup limit of 62,000 MWd/MTU.

3.4 Control Rod Drop Time

SRP Section 4.2 states that control rod reactivity must be maintained as a design basis. In the mid-1990s, several control rods failed to insert fully into the dashpot section during reactor scrams at some PWRs. The affected control rods were positioned in high burnup fuel assemblies. Upon inspection of the fuel assemblies, the control rods were found to be in good condition, but the guide thimbles were deformed. The deformed guide thimbles could cause longer control rod drop time and delay the reactor trip. The guide thimbles are made of Zircaloy tubes.

The staff issued Bulletin 96-01, "Control Rod Insertion Problems," requesting special actions to ensure compliance with the current licensing basis of shutdown margin and control rod drop times. The industry took action to redesign the affected fuel assemblies and improve core management to eliminate the problem. Although the staff resolved those issues in the Bulletin, the staff will continue monitoring the control rod performance, and require new fuel designs or burnup extensions to address this problem.

Framatome ANP's Mark-BW fuel design has a dashpot integral to the guide thimbles. Framatome ANP stated that no Mark-BW fuel assemblies had experienced any incomplete rod insertion problem. Framatome ANP presented control rod drop tests of Mark-BW fuel with M5 thimble tubes from four reactors. The results showed that there were no appreciable drop time changes from low to high burnup regimes. Based on the Framatome ANP control rod performance, the staff agrees with the observation.

Based on these drop tests and the fact that the M5 guide thimbles are less likely than Zircaloy guide thimbles to involve this problem, the staff concludes that the Mark-BW fuel control rod performance is acceptable for the peak rod average burnup limit of 62,000 MWd/MTU.

3.5 Reactivity Initiated Accident

The reactivity initiated accidents (RIAs) include a control rod ejection accident in PWRs. SRP Section 4.2 specifies that a fuel enthalpy limit of 280 cal/g should be observed during an RIA as a design basis.

Recent experimental data showed failure of high burnup fuel at lower enthalpy values than the 280 cal/g safety limit. However, there was a broad agreement among the staff and the industry, including the international community, that the effect of burnup degradation in the enthalpy safety limit for high burnup fuel is likely to be compensated by applying detailed three-dimensional analytical methods for RIAs. In addition, generic analyses performed by the industry assuming low enthalpy fuel failure, showed that the radiological consequences of rod ejection accidents met the acceptance criteria in the SRP.

The staff realizes that the fuel enthalpy safety limit in the SRP is not conservative and may decrease in the future. Further testing and evaluation are needed to better establish new limits. Recently, industry submitted a generic TR entitled, "Topical Report on Reactivity Initiated Accident: Bases for RIA Fuel and Core Coolability Criteria," for staff review. This TR intends to establish new safety limits of fuel failure and fuel coolability. Pending completion of the review, the staff considers that the current enthalpy safety limit continues to be acceptable until it is revised, and the use of M5 material in the Mark-BW fuel design is not expected to significantly impact the safety analyses. In addition, the staff considers that the probability of these accidents is low and the generic safety analyses provide reasonable assurance that radiological consequences will not violate the acceptance criteria in the SRP.

Since there are many similar features between Mark-B and Mark-BW fuel designs, the staff expects that Mark-BW fuel performs similarly as the Mark-B fuel under RIAs. Framatome ANP confirmed that the Mark-BW fuel design continues to meet the current fuel enthalpy limit to the peak rod average burnup limit of 62,000 MWd/MTU as the Mark-B fuel already did. Based on the similarity between the Mark-B and Mark-BW fuel designs, the staff concludes that the Mark-BW fuel design will have no impact in the RIA results for burnup limit extension from 60,000 to 62,000 MWd/MTU.

3.6 Post-Irradiation Examination

In the past few years, operating experiences have identified a series of fuel issues that raise important licensing questions. Among these issues are accelerated growth of rods and assemblies, higher cladding oxidation, incomplete control rod insertion events, etc. All of these issues are associated with high burnups. The NRC plan for addressing high burnup fuel issues is described in the document entitled, "Agency Program Plan for High Burnup Fuel," dated July 6, 1998 (ADAMS Accession Nos. ML011380085 and ML011380091). The staff has established a few basic burnup extension guidelines. In particular, the staff stresses the need for LTAs in the guidelines.

During the approval of TR BAW-10186P-A, Revision 1 and TR BAW-10227P-A, Framatome ANP made a commitment to acquire additional PIE data. The PIE program usually involves LTA irradiation in multiple plants to collect high burnup results. These high burnup results exceeding the current burnup limits will be able to support future licensing applications. Framatome ANP provided a list of completed and ongoing LTA inspections. The inspection includes various performance data such as cladding oxide, rod and assembly growth, shoulder gap, rod bow, control rod drop time, and cladding wear.

Based on Framatome ANP's LTA commitment, which is consistent with the staff guidelines, the staff concludes that the PIE program is acceptable for Mark-BW fuel design up to the peak rod average burnup limit of 62,000 MWd/MTU.

4.0 CONCLUSION

The staff has reviewed Supplement 1 to TR BAW-10186P-A, Revision 1 that describes the Mark-BW fuel design with the advanced cladding material M5. Based on the staff's review of the applicable data and many similar features with the Mark-B design, the staff concludes that

the Mark-BW fuel design with the M5 cladding is acceptable for burnup extension to the peak rod average burnup limit of 62,000 MWd/MTU.

Therefore, the staff concludes that Supplement 1 to TR BAW-10186P-A, Revision 1 provides adequate justification for the use of the Mark-BW fuel design with M5 cladding to the peak rod average burnup limit of 62,000 MWd/MTU. The approval of this Supplement supercedes the safety evaluation restrictions on burnup in TRs BAW-10186P-A, Revision 1 and BAW-10227P-A for the Mark-BW fuel design. In addition, Framatome ANP may incorporate this safety evaluation in the approved versions of TRs BAW-10186P-A, Revision 1 and BAW-10227P-A.

Principal Contributor: S. L. Wu

Date: June 18, 2003



UNITED STATES
NUCLEAR REGULATORY COMMISSION

WASHINGTON, D.C. 20555-0001

January 25, 1999

Mr. J. H. Taylor, Manager
Licensing Services
Framatome Cogema Fuels
3315 Old Forest Road
P. O. Box 10935
Lynchburg, VA 24506-0935

**SUBJECT: ACCEPTANCE FOR REFERENCING OF FRAMATOME COGEMA FUELS
TOPICAL REPORT BAW-10186P: "EXTENDED BURNUP EVALUATION"
(TAC NO. MA3705)**

Dear Mr. Taylor:

The staff has reviewed the subject report submitted by Framatome Cogema Fuels (FCF) by letter of November 24, 1992, and additional information submitted by letters dated July 19, August 22, and December 6, 1995; June 26, 1996; and January 23, 1997, to our requests for additional information. The staff approved the subject report in a letter including a safety evaluation (SE) from D. B. Matthews (USNRC) to J. H. Taylor (FCF) on April 29, 1997, and FCF published an approved version of the subject report BAW-10186P-A on June 12, 1997.

However, FCF raised a concern relating to the corrosion limit during the implementation of BAW-10186P-A. FCF submitted two letters dated August 29 and October 28, 1997, from J. H. Taylor to USNRC to clarify the corrosion issue. The staff determined that there was a need to revise and reissue the SE to avoid confusion in the future. Thus the enclosed revised SE will supersede the previous SE. On the basis of our review, the staff has found the subject report to be acceptable for referencing in license applications to the extent specified and under the limitations stated in the U.S. Nuclear Regulatory Commission (NRC) safety evaluation. The evaluation defines the basis for acceptance of the report.

The staff will not repeat its review of the matters described in FCF Topical Report BAW-10186P and found acceptable when the report appears as a reference in license applications, except to ensure that the material presented applies to the specific plant involved. NRC acceptance applies only to the matters described in FCF Topical Report BAW-10186P. In accordance with procedures established in NUREG-0390, the NRC requests that FCF publish accepted versions of the report, proprietary and non-proprietary, including the revised SE within 3 months of receipt of this letter. The accepted versions shall incorporate this letter and the enclosed evaluation between the title page and the abstract and an -A (designating accepted) following the report identification symbol. The accepted version should also incorporate the October 28, 1997, submittal. In addition, to avoid confusion in the future, the staff requests that FCF withdraw the version of BAW-10186P-A/BAW-10186-A that was submitted by letter dated June 12, 1997. Also please withdraw the letter dated August 29, 1997, because this letter has been superseded by the letter dated October 28, 1997.

J. H. Taylor

- 2 -

Should our acceptance criteria or regulations change so that our conclusions as to the acceptability of the report are no longer valid, applicants referencing this topical report will be expected to revise and resubmit their respective documentation, or submit justification for the continued applicability of the topical report without revision of their respective documentation.

Sincerely,



Thomas H. Essig, Acting Chief
Generic Issues and Environmental Projects Branch
Division of Reactor Program Management
Office of Nuclear Reactor Regulation

Enclosure:
FCF Topical Report BAW-10186P Safety Evaluation

REVISED SAFETY EVALUATION OF FRAMATOME COGEMA FUELS
TOPICAL REPORT BAW-10186P
"EXTENDED BURNUP EVALUATION"

1 INTRODUCTION

In a letter dated November 24, 1992, from J. H. Taylor, Babcock & Wilcox Nuclear Technologies (B&WNT), to the U.S. Nuclear Regulatory Commission (NRC), B&WNT submitted a Topical Report BAW-10186P, "Extended Burnup Evaluation," for NRC review. By letter dated July 19, 1995, B&WNT requested that the review be extended to include a change in the fuel rod power history uncertainty used in TACO3 licensing analyses. Since that time B&WNT has become Framatome Cogema Fuels (FCF).

BAW-10186P describes an improved extended burnup methodology that FCF intends to apply for fuel reload applications. The purpose of this improved methodology is to extend the analysis to a slightly higher burnup range than the previously approved range for different fuel designs. Additional material including responses to the NRC's requests for additional information was submitted by letters dated August 22, and December 6, 1995, June 26, 1996, and January 23, 1997.

The staff reviewed the topical report and the related documents, and approved BAW-10186P in a letter, including a safety evaluation (SE), from D. B. Matthews (USNRC) to J. H. Taylor (FCF) dated April 29, 1997. The NRC staff was supported in this review by its consultant, Pacific Northwest National Laboratory (PNNL). Our consultant's technical evaluation report (TER), which was attached, provided technical findings relative to the review. Subsequently, FCF published an approved version of the report BAW-10186P-A on June 12, 1997.

During the implementation of BAW-10186P-A, FCF raised a question about the limitations on the predicted cladding corrosion levels. FCF, NRC staff, and its contractor reviewer at PNNL held several telephone conferences to reach agreement on the interpretation of the limitations. FCF submitted two letters dated August 29 and October 28, 1997 from J. H. Taylor to USNRC to clarify the corrosion issue. The staff determined that the SE should be revised and reissued to avoid confusion in the future. Thus this revised SE will supersede the SE dated April 29, 1997.

2 EVALUATION

The staff reviewed the enclosed TER, and concluded that the TER provides an adequate technical basis to approve BAW-10186P. The staff agrees with PNNL's conclusion that the improved methodology described in BAW-10186P is acceptable for fuel reload licensing applications. Based on our review, the staff adopts the findings in the attached TER. In addition the staff provides an assessment of corrosion limit in the following.

2.1 Oxidation and Crud Buildup (TER Section 3.0(E))

In a letter dated October 28, 1997 from J. H. Taylor to USNRC, FCF stated that the predicted oxide/corrosion layers are limited to 100 microns for normal operation and anticipated operational occurrences (AOOs). This limit of oxide and corrosion depth is intended to address the concern of potential ductility reduction and other adverse effects on the cladding integrity for high burnup operations. This limit of 100 microns has been widely used in the industry for fuel rod designs. Thus, the staff considers that the limit of 100 microns for oxide/corrosion including the crud buildup is acceptable.

FCF further proposed a lead test assembly (LTA) program to continue collecting corrosion data during high burnup operations. The LTA program allows a total of eight fuel assemblies in each fuel cycle from different sub-batches to operate even though the predicted corrosion is greater than 100 microns. These assemblies will be designated as lead corrosion assemblies. Typically these assemblies will be placed in non-limiting core positions but with relative high powers to be able to simulate typical operation conditions. Corrosion measurements will be performed after these assemblies are discharged from the core. In any fuel core the total number of LTAs (lead corrosion assemblies plus other LTAs) will not exceed twelve. The staff reviewed the LTA program and determined that this LTA program satisfies the intent of the LTA programs as described in the Standard Review Plan (SRP) 4.2. Therefore, the staff approves the FCF's LTA program.

FCF will use the COROS02 corrosion model for best estimate calculations of corrosion. Best estimate models are used throughout the industry. While the staff recognizes that the corrosion data base has large uncertainty, and different measurement techniques can produce very different results, the staff considers that the use of a best estimate calculation for corrosion analysis is not unreasonable. FCF will continue assessing the corrosion model conservatism to ensure that the best estimate model is consistent and unbiased through high burnups. The NRC consultant PNNL has reviewed the COROS02 corrosion model and found it acceptable as described in the attached TER. Thus, the staff approves the use of a best estimate calculation in the corrosion model.

3 CONCLUSIONS

The staff has reviewed the FCF's extended burnup methodology described in BAW-10186P, and finds that the improved methodology is adequate and thus acceptable for fuel reload licensing applications subject to the following conditions to which FCF has agreed (References 6 and 7).

- 1) This methodology is acceptable for Mark-B fuel design up to 62 GWd/MTU rod average burnup.
- 2) This methodology is acceptable for Mark-BW fuel design up to 60 GWd/MTU rod average burnup.
- 3) This approval does not cover extended burnup operation of Mark-C fuel design.

- 4) The maximum predicted oxide thickness will be 100 microns.
- 5) Up to eight fuel assemblies from different sub-batches in each fuel cycle may have fuel rods with predicted oxide layers greater than 100 microns and will be designated as lead corrosion assemblies.
- 6) The total number of lead test assemblies (lead corrosion assemblies and other LTAs) in any fuel cycle will not exceed twelve.

In addition, as was stated in the TER, the NEMO code calculational uncertainty for use in the TACO3 fuel performance code for licensing analyses is acceptable.

4 REFERENCES

1. "Extended Burnup Evaluation," BAW-10186P, Babcock and Wilcox Fuel Company, Lynchburg, Virginia, transmitted by letter, J. H. Taylor (BWFC) to U.S. NRC Document Control Desk, dated November 24, 1992.
2. Letter, J. H. Taylor (B&W Nuclear Technologies) to R. C. Jones (NRC) dated July 19, 1995.
3. Letter, J. H. Taylor (B&W Nuclear Technologies) to R. C. Jones (NRC), JHT/95-88, dated August 22, 1995.
4. Letter, J. H. Taylor (B&W Nuclear Technologies) to R. C. Jones (NRC), JHT/95-119, dated December 6, 1995.
5. Letter, J. H. Taylor (B&W Nuclear Technologies) to R. C. Jones (NRC), JHT/96-042, dated June 26, 1996.
6. Letter, J. H. Taylor (Framatome Cogema Fuels) to NRC Document Control Desk, "Application of BAW-10186P," JHT/97-7, dated January 23, 1997.
7. Letter, J. H. Taylor (Framatome Cogema Fuels) to NRC Document Control Desk, JHT/97-39, dated October 28, 1997.
8. Babcock and Wilcox Fuel Company, March 1993, NEMO-Nodal Expansion Method Optimized, BAW-10180P-A, Rev 1, Babcock and Wilcox Fuel Company, Lynchburg, Virginia.

TECHNICAL EVALUATION REPORT

TECHNICAL EVALUATION REPORT OF THE
TOPICAL REPORT BAW-10186P (EXTENDED
BURNUP EVALUATION REPORT)

C. E. Beyer
D. D. Lanning

March 10, 1997

Prepared for
Office of Nuclear Reactor Regulation
U.S. Nuclear Regulatory Commission
Washington, D.C. 20014
under Contract DE-AC06-76RLO 1830
NRC FIN I2009

Pacific Northwest Laboratory
Richland, Washington 99352

ABBREVIATIONS LIST

| | | |
|-------|---|--|
| AOO | - | Anticipated Operational Occurrence |
| ASME | - | American Society of Mechanical Engineers |
| DNB | - | Departure from Nucleate Boiling |
| DNBR | - | Departure from Nucleate Boiling Ratio |
| ECCS | - | Emergency Core Cooling System |
| EOL | - | End of Life |
| FCF | - | Framatome Cogema Fuels |
| FGR | - | Fission Gas Release |
| GDC | - | General Design Criterion |
| LOCA | - | Loss of Coolant Accident |
| NRC | - | U.S. Nuclear Regulatory Commission |
| PCI | - | Pellet Cladding Interaction |
| PCT | - | Peak Cladding Temperature |
| PIE | - | Post Irradiation Examination |
| PNNL | - | Pacific Northwest National Laboratory |
| RIA | - | Reactivity Initiated Accident |
| SAFDL | - | Specified Acceptable Fuel Design Limit |
| SRP | - | Standard Review Plan |
| TER | - | Technical Evaluation Report |

CONTENTS

| | | |
|-----|--|----|
| 1.0 | Introduction | 1 |
| 2.0 | Fuel System Design | 2 |
| 3.0 | Fuel System Damage | 3 |
| | (A) Stress | 3 |
| | (B) Strain | 4 |
| | (C) Strain Fatigue | 5 |
| | (D) Fretting Wear | 6 |
| | (E) Oxidation and Crud Buildup | 7 |
| | (F) Rod Bowing | 8 |
| | (G) Axial Growth | 8 |
| | (H) Rod Internal Pressure | 9 |
| | (I) Assembly Ltoff | 10 |
| 4.0 | Fuel Rod Failure | 10 |
| | (A) Hydriding | 10 |
| | (B) Cladding Collapse | 11 |
| | (C) Overheating of Cladding | 11 |
| | (D) Overheating of Fuel Pellets | 12 |
| | (E) Pellet/cladding Interaction | 12 |
| | (F) Cladding Rupture | 13 |
| | (G) Fuel Rod Mechanical Fracturing | 13 |
| 5.0 | Fuel Coolability | 13 |
| | (A) Fragmentation of Embrittled Cladding | 13 |
| | (B) Violent Expulsion of Fuel | 14 |
| | (C) Cladding Ballooning and Flow Blockage | 15 |
| | (D) Fuel Assembly Structural Damage from External Forces | 15 |
| 6.0 | Fuel Surveillance | 16 |
| 7.0 | Conclusions | 17 |
| 8.0 | References | 17 |

1.0 INTRODUCTION

Framatome Cogema Fuels (FCF) has submitted to the U.S. Nuclear Regulatory Commission (NRC) a topical report, entitled "Extended Burnup Evaluation," BAW-10186P (Reference 1), for review and approval. This report requests an extension in fuel rod average burnups for their Mark-B (15X15) and Mark-C (17X17) fuel designs for Framatome type reactors, and Mark-BW15 (15X15) and Mark-BW17 (17X17) for Westinghouse type reactors. An additional request was made to extend the scope of this review (Reference 2) to include a change in the fuel rod power history uncertainty used in TACO3 licensing analyses. The original power uncertainty used for TACO3 were based on the calculational uncertainties associated with the FLAME3 neutronics code used at the time the TACO3 code was developed. Since that time FCF has developed the NEMO code (Reference 3) for neutronics and rod power calculations and the calculational uncertainties of the code are lower than for the previous FLAME3 code. This request is evaluated at the beginning of Section 3.0 of this report. This Technical Evaluation Report (TER) will only address the burnup extension of 62 GWd/MTU for Mark B and 60 GWd/MTU for Mark BW designs and the proposed change in the power uncertainties used in TACO3 for licensing analyses (Reference 2). The previously approved burnup extensions have limited the Mark-B fuel designs to a proprietary batch average burnup defined in Reference 5 and the Mark-BW fuel designs up to a lead rod-average burnup level of 60 GWd/MTU (Reference 6). The Mark-C design is not covered in this review because FCF has only a limited amount of performance data for this design and does not currently have an operating reactor utilizing this design.

It should be explained that Framatome Cogema Fuels was previously named the B&W Fuel Company (BWFC) a part of B&W Nuclear Technologies and prior to BWFC was named Babcock & Wilcox (B&W). Some of the references in this TER refer to these different company names depending on the date the reference was generated.

Pacific Northwest National Laboratory (PNNL) has acted as a consultant to the NRC in this review. As a result of the NRC staffs and their PNNL consultants review of the topical report, a list of questions were sent by the NRC to FCF requesting clarification of specific design criteria and licensing analyses (Reference 7). FCF partially responded to those questions in Reference 8 and provided the remaining responses in Reference 9. Following a February 26, 1996 telecon with NRC and PNNL, FCF agreed to supply additional information (Reference 10) to support their request for a burnup extension.

This review was based on those licensing requirements identified in Section 4.2 of the Standard Review Plan (SRP) (Reference 11). The objectives of this fuel system safety review, as described in Section 4.2 of the SRP, are to provide assurance that 1) the fuel system is not damaged as a result of normal operation and anticipated operational occurrences (AOOs), 2) fuel system damage is never so severe as to prevent control rod insertion when it is required, 3) the number of fuel rod failures is not underestimated for postulated accidents, and 4) coolability is always maintained. A "not damaged" fuel system is defined as fuel rods that do not fail, fuel

system dimensions that remain within operational tolerances, and functional capabilities that are not reduced below those assumed in the safety analysis. Objective 1, above, is consistent with General Design Criterion (GDC) 10 (10 CFR 50, Appendix A) (Reference 12), and the design limits that accomplish this are called specified acceptable fuel design limits (SAFDLs). "Fuel rod failure" means that the fuel rod leaks and that the first fission product barrier (the cladding) has, therefore, been breached. Fuel rod failures must be accounted for in the dose analysis required by 10 CFR 100 (Reference 13) for postulated accidents. "Coolable geometry" means, in general, that the fuel assembly retains its rod-bundle geometrical configuration with adequate coolant channels to permit removal of residual heat even after a severe accident. The general requirements to maintain control rod insertability and core coolability appear repeatedly in the GDC (e.g., GDC 27 and 35). Specific coolability requirements for the LOCA are given in 10 CFR 50, Section 50.46 (Reference 14).

In order to assure that the above stated objectives are met and follow the format of Section 4.2 of the SRP, this review covers the following three major categories: 1) Fuel System Damage Mechanisms, which are most applicable to normal operation and AOOs; 2) Fuel Rod Failure Mechanisms, which apply to normal operation, AOOs, and postulated accidents; and 3) Fuel Coolability, which are applied to postulated accidents. Specific fuel damage or failure mechanisms are identified under each of these categories in Section 4.2 of the SRP. This TER discusses under each fuel damage or failure mechanism listed in the SRP the FCF design limits, analysis methods and data used to demonstrate that the SAFDLs are met up to the rod-average burnup levels of 62 GWd/MTU for Mark B and 60 GWd/MTU for Mark BW designs.

The purpose of design criteria or limits are ^{to provide limiting CFM} ~~to provide limiting~~ values that prevent fuel damage or failure and fuel coolability/control rod insertability for postulated accidents with respect to each mechanism. Reviewed in this TER is whether FCF fuel designs have adequate data to demonstrate that their fuel designs can operate satisfactorily up to rod-average burnup levels of 62 GWd/MTU for Mark B and 60 GWd/MTU for Mark-BW designs as defined by the SAFDLs for normal operation, AOOs and postulated accidents. *CFM*

The Mark B and Mark BW fuel designs are briefly discussed in the following section (Section 2.0). The fuel damage and failure mechanisms are addressed in Sections 3.0 and 4.0, respectively, while fuel coolability is addressed in Section 5.0.

2.0 FUEL SYSTEM DESIGN

The Mark-B design is a 15X15 assembly with Zircaloy spacer grids. The fuel assembly consists of 208 fuel rods, 16 control rod guide tubes, 1 instrumentation tube assembly, 7 segmented spacer sleeves, 8 spacer grids, and bottom and top nozzles. The guide tubes, spacer grids and end nozzles form the structure of the assembly where the fuel rods and tubes are arranged in a 15X15 array. The center position in the assembly is reserved for instrumentation. The structural materials consist of Zircaloy-4 and Inconel except for the axial power shaping rod cladding which consists of stainless steel.

The Mark-BW designs are 15X15 and 17X17 assemblies with Zircaloy grids for Westinghouse type reactor reloads. The 15X15 assembly consists of 204 fuel rods, 20 control rod guide tubes, 1 instrumentation tube assembly, 8 spacer grids, and top and bottom nozzles with the holddown spring being a leaf configuration. The 17X17 assembly consists of 264 fuel rods, 24 control rod guide tubes, 1 instrumented tube assembly, 8 spacer grids, and top and bottom nozzles with the holddown spring being a leaf configuration.

3.0 FUEL SYSTEM DAMAGE

The design criteria presented in this section should not be exceeded during normal operation including AOOs. The evaluation portion of each damage mechanism evaluates the analysis methods, analyses and data used by FCF to demonstrate that their design criteria are not exceeded during normal operation including AOOs for their fuel designs up to rod-average burnup limits of 62 GWd/MTU for Mark B and 60 GWd/MTU for Mark BW designs.

A request was made by FCF to extend the scope of this review (Reference 2) to include a change in the fuel rod power history uncertainty used in TACO3 licensing analyses. The TACO3 code is used by FCF in many of the analysis methods discussed below to verify that the design criteria in this section and Sections 4.0 and 5.0 are met. The original power uncertainty used for TACO3 licensing applications were based on the calculational uncertainties associated with the FLAME3 neutronics code used at the time the TACO3 code was developed. Since that time FCF has developed the NEMO code for neutronics and rod power calculations and the calculational uncertainties of the code are lower than for the previous FLAME3 code. The NEMO neutronics code and calculational uncertainties have been approved by the NRC (Reference 3) for analysis of fuel powers and neutronics. Therefore, the use of the NEMO calculational uncertainty for use in TACO3 licensing applications is considered to be acceptable.

(A) STRESS

Bases/Criteria - In keeping with the GDC 10 SAFDLs, fuel damage criteria for cladding stress should ensure that fuel system dimensions remain within operational tolerances and that functional capabilities are not reduced below those assumed in the safety analysis. The FCF design criteria for fuel rod cladding and assembly stresses are based on guidelines established in Section III of the American Society of Mechanical Engineers (ASME) Boiler Pressure Vessel Code (Reference 15). FCF utilizes unirradiated values of yield and ultimate tensile stress to determine the stress limits based on Reference 15. The use of unirradiated values is conservative because irradiation has been shown to increase the yield and ultimate tensile stresses for Zircaloy. These criteria are consistent with the acceptance criteria established in Section 4.2 of the SRP and are acceptable up to the burnup limits established in Reference 4.

Evaluation - The stress analyses for FCF fuel assembly components and fuel rod cladding are based on standard stress analysis methods including finite-element analysis. Pressure and temperature inputs to the stress analyses are chosen so that the operating conditions for all

normal operation and AOOs are enveloped. The cladding wall thicknesses are reduced to those minimum values allowed by fabrication specifications and further reduced to allow for corrosion on the inside and outside diameter. FCF uses the cladding corrosion from COROSO2 to determine corrosion on the outside diameter. PNNL concludes that the FCF design analysis methods for stress analyses are consistent with the guidelines in Section 4.2 of the SRP and are acceptable up to the burnup limits established in Reference 4.

(B) STRAIN

Bases/Criteria - The FCF design criteria for fuel rod cladding strain is that maximum uniform hoop strain (elastic plus plastic) shall not exceed 1%. This criteria is intended to preclude excessive cladding deformation from normal operation and AOOs. This is the same criterion for cladding strain that is used in Section 4.2 of the SRP and, therefore, is acceptable.

The material property that could have a significant impact on the cladding strain limit at extended burnup levels is cladding ductility. The strain criterion could be impacted if cladding ductility were decreased, as a result of extended burnup operation, to levels that would allow cladding failure without the 1% cladding strain criteria being exceeded under normal operation and AOOs.

Recent out-of-reactor measured elastic and plastic cladding strain values from high burnup cladding from two PWR fuel vendors (References 16, 17 and 18) have shown a decrease in cladding ductilities when local burnups exceed 52 MWd/kgM. The cladding plastic strain values have a large scatter when local burnups were between 55 and 63 MWd/kgM with cladding ductility varying between 0.3% to 2% depending on testing methods (burst, tensile or ring tests), hydrogen levels in the cladding and fuel vendor. A quantitative separation of test methods and fuel vendor differences among the data is not possible at this time because of the large amount of scatter in the data and the relatively small amount of data at both high burnups and high corrosion levels. However, qualitatively the burst test data generally has the lowest cladding strains indicating that the stress state in the cladding appears to have some influence on measured uniform strain. Another complicating factor is that none of these testing methods, including the burst tests, simulate the stress state of pellet-cladding interaction (PCI) that contributes to cladding strain in operating fuel rods. However, all of these data do show that cladding ductility is decreasing with increasing burnup and hydrogen (corrosion) levels. In addition, the majority of the high burnup data (tensile or burst) shows that when hydrogen levels start to exceed 700 ppm the uniform strains begin to fall below 1%.

FCF has responded (Reference 8) with actual in-reactor strain data due to PCI above 1% strain without failure from segmented fuel rods ramped to peak powers of 12 to 13.4 kW/ft with peak burnups of 62 GWd/MTU and cladding hydrogen levels between 225 to 320 ppm (corrosion thickness between 39 to 55 microns). This demonstrates that the FCF cladding up to peak fuel burnups of 62 GWd/MTU can achieve elastic plus plastic strains of 1% or greater without failure but does not address FCF cladding ductility when hydrogen levels exceed 700 ppm. FCF's limit

on maximum cladding corrosion (Reference 4) is consistent with maintaining cladding hydrogen levels below 700 ppm. PNNL concludes that the 1.0% uniform strain limit on FCF Zircaloy-4 cladding strain is acceptable up to the burnup and corrosion limits established in Reference 4.

Evaluation - The subject topical report has stated that the TACO-3 fuel performance code (Reference 19) is used for cladding strain analyses. This fuel performance code has been previously reviewed and approved by NRC up to the burnup levels established in Reference 4. FCF uses conservative bounding values for input to TACO-3 for this calculation including worst case fabrication tolerances, pressure differentials and power histories (including AOOs). PNNL concludes that this analysis methodology is acceptable.

(C) STRAIN FATIGUE

Bases/Criteria - The FCF design criterion for cladding strain fatigue is that the cumulative fatigue usage factor be less than 0.9 when a minimum safety factor of 2 on the stress amplitude or a minimum safety factor of 20 on the number of cycles, which ever is the most conservative, is imposed as per the O'Donnell and Langer design curve (Reference 20) for fatigue usage.

The material property that could have a significant effect on the strain fatigue criterion is cladding ductility. As discussed in the above Section 3.0(B) for design strain, extended burnup operations above local burnups of 52 MWd/kgM have recently demonstrated a significant reduction in cladding ductilities. This could also reduce the cladding strain fatigue capability. However, as discussed in Section 3.0(B), Zircaloy-4 cladding ductility will not fall below the acceptable limit for total uniform strain if cladding corrosion and hydrogen levels are within the limits established by FCF in Reference 4. In addition, there is a considerable amount of conservatism in the FCF strain fatigue calculation and considerable lifetime margin in FCF strain fatigue results up to the burnup limits established in Reference 4. Also, the rod power for a FCF lead fuel rod at the extended burnup levels requested is relatively low so that cladding stress and strains will be relatively low at this burnup level. Therefore, PNNL concludes that the FCF strain fatigue criterion proposed in Reference 1 is acceptable for licensing applications to FCF fuel designs up to the burnup limits established in Reference 4.

Evaluation - The analysis methodology for evaluating strain fatigue for the FCF fuel designs uses the O'Donnell and Langer curve for irradiated Zircaloy (Reference 20). The use of O'Donnell and Langer's curve and analysis methods for determining strain fatigue life is consistent with SRP Section 4.2 and have been previously approved by the NRC. The analysis methodology also uses conservative inputs of minimum as-fabricated cladding thickness and oxide layer thickness. PNNL concludes that the strain fatigue analysis methods are acceptable for evaluating the above design criteria up to the burnup limits established in Reference 4.

(D) FRETTING WEAR

Bases/Criteria - Fretting wear is a concern for fuel, burnable poison rods, and guide tubes. Fretting, or wear, may occur on the fuel and/or burnable rod cladding surfaces in contact with the spacer grids if there is a reduction in grid spacing loads in combination with small amplitude, flow induced, vibratory forces. Guide tube wear may result when there is flow induced motion between the control rod ends and the inner wall of the guide tube.

While Section 4.2 of the SRP does not provide numerical bounding value acceptance criteria for fretting wear, it does stipulate that the allowable fretting wear should be stated in the safety analysis report and that the stress/strain and fatigue limits should presume the existence of this wear.

The FCF design criterion against fretting wear is that the fuel design shall provide sufficient support to limit fuel rod vibration and cladding fretting wear. This design criterion can also be applied to other fuel assembly components that are susceptible to fretting wear, such as the fuel assembly guide tubes. This criterion is consistent with Section 4.2 of the SRP and is found to be acceptable for the FCF fuel designs up to the burnup levels established in Reference 4.

Evaluation - FCF has stated that fretting wear is based on external life and wear testing performed in a flow loop and postirradiation examination (PIE) results. The life and wear tests are conducted at maximum reactor flow conditions for more than 1000 hours to evaluate the fretting characteristics of the fuel rods and spacer grids.

FCF was questioned on the recent fretting failures in a FCF designed plant and whether this was due to irradiation induced relaxation of the spacer grid springs. FCF responded that the failures were from a non-FCF fuel design from another vendor and that some FCF spacer grid fretting problems had been observed in an old discontinued fuel design with Inconel intermediate spacer grids. They further indicated that two fretting failures have been found with their newer Zircaloy spacer grids but these were thought to be due to fabrication problems with the spacer grid springs or fuel handling had damaged the spacer grid springs in these two failure incidents. PNNL agrees that these are likely reasons for these fretting failures. FCF stated that they have examined Mark B designs with Zircaloy spacer springs up to very near the burnup limit in Reference 4 without any unusual observed fretting wear. Therefore, PNNL concludes that the evaluation of fretting wear has been adequately addressed up to the burnup limits established in Reference 4.

It should be noted that, recently, there have been more cladding fretting failures due to fabrication problems or flow anomalies from different vendors. These fretting failures have resulted in high plant coolant activities. In the future further NRC inspections may be required to examine this problem.

(E) OXIDATION AND CRUD BUILDUP

Bases/Criteria - Section 4.2 of the SRP identifies cladding oxidation and crud buildup as potential fuel system damage mechanisms. The SRP does not establish specific limits on cladding oxidation and crud but does specify that their effects be accounted for in the thermal and mechanical analyses performed for the fuel. As noted in Sections 3.0(B) and 3.0(C), the cladding ductility can be significantly decreased at higher burnup levels where oxide thickness and hydrogen levels can become relatively large because of accelerated corrosion at rod-average burnups above 50 to 55 GWd/MTU. FCF originally proposed a maximum corrosion limit that could achieve cladding hydrogen levels of 700 ppm and greater using the new FRAPCON-3 hydrogen pickup fraction due to corrosion (Reference 21). Due to the lack of strain data from FCF cladding with 700 ppm of hydrogen and above, FCF has revised their maximum corrosion limit (Reference 4) to be more consistent with existing hydrogen and strain data to date that demonstrates adequate cladding ductility. This maximum corrosion limit is based on a localized axial position on a fuel rod. PNNL concludes that this revised maximum corrosion limit (Reference 4) is acceptable up to the burnup limits established in Reference 4.

Evaluation - Section 4.2 of the SRP states that the effects of cladding crud and oxidation needs to be addressed in safety and design analyses, such as in the thermal and mechanical analysis. The amount of cladding oxidation is dependent on fuel rod powers, water chemistry control and primary inlet coolant temperatures, but the amount of oxidation and crud buildup increases with burnup and cannot be eliminated. Therefore, extended burnups result in a thicker oxide layer that provides an extra thermal barrier, cladding thinning and ductility decrease that can affect the mechanical analysis. The degree of this effect is dependent on reactor coolant temperatures and the level of success of a reactors' water chemistry program. The following is an evaluation of the FCF corrosion model.

FCF has proposed a new cladding corrosion model, COROSO2 (Reference 9), that is more conservative, i.e., predicts more corrosion, than the original OXIDEPC model in TACO3 and predicts the accelerated corrosion observed in high burnup rods much better than the OXIDEPC model. The relatively small amount of maximum corrosion thickness data from FCFs low tin cladding (currently the cladding used by FCF for high burnup applications) indicates that the COROSO2 model predicts maximum corrosion thickness in a best estimate or slightly conservative manner but significantly overpredicts span average corrosion (span average thickness is the type of data most often collected by FCF). It is the maximum corrosion thickness within an assembly or on a fuel rod that is of greatest interest for licensing analyses because this is the most likely point of failure due to corrosion and is the basis for the FCF corrosion limit discussed above. For this reason FCF plans to collect more data based on maximum corrosion thickness in the future. The maximum corrosion thickness measured by FCF is a moving average of the eddy current data over the rod length. The average is based on less than a half inch length of the fuel rod. The best estimate or slightly conservative prediction of the COROSO2 model is considered to be acceptable because of the conservatism in the FCF maximum corrosion limit. PNNL concludes that the COROSO2 model is acceptable for use in predicting maximum corrosion

levels for verifying that they are within their proprietary maximum corrosion limit (Reference 4).

(F) ROD BOWING

Bases/Criteria - Fuel and burnable poison rod bowing are phenomena that alter the design-pitch dimensions between adjacent rods. Bowing affects local nuclear power peaking and the local heat transfer to the coolant. Rather than place design limits on the amount of bowing that is permitted, the effects of bowing are included in the departure from nucleate boiling (DNB) analysis by a DNB ratio (DNBR) penalty when rod bow is greater than a predetermined amount. This FCF approach is consistent with the Section 4.2 of the SRP and is acceptable up to the burnup limits established in Reference 4.

Evaluation - Rod bowing has been found to be dependent on the distance between grid spacers, the rod moment of inertia flux distribution and material characteristics of the cladding. FCF has presented rod bowing data up to assembly average burnups of 58.3 GWd/MTU that shows that rod bowing saturates above 30 GWd/MTU and does not increase between 30 to 58.3 GWd/MTU. FCF has proposed an "observed limit" on rod bowing that bounds all of their data for use in their DNB analyses at rod-average burnups above 29 GWd/MTU. This "observed limit" is much greater than the 95% tolerance limit curve for their current data and, therefore, is conservative. FCF has further stated that the local power peaking uncertainties, used to accommodate rod bow effects, equal or bound the "observed limit" for assembly-average burnups greater than 29 GWd/MTU. PNNL concludes that this approach is conservative and, therefore, acceptable up to the burnup limits established in Reference 4.

(G) AXIAL GROWTH

Bases/Criteria - The FCF design basis for axial growth is that adequate clearance be maintained between the rod ends and the top and bottom nozzles to accommodate the differences in the growth of fuel rods and the growth of the fuel assembly. Similarly, for assembly growth, FCF has a design basis that axial clearance between core plates and the bottom and top assembly nozzles should allow sufficient margin for fuel assembly irradiation growth during the assembly lifetime to prevent the holddown spring in the assembly upper end fitting from going solid at cold shutdown. These criteria are consistent with Section 4.2 of the SRP and are acceptable up to rod-average burnup limits identified in Reference 4.

Evaluation - FCF provides an initial fuel rod-to-nozzle growth gap in their fuel assembly designs to allow for differential irradiation growth and thermal expansion between the fuel rod cladding and the fuel assembly guide thimble tubes. The minimum gap required to allow for the irradiation growth and thermal expansion to preclude interference during operation is based on the assumption of worst case fuel rod (maximum) and fuel assembly growth (minimum) combined with worst case fabrication tolerances. In like manner FCF designs holddown springs for the assembly to have enough travel to prevent the holddown spring from bottoming out on reactor-internals assuming maximum assembly growth and worst case tolerances.

The FCF models used to predict fuel rod and assembly growth are based on axial growth data for the Mark-E fuel design up to near the extended burnup limit requested for this design. FCF utilizes lower and upper bound 95/95 tolerance lines of their axial assembly growth data to predict the rod-to-nozzle gap and the assembly-to-reactor-internals gap to prevent the holddown spring from going solid, respectively. The upper bound 95/95 tolerance line for rod growth is used in the rod-to-nozzle gap analysis. Worst case fabrication dimensions or 95/95 dimensional tolerances (when available) are used in determining minimum gap spacings. PNNL concludes that these analysis methods are conservative and, therefore, are acceptable up to the burnup limits established in Reference 4.

(H) ROD INTERNAL PRESSURE

Bases/Criteria - Rod internal pressure is a driving force for, rather than a direct mechanism of, fuel system damage that could contribute to the loss of dimensional stability and cladding integrity. Section 4.2 of the SRP presents a rod pressure limit of maintaining rod pressures below system pressure that is sufficient to preclude fuel damage. The FCF design basis for the fuel rod internal pressure is that the fuel system will not be damaged due to excessive fuel rod internal pressure and FCF has established the "Fuel Rod Pressure Criterion" (Reference 22) to provide assurance that this design basis is met. The internal pressure of the FCF lead fuel rod in the reactor is limited to a value below that which could cause 1) the diametral gap to increase due to outward cladding creep during steady-state operation, and 2) extensive DNB propagation to occur. This FCF design basis and the associated limits have been found acceptable by the NRC (Reference 22) up to the burnup limits established in Reference 4.

Evaluation - FCF utilizes the TACO3 fuel performance code (Reference 19) for predicting end-of-life (EOL) fuel rod pressures to verify that they do not exceed the FCF "Fuel Rod Pressure Criterion" during normal operation and AOOs. FCF was questioned (Reference 7) on the conservatism in the TACO3 code for predicting fission gas release (FGR) and rod pressures for steady-state and Condition 1 transients at extended burnups. FCF responded (Reference 8) by providing TACO3 predictions of two high burnup (62 GWd/MTU rod-average) fuel rods subjected to power ramps of 12 and 13.4 kW/ft and three high burnup (46 to 69 GWd/MTU) fuel rods operating at low steady state powers. The TACO3 code overpredicted the FGR of all five of these rods. A conservative power history is used by FCF in the EOL rod pressure analysis that includes several Condition 1 transients that bound any normal operation and AOOs. This application of power histories for the EOL rod pressure analysis were previously reviewed and approved (Reference 5) and are considered to be applicable to the burnups established in Reference 4. However, FCF has requested that a new power uncertainty factor derived from their newly approved neutronics methods based on the NEMO neutronics code (Reference 3) also be applied to their thermal-mechanical analyses including the EOL rod pressure analysis. PNNL concludes that the TACO3 analysis methods including the new power uncertainty factor from Reference 3 are applicable up to the burnup limits established in Reference 4.

(I) ASSEMBLY LIFTOFF

Bases/Criteria - The SRP calls for the fuel assembly hold-down capability (wet weight and spring forces) to exceed worst-case hydraulic loads for normal operation, which includes AOOs. The FCF assembly holddown criteria is "the holddown spring shall be capable of maintaining fuel assembly contact with the lower support plate during Condition I and II events." PNNL concludes that this is consistent with the SRP guidelines and, therefore, is acceptable up to the burnups established in Reference 4.

Evaluation - The fuel assembly liftoff forces are a function of primary coolant flow, holddown spring forces, and assembly dimensional changes. Extended burnup operation will result in additional irradiation relaxation of holddown springs and increase the fuel assembly length [assembly length changes are discussed in Section 3.0(G)]. These two phenomena have opposing effects on assembly holddown forces. For extended burnup operation the primary concern is that the holddown spring will go solid or increase spring forces to the point that fuel assembly bowing will occur and limit control rod insertion. Therefore, PNNL concludes that assembly liftoff is not a problem for FCF designs up to the burnup limits established in Reference 4.

4.0 FUEL ROD FAILURE

In the following paragraphs, fuel rod failure thresholds and analysis methods for the failure mechanisms listed in the SRP will be reviewed. When the failure thresholds are applied for normal operation including AOOs, they are used as limits (and hence SAFDLs) since fuel failure under those conditions should not occur according to the traditional conservative interpretation of the GDC 10. When these thresholds are used for postulated accidents, fuel failures are permitted, but they must be accounted for in the dose assessments required by 10 CFR 100. The basis or reason for establishing these failure thresholds is thus established by GDC 10 and Part 100 and only the threshold values and the analysis methods used to assure that they are met are reviewed below.

(A) HYDRIDING

Bases/Criteria - Internal hydriding as a cladding failure mechanism is precluded by controlling the level of hydrogen impurities in the fuel during fabrication; this is generally an early-in-life failure mechanism. FCF has not discussed their criteria for internal hydriding in the subject topical report; however, a limit on hydrogen level for FCF pellets is discussed in Reference 5. The hydrogen level of FCF fuel pellets is controlled by drying the pellets in the cladding and taking a statistical sample to ensure that the hydrogen level is below a specified level. Previous FCF design reviews, e.g., Reference 5, have shown that this level is below the value recommended in the SRP. Consequently, PNNL concludes that the FCF limit on hydrogen in their fuel pellets is acceptable.

External hydriding of the cladding due to waterside corrosion is the other source and is discussed in Section 3.0(E) of this TER. As noted in this section the level of external hydriding is controlled by FCF by a proprietary limit on corrosion thickness. PNNL concludes that this corrosion limit is acceptable for limiting the level of external hydriding in the cladding up to the burnup limits established in Reference 4.

Evaluation - Internal hydriding is controlled by FCF by taking statistical samples following pellet fabrication prior to loading the pellets in the fuel rods and confirming that hydrogen is below a specified level. Therefore, no analyses are necessary other than to confirm that the statistical pellet sampling is below the specified level.

External hydriding is controlled by the FCF limit on corrosion thickness discussed in Section 3.0 (E) of this TER.

PNNL concludes that FCF has addressed the issue of hydriding up to the burnup limits established.

(B) CLADDING COLLAPSE

Bases/Criteria - If axial gaps in the fuel pellet column were to occur due to fuel densification, the potential would exist for the cladding to collapse into a gap (i.e., flattening). Because of the large local strains that would result from collapse, the cladding is then assumed to fail. It is a FCF design criteria that cladding collapse is precluded during the fuel rod design lifetime. This design basis is the same as that in the SRP and, thus, is acceptable up to the burnup limits established in Reference 4.

Evaluation - The FCF analytical models for evaluating cladding creep collapse are the CROV and TACO3 computer codes that have been reviewed and approved by NRC (References 23 and 19). The application of these codes to calculating creep collapse are discussed in Reference 23. PNNL concludes that the application of these codes and methods are conservative for evaluating cladding creep collapse and, therefore, are acceptable up to the burnup limits established in Reference 4.

(C) OVERHEATING OF CLADDING

Bases/Criteria - The FCF design criteria for the prevention of fuel failures due to overheating is that there will be at least 95% probability, at a 95% confidence level, that DNB will not occur on a fuel rod during normal operation and AOOs. This design limit is consistent with the thermal margin criterion of the SRP guidelines and, therefore, is acceptable.

Evaluation - As stated in the SRP, Section 4.2, adequate cooling is assumed to exist when the thermal margin criterion to limit DNB or boiling transition in the core is satisfied. The principle physical phenomenon that is both burnup dependent and impacts DNB is fuel rod bowing and

this is addressed in Section 3.0(F) of this report. This section demonstrates that rod bowing saturates at a burnup of 30 GWd/MTU and, therefore, DNB is not impacted up to the burnup levels established in Reference 4. PNNL concludes that FCF has addressed the issue of DNB.

(D) OVERHEATING OF FUEL PELLETS

Bases/Criteria - To preclude overheating of fuel pellets, FCF has indicated that no fuel centerline melting is allowed for normal operation and AOOs. This design limit is the same as given in Section 4.2 of the SRP and, therefore, is acceptable.

Evaluation - FCF was questioned about the recently observed reduction in fuel thermal conductivity reduction at extended burnups and its impact on TACO3 calculated fuel temperatures in relation to their fuel melt temperature analyses (Reference 7). FCF responded (Reference 8) that they evaluated the impact of the decrease in fuel thermal conductivity in TACO3 calculations based on both currently published information on the thermal conductivity decrease and previous TACO3 comparisons to fuel centerline temperature data up to a rod-average burnup of 40 GWd/MTU (Reference 19). FCF concluded that the TACO3 code provided a satisfactory prediction of fuel centerline temperature up to the burnup level that they had data (40 GWd/MTU rod-average), but because they had no data above this burnup level they would apply a penalty factor as a function of burnup above 40 GWd/MTU on TACO3 calculated fuel centerline temperatures for their fuel melting analyses. PNNL has evaluated FCF's methodology for developing and applying their penalty factor to TACO3 calculated fuel centerline temperatures for their fuel melting analyses. PNNL agrees that TACO3 provides an adequate prediction of fuel centerline temperature up to a rod-average burnup of 40 GWd/MTU and also finds that the penalty factor is satisfactory based on fuel thermal conductivity data available at this time.

Therefore, PNNL concludes that the new FCF penalty factor for fuel melting analyses, that accounts for the reduction in fuel thermal conductivity with burnup, is acceptable up to the burnup limits established in Reference 4.

(E) PELLETT-CLADDING INTERACTION

Bases/Criteria - As indicated in Section 4.2 of the SRP, there are no generally applicable criteria for PCI failure. However, two acceptable criteria of limited application are presented in the SRP for PCI: 1) less than 1% transient-induced cladding strain, and 2) no centerline fuel melting. Both of these limits are used by FCF as discussed in Sections 3.0(B) and 4.0(D) of this report and, therefore, have been addressed by FCF.

Evaluation - As noted earlier, FCF utilizes the TACO-3 (Reference 19) code to show that their fuel meets both the cladding strain and fuel melting criteria. This code is acceptable per the recommendations in Sections 3.0(B) and 4.0(D).

(F) CLADDING RUPTURE

Bases/Criteria - There are no specific design limits associated with cladding rupture other than the 10 CFR 50 Appendix K (Reference 24) requirement that the incidence of rupture not be underestimated. A cladding rupture temperature correlation must be used in the loss-of-coolant accident (LOCA) emergency core cooling system (ECCS) analysis. FCF uses a rupture temperature correlation consistent with NUREG-0630 guidance (Reference 25). PNNL therefore concludes that FCF has adequately addressed the criteria for cladding rupture.

Evaluation - FCF has adopted the cladding deformation and rupture models from NUREG-0630 guidance (Reference 25) which has been approved by the NRC for ECCS evaluation. The increase in fuel rod pressures with increasing burnup can impact cladding deformation and rupture. As noted in Sections 3.0(H) and 5.0(A) of this report, FCF uses the TACO3 fuel performance code to provide initial rod pressures and stored energy for the LOCA analysis and the code application of this code is found to be satisfactory for these applications up to the burnup levels established in Reference 4. PNNL concludes that FCF has adequately addressed the issue of cladding rupture.

(G) FUEL ROD MECHANICAL FRACTURING

Bases/Criteria - The term "mechanical fracture" refers to a fuel rod defect that is caused by an externally applied force such as a hydraulic load or a load derived from core-plate motion. The design limit proposed by FCF to prevent fracturing is that the stresses due to postulated accidents in combination with the normal steady-state fuel rod stresses should not exceed the yield strength of the components in their fuel assemblies. This design limit for fuel rod mechanical fracturing is consistent with the SRP guidelines, and, therefore, is acceptable.

Evaluation - The mechanical fracturing analysis is done as a part of the seismic-and-LOCA loading analysis. A discussion of the seismic-and-LOCA loading analysis is given in Section 5.0(D) of this TER.

5.0 FUEL COOLABILITY

For postulated accidents in which severe fuel damage might occur, core coolability must be maintained as required by several GDCs (e.g., GDC 27 and 35). In the following paragraphs, limits and methods to assure that coolability is maintained are discussed for the severe damage mechanisms listed in the SRP.

(A) FRAGMENTATION OF EMBRITTLED CLADDING

Bases/Criteria - The most severe occurrence of cladding oxidation and possible fragmentation during a postulated accident is the result of a LOCA. In order to reduce the effects of cladding oxidation during a LOCA, FCF uses a limiting criterion of 2200°F on peak cladding temperature

(PCT) and a limit of 17% on maximum cladding oxidation as prescribed by 10 CFR 50.46. These criteria are consistent with SRP criteria and, thus, are acceptable.

Evaluation - FCF has stated that they will only use NRC reviewed and approved LOCA models for evaluating the above criteria. However, the initial fuel stored energy can impact the cladding embrittlement. FCF uses the TACO3 code to calculate initial stored energy for input to the LOCA analyses. FCF was questioned (Reference 7) about the impact on the calculated stored energy for LOCA due to the observed decrease in fuel thermal conductivity and the shift in radial power distributions at extended burnups because the TACO3 code does not accurately model these effects. FCF responded (Reference 8) that they have evaluated the impact of these effects on stored energy at extended burnup and propose to apply a penalty factor that increases their multiplicative uncertainty factors for TACO3 calculated stored energy to account for these effects. FCF further responded that the additional uncertainty factors would only be applied at burnups greater than 40 GWd/MTU (rod-average) because the TACO3 code has conservatism built in that compensate for these effects below 40 GWd/MTU. This is demonstrated by the fact that the TACO3 code predictions and uncertainties have been shown to be satisfactory by comparison to fuel temperature data up to 40 GWd/MTU (rod-average). PNNL concurs with FCF that the conservatism in TACO3 account for the effects of the thermal conductivity degradation and change in radial power distribution because the effects are small below 40 GWd/MTU. PNNL also concurs that the FCF proposed additional uncertainty factors on stored energy above 40 GWd/MTU (rod-average) are satisfactory based on the thermal conductivity data available at this time.

FCF has indicated that the LOCA analyses ^{will continue to CDH} ~~will continue to~~ be limiting at beginning-of-life even with the use of these penalty factors above burnups of 40 GWd/MTU up to currently approved burnup levels. PNNL concludes that FCF has adequately addressed the impact of extended burnup on stored energy and LOCA up to the ~~burnup~~ ^{burnup CDH} levels established in Reference 4.

(B) VIOLENT EXPULSION OF FUEL

Bases/Criteria - In a severe reactivity insertion accident (RIA), such as a control rod ejection accident, large and rapid deposition of energy in the fuel could result in melting, fragmentation, and dispersal of fuel. The mechanical action associated with fuel dispersal might be sufficient to destroy the fuel cladding and rod bundle geometry and to provide significant pressure pulses in the primary system. To limit the effects of an RIA event, Regulatory Guide 1.77 (Reference 26) recommends that the radially-averaged energy deposition at the hottest axial location be restricted to less than 280 cal/g. In addition, the fuel failure limit is the onset of DNB for the close consequences of an RIA. The limiting RIA event for FCF fuel designs is a control rod ejection accident.

The FCF safety criteria for the control rod ejection accident is: the radial average peak fuel enthalpy for the hottest fuel rod shall not exceed

280 cal/g. This is identical to the guidance in Section 4.2 of the SRP and Regulatory Guide 1.77 (References 11 and 26). It is noted that the NRC staff are currently reviewing the 280 cal/gm limit and the limit for fuel failure may be decreased to a lower limit at high burnup levels. Recent RIA testing has indicated the fuel expulsion and fuel failure may occur before the 280 cal/gm limit and the onset of DNB, respectively (References 27 and 28). However, further testing and evaluation is needed to establish limits. The fuel expulsion and failure limits for an RIA may decrease in the future but the current limits remain valid at this time.

Evaluation - FCF verifies that this acceptance criterion is met for each fuel cycle through design and cycle specific analyses and by limiting the ejected rod worth. The industry and NRC have both done preliminary evaluations of the worst impact of both a lower enthalpy limit for fuel expulsion and lower failure limit at current burnup limits are acceptable. The very conservative analyses indicate that maximum enthalpies for high burnup rods are at least a factor of three lower than the current limit and violent expulsion is unlikely. The dose consequences are within those specified in 10 CFR 100. FCF uses NRC-approved methods to perform these analyses and the methods remain valid at this time up to the burnups established in Reference 4. PNNL concludes that FCF has adequately addressed this issue.

(C) CLADDING BALLOONING

Bases/Criteria - Zircaloy cladding will balloon (swell) under certain combinations of temperature, heating rate, and stress during a LOCA. There are no specific design limits associated with cladding ballooning other than the 10 CFR 50 Appendix K requirement that the degree of swelling not be underestimated. To meet the requirement of 10 CFR 50 Appendix K, the burst strain and the flow blockage resulting from cladding ballooning must be taken into account in the overall LOCA analysis. FCF has stated that they utilize the approved burst strain and flow blockage models developed from NUREG-0630 (Reference 25). It is noted that NRC is currently looking at the impact of the reduction in cladding ductility at extended burnups on cladding ballooning and rupture during LOCAs. However, the NUREG-0630 models remain applicable and valid at this time up to the burnup limits established in Reference 4.

Evaluation - FCF has adopted the cladding rupture and ballooning models from NUREG-0630 (Reference 25) as recommended by Section 4.2 of the SRP and these models have been previously approved by the NRC. Therefore, PNNL concludes that FCF has addressed the issue of cladding ballooning.

(D) FUEL ASSEMBLY STRUCTURAL DAMAGE FROM EXTERNAL FORCES

Bases/Criteria - Earthquakes and postulated pipe breaks in the reactor coolant system would result in external forces on the fuel assembly. Appendix A to SRP Section 4.2 states that the fuel system coolable geometry shall be maintained and damage should not be so severe as to prevent control rod insertion during seismic and LOCA events. FCF has adopted the SRP guidelines as

their design criteria. PNNL concludes that the FCF design criteria for seismic and LOCA loads are acceptable.

Evaluation - FCF stated that they have used NRC-approved methodologies provided in Reference 27 for evaluating seismic and LOCA loads. Extending fuel rod burnup levels could result in adverse effect on fuel assemblies due to seismic and LOCA events. FCF responded that the following parameters could impact seismic/LOCA events: spacer grid spring relaxation [see Section 3.0(D)], holddown spring relaxation, and reduction in the rod-to-nozzle and assembly-to-reactor-internals gaps [see Sections 3.0(G) and 3.0(I)], and changes in Zircaloy material properties [see Sections 3.0(A) and 3.0(B)]. FCF claims (Reference 1) that the relaxation of the spacer grid springs only decrease the natural frequencies of the assembly slightly based on post-irradiation-examination (PIE) data, and this small decrease has an insignificant effect on the spacer grid impact loads based on analysis studies. The reduction in the rod-to-nozzle and assembly-to-reactor-internals gaps are incorporated into the FCF dynamic response analysis for seismic/LOCA loads and the holddown spring relaxation has little effect because the spring rate is not affected (Reference 1). The change in material properties are primarily the increase in yield and ultimate tensile strength and the decrease in Zircaloy ductility. The increase in material strength results in greater assembly strength that is not accounted for by FCF for this analysis and, therefore, is conservative and acceptable. The reduction in Zircaloy ductility is controlled by the limit on corrosion discussed in Section 3.0(E) of this TER and, therefore, is acceptable. PNNL concurs that the extended burnup levels established in this TER will have an insignificant effect on seismic/LOCA loads. PNNL concludes that FCF has adequately addressed the issue of assembly loads due to seismic/LOCA.

6.0 FUEL SURVEILLANCE

FCF was questioned about what future fuel surveillance would be performed to justify operation for each of their fuel designs for future burnup extensions. FCF responded (Reference 4) that their lead assembly programs generally consist of four to eight fuel assemblies with varying levels of extended burnup operation. Each lead assembly will be subjected to PIE that varies depending on utility support but generally consists of fuel rod oxide and diameter, fuel rod and assembly bow, and assembly holddown spring height measurements. The guide tube and overall assembly condition are also visually examined. FCF further stated that the appropriate data would be submitted to NRC for review and approval prior to any extensions in burnup beyond the limits approved in this TER.

PNNL notes that the NRC may also request data on control rod drop times or drag tests for assembly burnups beyond current FCF burnup limits. In addition, the NRC may want to see rod drop test or drag test data for new fuel designs. This is because of the decrease in control rod drop times recently observed in some Westinghouse fuel designs/plants that have achieved high burnups. PNNL concludes that FCF has addressed the issue of fuel surveillance.

7.0 CONCLUSIONS

PNNL has reviewed the extended burnup request submitted in BAW-10186P and the responses to requests for additional information (RAIs) in accordance with the SRP, Section 4.2. PNNL concludes that topical report BAW-10186P is acceptable for licensing application for FCF Mark B, BW15 and BW17 designs up to the burnup levels of 62 GWd/MTU for the former and 60 GWd/MTU for the latter two designs. This approval does not include extended burnup operation of the FCF Mark-C fuel designs. In addition, FCF's request to apply the NEMO calculational uncertainty for use in TACO3 licensing analysis is also acceptable.

8.0 REFERENCES

1. Babcock and Wilcox Fuel Company. November 1992. Extended Burnup Evaluation. BAW-10186P, Babcock and Wilcox Fuel Company, Lynchburg, Virginia, transmitted by letter, J. H. Taylor (BWFC) to U.S. NRC Document Control Desk, "Submittal of Topical Report BAW-10186P," dated November 24, 1992.
2. Letter, J. H. Taylor (B&W Nuclear Technologies) to R. C. Jones (NRC), dated July 19, 1995.
3. Babcock and Wilcox Fuel Company. March 1993. NEMO - Nodal Expansion Method Optimized. BAW-10180P-A. Rev. 1, Babcock and Wilcox Fuel Company, Lynchburg, Virginia.
4. Letter from J. H. Taylor (Framatome Cogema Fuels) to NRC Document Control Desk, "Application of BAW-10186P" JHT/97-7, dated January 23, 1997.
5. Babcock and Wilcox. April 1986. Extended Burnup Evaluation. BAW-10153P-A, Babcock and Wilcox, Lynchburg, Virginia.
6. Babcock and Wilcox Fuel Company. June 1988. Mark-BW Mechanical Design Report. BAW-10172P, Babcock and Wilcox Fuel Company, Lynchburg, Virginia.
7. Letter, Edward Kendrick (NRC) to J. H. Taylor (B&W Nuclear Technologies), "Request for Additional Information on Report BAW-10186-P, dated June 28, 1995.
8. Letter, J. H. Taylor (B&W Nuclear Technologies) to R. C. Jones (NRC), JHT/95-88, dated August 22, 1995.
9. Letter, from J. H. Taylor (B&W Nuclear Technologies) to R. C. Jones (NRC), JHT/95-119, dated December 6, 1995.

10. Letter, from J. H. Taylor (Framatome Cogema Fuels) to R. C. Jones (NRC), JHT/96-042, dated June 26, 1996.
11. U.S. Nuclear Regulatory Commission. July 1981. "Section 4.2, Fuel System Design." In Standard Review Plan for the Review of Safety Analysis Reports for Nuclear Power Plants--LWR Edition. NUREG-0800, Revision 2, U.S. Nuclear Regulatory Commission, Washington, D.C.
12. United States Federal Register. "Appendix A, General Design Criteria for Nuclear Power Plants." 10 Code of Federal Regulations (CFR), Part 50. U.S. Printing Office, Washington, D.C.
13. United States Federal Register. "Reactor Site Criteria." 10 Code of Federal Regulations (CFR), Part 100. U.S. Printing Office, Washington, D.C.
14. United States Federal Register. 10 Code of Federal Regulations (CFR), Part 50.46. U.S. Printing Office, Washington, D.C.
15. American Society of Mechanical Engineers. 1983 Edition. "Section III, Nuclear Power Plant Components." ASME Code. American Society of Mechanical Engineers, New York.
16. Smith, Jr. G. P., R. C. Pirek and M. Griffiths. July 1994. *Hot Cell Examination of Extended Burnup Fuel from Calvert Cliffs-1*. EPRI TR-103302-V2, Final Report, Electric Power Research Institute, Palo Alto, California.
17. Newman, L. W. et al. 1986. *The Hot Cell Examination of Oconee Fuel Rods After Five Cycles of Irradiation*. DOE/ET/34212-50 (E-W-1874), Babcock & Wilcox, Lynchburg, Virginia.
18. Garde, A. M. 1989. "Effects of Irradiation and Hydrating on the Mechanical Properties of Zircaloy-4 at High Fluence." In *Zirconium in the Nuclear Industry: Eighth International Symposium*, ASTM STP 1023, pp. 548-569, Eds. L.F.P. VanSwam and C. M. Eucken. American Society for Testing and Materials, Philadelphia, Pennsylvania.
19. Wesley, D. A., and K. J. Firth. October 1989. TACO-3 Fuel Pin Thermal Analysis Code. BAW-10162P-A, Babcock & Wilcox, Lynchburg, Virginia.
20. O'Donnell, W. J., and B. F. Langer. 1964. "Fatigue Design Basis for Zircaloy Components." In Nuc. Sci. Eng. 20:1.

21. Lanning, D. D., C. E. Beyer, and C. L. Painter. March 1996. "New High Burnup Fuel Models for NRC's Licensing Code, FRAPCON." Proceedings of the U.S. Nuclear Regulatory Commission 23rd Water Reactor Safety Information Meeting, NUREG/CP-0249, Vol. 1, p. 141, Office of Nuclear Regulatory Research, U.S. NRC, Washington D.C.
22. D. A. Wesley, D. A. Farnsworth and G.A. Meyer, July 1995. Fuel Rod Gas Pressure Criterion (FRGPC), BAW-10183P-A.
23. Miles, T., et. al., August 1995. Program to Determine In-Reactor Performance of B&W Fuel Cladding Creep Collapse, BAW-10084P-A Rev.3, B&W Fuel Company, Lynchburg, Virginia.
24. United States Federal Register. "Appendix K, ECCS Evaluation Models." 10 Code of Federal Regulations (CFR), Part 50. U.S. Printing Office, Washington, D.C.
25. Powers, D. A., and R. O. Meyer. 1980. Cladding Swelling and Rupture Models for LOCA Analysis. NUREG-0630, U.S. Nuclear Regulatory Commission, Washington, D.C.
26. U.S. Nuclear Regulatory Commission. 1974. Assumptions Used for Evaluating a Control Rod Ejection Accident for Pressurized Water Reactors, Regulatory Guide 1.77, U.S. Nuclear Regulatory Commission, Washington D.C.
27. Schmitz, F., et. al., March 1996. "New Results from Pulse Test in the CABRI Reactor," Proceedings of the 23rd Water Reactor Safety Information Meeting October 23-25, 1995.
28. Fuketa, T., et. al., March 1996. "New Results from the NSRR Experiments with High Burnup Fuel," Proceedings of the 23rd Water Reactor Safety Meeting, October 23-25, 1995.
29. Babcock and Wilcox. May 1979. Analytical Methods Description - Reactor Coolant System Hydrodynamic Loadings During a Loss-of-Coolant-Accident - Supplement 1, BAW-10132P-A Supp.1, Babcock and Wilcox, Lynchburg, Virginia.

ABSTRACT

This document serves to revise the report BAW-10153P-A⁽¹⁾ EXTENDED BURNUP EVALUATION. In that baseline document, information was presented that supported the operation and licensing of PWR fuel assemblies designed and manufactured by B&W (now FCF) up to batch average burnups of [c,d,e] MWd/mtU recognizing that higher values could be sought contingent on feed-back from demonstration and test assembly programs. The document also concluded that there was no inherent limitation to licensing B&W designed fuel to assembly burnups of [c,d,e] MWd/mtU. The document was approved by the NRC in December 1985.⁽²⁾ Subsequent to the approval, BAW-10172P⁽³⁾ was submitted to justify the operation of Mark-BW fuel in Westinghouse reactors to assembly average burnups of [c,d,e] MWd/mtU. Approval was received for this second document in December 1989.⁽⁴⁾

Since these approvals, improvements and refinements in the FCF codes and in the materials and designs employed, together with data from Lead Test Assemblies at extended burnups, have reinforced the earlier belief that fuel assemblies can operate safely and satisfactorily to higher burnups. To date, the FCF design methodology, materials specifications, and analytical techniques have been applied to four general types of fuel assembly. In all cases, assemblies can be designed that are capable of operating to high burnups. The burnups targeted by these designs are [c,d,e] MWd/mtU maximum for fuel assemblies and [c,d,e] MWd/mtU maximum for fuel rods. This document presents a summary of data, methods and analysis that support operation of FCF fuel at these burnups. In some cases, the analyses presented in BAW-10153P-A are applicable to the higher burnup limits and are either referenced or repeated from the original text.

TABLE OF CONTENTS

| | | |
|---------|---|----|
| 1.0 | Introduction | 7 |
| 2.0 | Fuel Assembly Performance and Extended Burnup | 11 |
| 2.1 | Introduction | 11 |
| 2.2 | Fuel Assembly Design Factors..... | 13 |
| 2.2.1 | Fuel Rod and Fuel Assembly Growth..... | 13 |
| 2.2.2 | Spacer Grid Relaxation and Fuel Rod Fretting | 14 |
| 2.2.3 | Fuel Assembly Skeleton Structure Oxidation | 15 |
| 2.2.4 | Guide Tube Wear..... | 17 |
| 2.2.5 | Spacer Grid Irradiation Growth | 18 |
| 2.2.6 | Structural Analysis | 19 |
| 2.2.7 | Conclusion | 25 |
| 2.3 | Fuel Rod Design Factors | 25 |
| 2.3.1 | Fuel Rod Cladding | 25 |
| 2.3.1.1 | Stress Analysis | 26 |
| 2.3.1.2 | Strain Analysis | 26 |
| 2.3.1.3 | Fatigue..... | 27 |
| 2.3.2 | Oxidation, Corrosion, and Crud..... | 27 |
| 2.3.3 | Cladding Hydriding and Ductility | 31 |
| 2.3.4 | Creep Collapse | 32 |
| 2.3.5 | Fuel Rod Bowing..... | 33 |
| 2.3.5.1 | Thermal-Hydraulic Evaluation | 33 |
| 2.3.5.2 | Local Power Changes Due to Rod Bowing | 35 |
| 2.3.5.3 | Mechanical Evaluation | 36 |
| 2.3.6 | Pellet Cladding Interaction | 36 |
| 2.3.7 | Defects..... | 37 |
| 2.3.8 | DNBR 39 | |

| | | |
|------------|---|-----|
| 2.4 | Fuel Pellet Factors | 39 |
| 2.4.1 | Densification and Swelling | 40 |
| 2.4.2 | Gap Closure | 41 |
| 2.4.3 | Gap Conductance | 42 |
| 2.4.4 | Fission Gas Release | 44 |
| 2.4.5 | Fuel Rod Internal Pressure | 46 |
| 2.4.6 | Stored Energy | 47 |
| 2.4.7 | Fuel Melt | 49 |
| 2.4.8 | Fuel Thermal Conductivity | 49 |
| 2.5 | Neutronics | 50 |
| 2.6 | Materials Qualification | 51 |
| 3.0 | Fuel Assembly Burnup Capabilities | 64 |
| 3.1 | Introduction | 64 |
| 3.2 | Fuel System Evaluation Summary | 64 |
| 3.3 | Neutronic Evaluation Summary | 65 |
| 4.0 | Safety Aspects of Extended Burnup | 65 |
| 4.1 | Introduction | 65 |
| 4.2 | Radiological Evaluation | 66 |
| 4.3 | ECCS Evaluation | 66 |
| 4.4 | Decay Heat | 67 |
| 4.5 | Seismic and LOCA Evaluation | 68 |
| 5.0 | Conclusion | 69 |
| 6.0 | References | 71 |
| Appendix A | | A-1 |
| Appendix B | | B-1 |
| Appendix C | | C-1 |
| Appendix D | | D-1 |
| Appendix E | | E-1 |

LIST OF FIGURES

| | | |
|---------|---|----|
| 2.2.1-1 | Fuel Rod Growth..... | 53 |
| 2.2.1-2 | Fuel Assembly Growth for RXA Guide Tubes..... | 54 |
| 2.3.1-1 | LHR vs Burnup Limits for CFM and 1% Strain | 55 |
| 2.3.2-1 | Oxide Thickness Comparison..... | 56 |
| 2.3.3-1 | Axial Variation of Hydrogen in Cladding | 57 |
| 2.3.3-2 | Average % Total Ductility vs Burnup..... | 58 |
| 2.3.3-3 | Average Uniform Ductility (Axial & Ring) vs Burnup | 59 |
| 2.3.3-4 | Tensile Strength (Axial & Ring) vs Burnup..... | 60 |
| 2.3.3-5 | Yield Strength (2% Offset) vs Burnup..... | 61 |
| 2.3.5-1 | Rod Bow Data for Mark-B, Mark-C, and Mark-BW Fuel Designs..... | 62 |
| 2.3.5-2 | Worst Span Water Channel Closure vs Burnup | 63 |

LIST OF TABLES

| | | |
|---------|--|----|
| 1-1 | FCF Design Approvals and Requests | 8 |
| 1-2 | Typical FCF Assembly Parameters (FCF Reactor System)..... | 9 |
| | Typical FCF Assembly Parameters (Westinghouse Reactor System) | 10 |
| 2.1-1 | Major High-Burnup Fuel Performance Programs. | 12 |
| 2.2.6-1 | Limiting Load Conditions for Mark-B Fuel Assembly Components For Normal Operation | 21 |
| 2.2.6-2 | Limiting Load Conditions for Mark-B Fuel Assembly Components For OBE and Combined SSE plus LOCA..... | 22 |
| 2.2.6-3 | Limiting Load Conditions for Mark-BW Fuel Assembly Components for Normal Operation..... | 23 |
| 2.2.6-4 | Limiting Load Conditions for Mark-BW Fuel Assembly Components for SSE and combined SSE plus LOCA Conditions | 24 |
| 2.3.7-1 | Average Steady State Coolant Iodine Activity for B&W Designed Plants. | 39 |

1.0 INTRODUCTION

In this report, operation of FCF (previously BWFC) designed fuel at extended burnups is evaluated against the phenomena, performance factors, and the fuel system considerations provided in Regulatory Guide 1.70 and NUREG 0800.⁽⁵⁾ The report serves to revise and update an earlier report, BAW-10153P-A EXTENDED BURNUP EVALUATION, although other later reports also addressed specific aspects of extended burnup operation. The base extended burnup topical report BAW-10153P-A addressed the high burnup effects for one generic fuel design, the Mark-B. With the approval of that report, Mark-B fuel was justified to operate to batch average burnups of [c,d,e] MWd/mtU (see Table 1-1). Since that time, improved evaluation methods combined with data obtained from post irradiation examinations after extended exposures have enabled FCF to design for higher burnups. In addition to the original Mark-B design, this capability is also applicable to three other FCF fuel designs. Two of the (four) designs are for B&W-type reactors, the Mark-B (15x15)^(6,7) and the Mark-C (17x17)⁽⁸⁾. The other two designs are for Westinghouse-type reactor reloads. These latter are the Mark-BW15 (15x15)⁽⁹⁾ and the Mark-BW17 (17x17)⁽³⁾, approved for rod burnups of [c,d,e] MWd/mtU.

The utilities that are purchasing fuel assemblies for the above reactor systems are now designing fuel cycles for future use that will require burnups beyond the currently approved levels. Some of these fuel cycles will require assembly burnups of [b,c,d,e] MWd/mtU and associated fuel rod burnups of [c,d,e] MWd/mtU. This document provides the justification for such burnups.

Table 1-2 lists various parameters and values for the four FCF fuel designs discussed above. The values are representative of the general designs with certain dimensions, such as those for guide tube and fuel rod lengths, being changed slightly, but within acceptable code predictions as fuel designs are optimized for new materials and higher burnups.

Section 2 discusses factors that affect fuel assembly performance and burnup capability. Predicted and actual results are compared. In Section 3, the burnup capabilities of the fuel designs are summarized. Safety aspects of extended burnup are discussed in Section 4. The report conclusion and references are provided in Sections 5 and 6, respectively.

Table 1-1. FCF Design Approvals and Requests

| | Currently Approved Burnups | | Requested Allowable Burnup |
|------------------------------|-----------------------------|---------------------------|----------------------------|
| Reference | BAW-10153P-A ⁽¹⁾ | BAW-10172P ⁽³⁾ | BAW-10186P (This Report) |
| Fuel Type | Mark B | Mark BW | All |
| Batch Average Burnup MWd/mtU | [b,c,d,e] | | |
| Fuel Assembly Burnup MWd/mtU | | | |
| Fuel Rod Burnup MWd/mtU | | | |

- * Burnup Requested and Approved
- ** Burnup Considered Feasible with Design

**Table 1-2. Typical FCF Fuel Assembly Parameters†
(B&W Reactor Systems)**

| Assembly Designation | Mark-B | Mark-C |
|--|---|--|
| Fuel Rod Array | 15x15 | 17x17 |
| Holddown Spring | Helical Coil Spring/ Multiple Leaf Option | Helical Coil Spring/ Multiple Leaf Option |
| Cladding Material | Zircaloy-4 | Zircaloy-4 |
| Guide Tube Material | Zircaloy-4 | Zircaloy-4 |
| Assemblies per Core | 177 | 205 |
| Fuel Rods per Assembly | 208 | 264 |
| Control Rod/Guide Tube/Instrument Tube Locations per Assembly | 17 | 25 |
| Debris Protection Feature | | |
| Rod Pitch, mm (inch) | [b,c,d,e] | |
| Fuel Rod Length, cm (inch) | | |
| Active Fuel Height, cm (inch) | 360.2 (141.8) | 363.2 (143.0) |
| Plenum Length, cm (inch) | | |
| Fuel Rod O.D., mm (inch) | | |
| Cladding I.D., mm (inch) | | |
| Cladding Thickness, mm (inch) | [b,c,d,e] | |
| Diametrical Gap, microns (mils) | | |
| Fuel Pellet O.D., mm (inch) | | |
| Fuel Pellet Density, % TD | | |
| Average LHGR, W/cm (kW/ft) | 203 (6.20) | 188 (5.73) |
| System Pressure, MPa (psia) | 15.2 (2200) | 15.5 (2250) |
| Core Inlet Temp., °C (°F) | 292.07 (557.7) | 300.0 (572.6) |
| Core Outlet Temp., °C (°F) | 315.7 (600.3) | 331.4 (628.6) |

† Designs, materials and dimensions are representative of those used to date. Alternates may be used if they are demonstrated to meet the burnup requirements.

* Other Options Available

**Table 1-2. Typical FCF Fuel Assembly Parameters†
(Westinghouse Reactor Systems)**

| Assembly Designation | Mark-BW17 | Mark-BW15 |
|---|------------------|------------------|
| Fuel Rod Array | 17x17 | 15x15 |
| Holddown Spring | Leaf Springs | Leaf Springs |
| Cladding Material | Zircaloy-4 | Zircaloy-4 |
| Guide Tube Material | Zircaloy-4 | Zircaloy-4 |
| Assemblies per Core | 193 (157) | 193 (157) |
| Fuel Rods per Assembly | 264 | 204 |
| Control Rod/Guide Tube/Instrument Tube Locations per Assembly | 25 | 21 |
| Debris Protection Feature | [b,c,d,e] | |
| Rod Pitch, mm (inch) | | |
| Fuel Rod Length, cm (inch) | | |
| Active Fuel Height, cm (inch) | | |
| Plenum Length, cm (inch) | | |
| Fuel Rod O.D., mm (inch) | | |
| Cladding I.D., mm (inch) | | |
| Cladding Thickness, mm (inch) | | |
| Diametrical Gap, microns (mils) | | |
| Fuel Pellet O.D., mm (inch) | | |
| Fuel Pellet Density, % TD | | |
| Average LHGR, W/cm (kW/ft) | 178 (5.43) | 184 (5.60) |
| System Pressure, MPa (psia) | 15.5 (2250) | 13.9 (2015) |
| Core Inlet Temp., °C (°F) | 294.2 (561.6) | 271.1 (519.9) |
| Core Outlet Temp., °C (°F) | 326.7 (620) | 304.5 (580.2) |

† Designs, materials and dimensions are representative of those used to date. Alternates may be used if they are demonstrated to meet the burnup requirements.
 * Other Options Available
 ** Design has used both densities.

2.0 FUEL ASSEMBLY PERFORMANCE AND EXTENDED BURNUP

2.1 INTRODUCTION

In this section, extended burnup performance factors and phenomena are discussed and assessed relative to existing information and modeling. This evaluation supports operation of fuel designs to burnups of [c,d,e] MWd/mtU for fuel assemblies and [c,d,e] MWd/mtU for fuel rods.

This evaluation for extended burnup operation uses fuel performance and materials models that are based on extensive operating experience and examination. Through 1991 over 600 fuel assemblies were discharged with burnups greater than 36,000 MWd/mtU. [c,d,e] fuel assemblies have reached burnups greater than [c,d,e] MWd/mtU with a maximum fuel assembly burnup of [c,d,e] MWd/mtU. More than 14 separate fuel performance programs have been conducted with extensive poolside and hot cell examinations as part of that effort. A summary of these major programs is given in Table 2.1-1. The programs provide information on the four FCF fuel designs and provide confidence that the methods described in this report can produce designs that meet all criteria at the burnups requested.

In support of this effort extending fuel burnup, new materials have been developed to improve fuel performance parameters. An example of this are the studies on various low corrosion fuel rod cladding alloys. The analysis and test methods needed to qualify these advanced materials for production use are summarized in section 2.6.

Table 2.1-1
Major High-Burnup Fuel Performance Programs

| <u>PROGRAM</u> | <u>COMPLETED IRRADIATION CYCLES</u> | <u>MAX FA BURNUP GWd/mtU</u> | <u>POST IRRADIATION EXAMINATIONS</u> |
|---------------------------------------|-------------------------------------|------------------------------|--------------------------------------|
| Mark-B | 5 ^(a) | | Poolside & Hotcell |
| Mark-BEB | 4 ^(b) | | Poolside & Hotcell |
| Mark-GdB | 4 ^(c) | | Poolside & Hotcell |
| Mark-BZ | 3 ^(d) | | Poolside |
| Mark-BAB | 3 ^(e) | [b,c,d,e] | Poolside |
| Mark-B, Fuel Failures | 3 ^(f) | | Poolside & Hotcell |
| Mark-C | 3 ^(g) | | Poolside |
| Mark-B, Pathfinder | 3 ^(h) | | Poolside |
| Mark-BW15 Zircaloy LTAs | 3 ⁽ⁱ⁾ | | Poolside |
| Mark-BW17 Advanced Clad | 2 ^(j) | | Poolside |
| Mark-BW17 LAs | 3 ^(k) | | Poolside |
| Mark-BW17 Special Clad ^(l) | | | |

- (a) Base FA design irradiated to high burnup for evaluation and modeling as part of a B&W/DOE/Duke Power joint program.
- (b) LTAs of an advanced, extended-burnup design.
- (c) An extended burnup fuel assembly design with selected rods loaded with Gadolinia ($Gd_2O_3 - UO_2$) fuel pellets as an integral burnable poison.
- (d) LTAs utilizing Zircaloy-4 intermediate spacer grids for low absorption.
- (e) LTAs containing axially-blanketed fuel columns.
- (f) Fuel assemblies examined poolside, and selected fuel rods pulled and examined in a hotcell as part of a joint FCF/EPR/Duke Power fuel failure investigation.
- (g) Mark-C LTAs with 17 x 17 rod array, two of these four LTAs are reconstitutable.
- (h) Pathfinder LTA with advanced Zircaloy-4 cladding materials.
- (i) Four LTAs using Zircaloy-4 clad fuel rods to replace stainless steel clad fuel rod assemblies.
- (j) One Lead Assembly (17x17, Mark-BW17 LA) with [c,d] different advanced cladding alloys within the Zircaloy-4 specification.
- (k) Three Lead Assemblies (17x17, Mark-BW17 LA)
- (l) Two LAs with [c,d,e] advanced cladding alloys, [c,d] are within the zircaloy-4 specification, [c,d] are outside of the specification.

2.2 FUEL ASSEMBLY DESIGN FACTORS

The effects of irradiation on fuel assembly behavior have been identified and evaluated. The evaluations include fuel rod, fuel assembly, and spacer grid growth, holddown spring design, material relaxation, fretting, fuel assembly oxidation effects, and guide tube wear. FCF has accumulated a comprehensive design base including analytical evaluations, evaluations of tests, and operating experience that establishes the relationship between the design factors and burnup. The use of this design base permits the licensing of an extended burnup fuel assembly design capable of safely and reliably obtaining maximum assembly average burnups in excess of [c,d,e] MWd/mtU.

2.2.1 FUEL ROD AND FUEL ASSEMBLY GROWTH

The irradiation and thermal growth of the fuel rod (Figure 2.2.1-1) and fuel assembly (Figure 2.2.1-2) affect guide tube axial loads, holddown spring compression, and relative axial clearances between the fuel rods and the upper end fitting (shoulder gap). Because irradiation growth continues with burnup, the effect has been considered and is addressed in the assembly design using modifications that assure extended burnup capability.

Zircaloy-4 guide tubes are now specified in the fully annealed recrystallized condition (RXA) rather than the cold-worked, stress-relieved (SRA) condition used initially. The RXA (annealed) condition has a lower stress free irradiation growth than that of the SRA material. This lower stress free growth results in a lower growth rate for RXA guide tubes compared to SRA guide tubes. The resulting RXA guide tube growth rate is low enough that the fuel assembly growth through [c,d,e] MWd/mtU can be accommodated by current holddown spring designs. This means that the holddown spring will supply sufficient holddown force at the beginning of life without excessively loading the guide tubes or being compressed solid at maximum discharge burnups. The relative growth data for FCF designed fuel assemblies with RXA guide tubes are shown in Figure 2.2.1-2. The design [b,c,d,e] growth curve for RXA guide tubes is plotted with the data.

The holddown spring system in the fuel assembly upper end fitting provides allowance for irradiation and thermal growth while providing holddown against hydraulic lift forces. FCF has utilized several types of spring designs, including single and multiple helical holddown springs, single and multiple leaf design springs, and a cruciform (leaf) design.⁽⁷⁾ Material for these springs may be Inconel-750 or Inconel-718 with heat treatment to maximize the stress margins throughout life. For extended burnup applications, the fuel assemblies are designed to the criterion that the holddown springs [b,c,d,e]. The holddown spring preload is set so that[b,c,d,e]in accordance with ASME guidelines⁽¹⁰⁾ under the increased number of operational cycles experienced for extended burnup operation.

2.2.2 SPACER GRID RELAXATION AND FUEL ROD FRETTING

The fuel assembly has five or six intermediate spacer grids and two end spacer grids fabricated by welding thin strips in an egg-crate fashion forming the fuel rod cell matrix. These strips are manufactured from Zircaloy-4 or Inconel and are formed with protrusions or "stops" on each side of the cell to grip the fuel rod or guide tube.⁽⁶⁾ These stops control the magnitude of the fuel rod lateral vibration to prevent fretting wear at the interface contact area. Lateral positioning of the spacer grids is maintained by the cell stops in contact with guide tubes or fuel rods on all four sides. Axial positioning is controlled not only through frictional grip forces, but also by sleeves or ferrules on the instrument tube and guide tubes. These sleeves are sized and spaced between grids to prevent gross movement of the spacer grids.

Due to exposure to a fast neutron flux, Zircaloy intermediate spacer grids will undergo growth and stress relaxation effects. The effects of spacer grid growth are reported in section 2.2.5. The effect of stress relaxation is to reduce the grip force on the fuel rod. When a fuel rod is inserted into a spacer grid cell, the spring stop is compressed and a high bending stress develops. The grip force is proportional to the stresses in the spring stop. During irradiation, the creep driven stress relaxation is affected by those same stresses. This means that the reduction in grip force is rapid during early irradiation and

significantly slower at higher burnups where the grid spring stop contact force and bending stress are low. This is confirmed by rod pull data from irradiated fuel assemblies. The difference in pull force through the intermediate spacer grids between one cycle and three cycle fuel assemblies is insignificant. Measurement of grip forces at [b,c,d,e] MWd/mtU was conducted on Zircaloy intermediate spacer grids. A total of [c] measurements on [c] grids were made with an average preload of [b,c,d,e] Visual examination of spacer grid contact sites on fuel rods pulled from the fuel assemblies examined showed no discernible wear depth.⁽¹²⁾ Life-and-wear testing and operational experience show no indication of adverse fretting wear or progressive wear of fuel rods with fully relaxed Zircaloy grids.⁽⁶⁾ The magnitude of long-term progressive fretting wear, due to grid relaxation, is therefore insignificant and it is concluded that the possibility of fuel rod failures due to fretting wear in Zircaloy spacer grids is unlikely.

2.2.3 FUEL ASSEMBLY SKELETON STRUCTURE OXIDATION

To date, the focus of the Zircaloy oxidation rate has been its effect on fuel rod cladding integrity. However, the main structural components of the fuel assembly are the Zircaloy guide tubes and the intermediate spacer grids whose structural performance could be adversely affected by excessive oxidation. Since coolant comes into contact with both sides of these structural components, oxide growth or material loss rate could be a concern (i.e. twice as much material lost). Oxide growth is a strong function of temperature. The FCF oxide growth model is based on the

Garzarolli model and is benchmarked to high burnup fuel rod oxide data.⁽¹³⁾ The model is in the following form:

| | |
|--|--|
| $ds/dt = (A/S^2) \cdot \exp(-Q_1/RT)$ | Pre-Transition |
| $ds/dt = (C_0 + U \cdot (M \cdot \phi)^p) \cdot \exp(-Q_2/RT)$ | Post-Transition |
| $S_t = D \cdot \exp(-Q_3/RT - ET)$ | Thickness of oxide layer at transition |

where

- ds/dt: Oxide growth rate
- T: Temperature, K
- S: Oxide thickness, μm .
- R: Universal gas constant
- Q_1, Q_2, Q_3 : Activation Energy
- ϕ : Fast neutron flux, $\text{n/cm}^2\text{-s}$, $E > 1 \text{ MEV}$.
- A, C, D, M, U, & p: Fitting constants

Because the structural components operate essentially at coolant temperature, the guide tube and intermediate spacer grid corrosion rate is much less than for the fuel rod. This gives a high burnup corrosion thickness about [b,c,d,e] of that on the fuel rod cladding. In practice, the oxide thickness is expected to be even less than the model predicts because of the material properties. The guide tubes and intermediate spacer grids are of RXA material which has a significantly lower initial corrosion rate than the SRA material of the fuel rods.⁽¹⁴⁾ The thinner material and two-sided corrosion at the lesser thickness results in similar predicted hydrogen concentrations in fuel rods and guide tubes as a function of burnup. Operating analyses have conservatively incorporated corrosion allowances for guide tube cladding and the results show favorable design margins. Operational experience has produced no guide tube or spacer grid failure due to oxidation to date and it is predicted that oxide buildup will be acceptable with extended burnup.

2.2.4 GUIDE TUBE WEAR

An extensive control rod guide tube wear measurement program has been conducted for the Mark-B design.⁽¹⁵⁾ The SRA Zircaloy guide tubes were examined. It was found that the most significant guide tube wear occurs adjacent to the tip of the control rod when in the fully withdrawn or "parked" position. Flow-induced vibration of the control rod against the inner wall of the guide tube results in fretting wear. Guide tube wear is typically localized on one side of the guide tube and was found to [b,c,d,e]. The range of wear rate [b,c,d,e] for a fuel assembly design is dependent on overall plant flow rates and control rod geometry. Therefore, [b,c,d,e] cannot be used to predict the relative wear rates of different designs in different plants. A statistical analysis of the results of operational testing has shown [b,c,d,e].

Structural analysis of the Mark-B fuel design (15x15) has shown that [c,d] wall thinning of the guide tube is acceptable for uniform circumferential wear caused by the control rod and [b,c,d,e] is acceptable for one-sided, localized wear, values that are much greater than any wear seen on FCF fuel. For 17 x 17 designs, the general industry experience indicates higher control rod wear rates compared to 15x15 designs. [b,c,d,e]

The use of RXA material to obtain lower guide tube growth is not expected to have any significant effect on guide tube wear. High burnup fuel cycle designs typically use BPRAs throughout the first cycle of operation, with the consequence that fuel assemblies may contain control rods during their second or third cycle only or for a maximum of two cycles (second and third cycles). However, irradiation effects on the guide tube material during the first cycle of operation will increase the yield strength of the RXA material to

approximately that of SRA material ⁽¹⁶⁾. Since hardness correlates to yield strength, the hardness and wear resistance of SRA and RXA claddings are expected to be similar during second and third cycle exposure.

In general, operational experience shows that guide tube wear is low and within acceptance criteria. A guide tube wear measurement program is currently in progress and is a part of future PIE campaigns.

2.2.5 SPACER GRID IRRADIATION GROWTH

Although the probability that irradiation growth will cause the spacer grids on two adjacent fuel assemblies to lock in contact with each other is extremely low, the condition has been addressed.

In assessing the probability of fuel lockup, two factors need to be considered. These are the growth rate of the grid material as a function of burnup and the gap within the core available to accommodate the growth. With regard to the materials issue, FCF fuel assembly intermediate spacer grids are made of fully recrystallized (RXA) Zircaloy-4 strip material, whereas the top and bottom end grids are made of Nickel Alloy (Inconel) 718. Since Zircaloy-4 has the higher irradiation growth rate, the lateral growth of the Zircaloy grids is the limiting case for analysis. Although a number of reports have shown that irradiation growth of SRA Zircaloy is affected by the rolling direction of the sheet, the RXA condition is not expected to show any directional effect. (Irradiation growth is due to an irradiation induced expansion of the "a" axis and a contraction of the "c" axis of the hexagonal crystals⁽¹⁷⁾ which, in the case of the recrystallized structure, are randomly distributed). The Mark-B Zircaloy grid strip is typically cut[b,c,d,e], whereas the Mark-BW Zircaloy grid strips are cut[b,c,d,e], but the results from one design will be equally applicable to the other for RXA material. The Mark-BW spacer grid design has been evaluated using typical RXA growth data from guide tubes to predict a postulated conservative condition for EOL, where irradiation growth is

greatest. A value of [c,d] growth was used as this worst case value compared to a value of about [c,d] estimated from Ref 17 at [b,c,d,e]. The analyses showed that two EOL burnup assemblies on the diagonal would not have interference. In the case of two adjacent assemblies and assuming [b,c,d,e]

]. However, the analysis showed that in the unlikely event of interference, there would be no negative impact on fuel assembly performance or structural integrity. Finally, the evaluation determined that given worst case burnup/placement scenarios, the core would not go solid. Some interference is allowed by the gaps between fuel assemblies and core baffle walls.

Lateral Mark-BZ (Zircaloy) grid width measurements have been made after one-cycle at [c,d,e] MWd/mtU burnup and show that virtually no lateral expansion occurred. In addition, experience with the same type of design has shown no grid interference problems at average batch discharge burnups up to [c,d,e] MWd/mtU and a peak assembly burnup of [c,d,e] MWd/mtU.

2.2.6 STRUCTURAL ANALYSIS

Structural analyses have been performed for all major fuel assembly components to determine the effect of extended burnup. In particular, longer operating times lead to additional fatigue cycles. The structural analysis is affected by the extended time of operation and not by the power history. The longer residence, together with the irradiation-induced relaxation and growth discussed earlier, have been conservatively addressed for all major fuel assembly components under normal operating and faulted conditions, including Operating Basis Earthquake (OBE) and Safe Shutdown Earthquake (SSE) with Loss of Coolant Accident (LOCA).^(18, 19, 20) In all cases, positive design margins have been identified for extended burnup fuel assemblies (Tables 2.2.6-1,2,3,4).

To provide an analytical basis for the Mark-B fuel assembly design, tests were performed on the guide tube skeleton structure (i.e. fuel assembly minus fuel rods, but with spacer grids in place) to determine the axial lower bound static buckling load capability. In the Mark-B design (B&W plants), control drives decelerate, therefore no impact loads exist during scram. In the Mark-BW fuel assembly design, guide tube segments representing a particular span between spacer grids were tested individually in axial compression to determine their buckling characteristics. Tests in this manner provide very conservative values for buckling analysis of the guide tube.

The stress limits for different spring designs are based on their deformation mode. For helical coil springs, the limit is the torsional stress limit for the spring wire. For leaf springs, the limit is the material ultimate strength limit in tension. Leaf spring designs, especially when used in multiple leaf spring packs are capable of higher holddown forces or greater margins. The most recent Mark-B holddown spring design uses a variation of the multiple leaf spring to provide additional holddown capability.⁽⁷⁾

Table 2.2.6-1

**Limiting Load Conditions for Mark-B Fuel Assembly Components
For Normal Operation**

| COMPONENTS | LOAD CONDITION | ASME CODE STRESS CATEGORY | ALLOWABLE LOAD LIMIT | APPLIED LOAD |
|---------------------|----------------|------------------------------|-------------------------|-----------------|
| End Spacer Grid | [b,c,d,e] | | | |
| Guide Tube Assembly | | | | |
| Upper End Fitting | | | | |
| Lower End Fitting | | | | |
| Holddown Spring | | | | |
| Instrument Tube | | | | |

Table 2.2.6-2

**Limiting Load Conditions for Mark-B Fuel Assembly Components
for OBE and Combined SSE Plus LOCA**

| COMPONENT | STRESS CATEGORY | | ALLOWABLE LOAD LIMIT | | APPLIED LOAD | |
|---------------------|-----------------|----------|----------------------|----------|--------------|----------|
| | ORE | SSE+LOCA | OBE | SSE+LOCA | OBE | SSE+LOCA |
| Guide Tube Assembly | [b,c,d,e] | | | | | |
| End Grid Assembly | | | | | | |
| Upper End Fitting | | | | | | |
| Lower End Fitting | | | | | | |
| Spacer Grid | | | | | | |

Table 2.2.6-3
Limiting Load Conditions for Mark-BW Fuel Assembly Components for Normal Operation

| COMPONENT | LOAD CONDITION | BASIS FOR DESIGN LIMIT | DESIGN LIMIT | ACTUAL LOAD | % MARGIN | |
|-----------------|----------------|------------------------|--------------|-------------|----------|-------------|
| Guide Thimble | | | | | | |
| Upper Nozzle | | | | | | |
| Lower Nozzle | | | | | | [b,c,d,e] |
| Holddown Spring | | | | | | |
| Instrument | | | | | | |

Table 2.2.6-4

**Limiting Load Conditions for Mark-BW Fuel Assembly Components
for SSE and Combined SSE Plus LOCA Conditions**

| COMPONENT | DOMINANT APPL. LOAD ^(a) | | BASIS FOR ALLOW. LOAD | | ALLOWABLE LOAD | | % MARGIN | |
|------------------------------------|------------------------------------|------------|-----------------------|------------|----------------|------------|----------|------------|
| | SSE | SSE + LOCA | SSE | SSE + LOCA | SSE | SSE + LOCA | SSE | SSE + LOCA |
| Guide Thimble ^(b) , lbs | [b,c,d,e] | | | | | | | |
| Fuel Rod ^(b) , ksi | | | | | | | | |
| Upper Nozzle, ksi | | | | | | | | |
| Lower Nozzle, ksi | | | | | | | | |
| Spacer Grid, lbs | | | | | | | | |

^(a) Dominant load is reported, analysis considers effects of load in other directions.

^(b) Load reported as load/tube.

^(c) Applied load considers a load factor[c,d,e] to account for unequal loading.

^(d) [b,c,d,e]

^(e) [b,c,d,e]

2.2.7 CONCLUSION

The fuel assembly design factors affecting the successful development and in-core operation of extended burnup fuel assemblies have been evaluated. The effects of irradiation and longer operation have been addressed in a conservative manner to ensure all safety and structural criteria have been met with positive margin. Based upon these evaluations, extended burnup fuel assembly structural designs support maximum fuel assembly burnups of [c,d,e] MWd/mtU and rod burnups of [c,d,e] MWd/mtU.

2.3 FUEL ROD DESIGN FACTORS

Fuel rods are designed to provide high performance and reliability. In particular, fuel rods are designed to prevent mechanical failure due to overstressing or overstraining, fatigue due to power cycling, oxidation, corrosion, hydriding, reduction of ductility, creep collapse, cladding stress corrosion cracking (SCC) due to pellet-cladding interaction (PCI), and fuel rod bowing. These design considerations are discussed in the following sections as they relate to extended burnup application up to [c,d,e] MWd/mtU fuel assembly and [c,d,e] MWd/mtU rod burnup.

2.3.1 FUEL ROD CLADDING

Fuel rods are designed to achieve a [c,d,e] MWd/mtU burnup recognizing the licensing criteria specified in NUREG 0800, section 4.2.⁽⁵⁾ These criteria require that mechanical analyses such as those for stress, strain, and fatigue be performed under conditions representing "worst case" operation. These analyses are primarily a function of fuel rod design parameters, [b,c,d,e] cladding strength, irradiated cladding fatigue and ductility properties, and reactor operational conditions. The [b,c,d,e] strength of the cladding is used in analyses for fuel rod clad loading as it is the most conservative. The cladding yield and ultimate strength both increase with irradiation. For analyses, the cladding ductility limit used is 1%. Ductility testing has been performed on irradiated cladding to ensure that the actual ductility is greater than the analysis limit. The fatigue

curve used has been modified for irradiation effects. The use of worst case properties in the analyses presented in the following paragraphs conservatively verifies the adequacy of the fuel rod design for all burnup applications.

2.3.1.1 STRESS ANALYSIS

Stress analyses have been performed to demonstrate that the fuel rod design complies with the design criterion that all stresses not exceed the minimum unirradiated yield strength of the cladding for all upset and faulted conditions. The ASME code⁽¹⁰⁾ has been used as a guide in classifying and combining stresses and establishing appropriate stress limits. The analyses determine worst-case stresses due to pressure, thermal cycling, spacer grid contact with the fuel rods, fuel rod ovalization, differential rod growth, cladding corrosion, and flow-induced vibrational loads, and then assume that these worst-case conditions will occur simultaneously during operation. Pressure stresses are based on worst-case conditions as well, i.e., fuel rod minimum internal pressure and maximum system pressure at beginning of life, and fuel rod maximum internal pressure and minimum system pressure at end of life. The analyses show the cladding stresses to be acceptable for all upset and faulted conditions independent of burnup.

2.3.1.2 STRAIN ANALYSIS

The TACO3 code⁽²¹⁾ is used to evaluate pellet/cladding strain as a function of a steady-state power history envelope with power transients superimposed until either a 1% maximum transient hoop strain or linear heat rate to melt (LHRM) is reached. Cladding strain is more limiting than LHRM only at high burnups. The operational transients imposed extend throughout a total rod-average burnup of [c,d,e] MWd/mtU. TACO3 models the effects of fission gas release, thermal expansion, irradiation growth, fuel densification and swelling, cladding creep, and elastic strain. "Worst case" analysis using a conservative power history shows that the strain criterion does not constrain fuel cycle designs for high burnup fuel. Figure 2.3.1-1 shows LHRs for centerline melt and 1% cladding strain vs burnup for a Mark-B fuel rod.

2.3.1.3 FATIGUE ANALYSIS

The fatigue analysis is conservative, insuring that the designs comply with a design criterion requiring a cumulative fatigue usage factor of less than [c,d] for the fuel rod cladding.⁽⁵⁾

Procedures for the fatigue analysis follow those outlined in the ASME Boiler and Pressure Vessel Code ⁽¹⁰⁾, using the O'Donnell-Langer fatigue curve for irradiated Zircaloy⁽²²⁾ as a design basis. To determine the total fatigue usage factor of the cladding, all Condition I and II events are considered together with any one of the Condition III events. Conservatisms include cladding thickness, oxide layer buildup, external pressure, internal fuel rod pressure and pressure differential. The fatigue usage factors for Mark-B and Mark-BW17 were calculated using a [c,d] year lifetime. This resulted in a [b,c,d,e] fraction of the pressure vessel transients which easily envelopes the conditions a fuel rod at [c,d,e] MWd/mtU would experience. Using these inputs, fatigue usage factors of [c,d,e] and [c,d,e] were calculated for the Mark-B and Mark-BW17 designs, respectively. The same methodology can be used for other designs as required.

2.3.2 OXIDATION, CORROSION AND CRUD

In reactor, Zircaloy-4 fuel cladding acquires a thin adherent oxide layer. A fraction of the hydrogen released from the corrosion process becomes dissolved in the base metal. The oxide expands in volume compared to the base metal consumed. Sufficient buildup of oxide layers, cladding hydrogen concentration, and crud can adversely affect the thermal and mechanical performance of the cladding. If the oxide layer is thick enough, oxide flakes will spall off the cladding. This behavior reduces cladding thickness but also lowers the cladding temperature to slow the corrosion process. Because extended burnup implies longer residence times in-core for the fuel, the potential oxide thickness growth has been assessed.

For fuel components manufactured from Zircaloy-4, the corrosion of the base metal

has the following effects:

- a. Loss of base metal and increase of clad stress.
- b. Increased thermal resistance across the oxide layer.
- c. Spalling of the oxide at high thickness. Oxide material is then lost into the primary coolant system. Those oxide flakes then contribute to the total system crud.
- d. Decrease of ductility due to hydrogen loading. The ductility of Zircaloy-4 decreases due to irradiation effects.⁽¹⁶⁾ Further decrease in ductility is a function of hydride formation.⁽²³⁾ Hydrides form when the hydrogen concentration exceeds the solubility of the Zircaloy. The hydrogen concentration is controlled by the oxide thickness, hydrogen pickup fraction, and the volume of the base metal.⁽¹³⁾ For a fuel rod, the cladding hydrogen concentration is a function of the oxide thickness and the thickness of the original base metal. FCF fuel rod designs use thick-walled cladding to decrease the hydrogen concentration at extended burnups. Other Zircaloy-4 components that are modeled are guide tubes and spacer grids. These materials are thinner and corrode from two sides compared to fuel rods. As discussed earlier, the rate of corrosion for these components is lower because the metal/oxide interface temperature is significantly cooler than that of fuel rods.
- e. Possible loss of cladding integrity at extended burnups due to spalling and hydride migration to local cool spots. At high oxide thicknesses, the hydrides formed from hydrogen pickup may migrate and concentrate due

to local temperature variations. These temperature variations tend to form from two causes.

1. An axial gap in the fuel column reduces the cladding temperature. It has been found that an axial gap of [c,d,e] inches can result in local temperature variation of [c,d] between adjacent claddings at a LHR of [] kW/ft.⁽²⁴⁾
2. Spalling of the oxide layer. Spalling of the entire thickness of the oxide layer has not been observed below [c,d,e] thickness which is the current FCF maximum span average oxide thickness limit for fuel rod integrity. The newly exposed cladding is now much cooler than the metal-oxide interface around it, and hydrogen migrates to the exposed cladding surface.

The local hydrogen concentrations and hydride formations due to local cool spots result in a local area that could be brittle and susceptible to cracking and failure.

Items a) and b) above are evaluated in the various analyses performed on Zircaloy-4 components. Through post-irradiation examination, the amount of metal lost to the oxidation process has been determined for various burnups. In addition, the amount of oxide buildup is input as a function of burnup in TACO3. Items c), d) and e) are controlled by limiting the allowable maximum oxide thickness.

Oxide measurements have been performed on fuel rods with up to 5 cycles of operation and with burnups up to [c,d,e] MWd/mtU. The rods examined were from three reactors. The results are plotted in Figure 2.3.2-1. No evidence of excessive local oxide buildup has been seen to date; parameters are well within the design models.

During operation, corrosion products suspended and dissolved in the primary coolant (crud) will be deposited on primary system surfaces. The deposition of crud on fuel has the potential for affecting core pressure drop and corresponding lift force. If the amount of deposition is significant, fuel assembly pressure drop could be increased due to a decrease in the fuel assembly flow area or an increase in the fuel cladding surface roughness. An increase in fuel assembly pressure drop would cause an increase in the hydraulic lift forces acting on the fuel assembly. Operating experience, however, has shown no evidence of fuel assembly lift. Direct measurement has shown crud thickness to be [c,d] or less. This was determined by repeat measurements of oxide thickness. After the base scan, the cladding was cleaned of crud using mildly abrasive material and then rescanned. The difference in oxide thickness was due to crud removal. If crud levels significantly increase above established values, the immediate past operating history of the plant is reviewed to determine whether or not a change in operating conditions could have been the cause.

FCF and industry post-irradiation examinations have shown a predominance of crud deposition on heated surfaces (fuel cladding) with insignificant deposition on spacer grids and other fuel assembly components. Oxide thicknesses vary with axial position; Oxide layers are thinner near the bottom and thicker toward the top of the rods. This trend is consistent with the cladding outer diameter surface temperature profile. A typical oxide profile from a five cycle fuel rod examined in the hot cell provided thickness values ranging from [b,c,d,e]. Maximum oxide thickness values for FCF fuel as a function of burnup are shown in Figure 2.3.2-1.

The decrease in fuel assembly flow area, normally expected because of the increase in effective fuel clad outside diameter due to crud, is offset by the effects of fuel cladding creepdown which continues until pellet-cladding-contact (PCC) prevents further cladding creepdown. After PCC occurs, there is a very slight increase in the effective fuel clad outside diameter which is insignificant up to burnups of [c,d,e] MWd/mtU. Flow area will always be greater at extended burnup than at beginning of life.

2.3.3 CLADDING HYDRIDING AND DUCTILITY

Hydriding of the cladding occurs when the terminal solubility of hydrogen in Zircaloy is exceeded.⁽²³⁾ This leads to a loss of ductility in the cladding.

Control of hydriding within the cladding is accomplished by minimizing the source of hydrogen. Advances in manufacturing techniques such as high density (95 to 96% TD) pellets have effectively eliminated manufacturing as a significant source of hydrogen. High hydrogen levels in the cladding are due to pickup of hydrogen released from cladding corrosion.

Based on cladding burst tests, brittle fracture occurs at approximately [c,d] ppm.⁽²³⁾ The highest localized five-cycle data point was [c,d] ppm, well below this value.⁽¹³⁾ At limiting oxide thicknesses, cladding hydrogen levels are predicted to be less than [c,d] ppm. More recent data detailed in BAW-10183P⁽³³⁾ also supports this position.

FCF has performed cladding hydrogen content measurements on samples taken from five-cycle rods.⁽¹³⁾ The axial variation of hydrogen content is plotted in Figure 2.3.3-1, which shows that hydrogen content increases with axial elevation and then decreases sharply above the fuel column. This axial trend is similar to that exhibited by the oxide thickness data in that it mimics the axial profile of fuel cladding temperature.

Cladding ductility tests show that the strength levels of the five-cycle samples were the same as after four cycles, but a decrease in uniform elongation was observed. Overall, results imply that any radiation damage has saturated at a lesser fluence than shown because the strength and uniform elongation for the irradiated specimens show little variation even though the fast neutron fluence experienced by the specimens varies by [c,d]. Tensile testing results are shown in Figures 2.3.3-2

through 2.3.3-5. Based on the tests, loss of ductility or strength is not a problem for [c,d,e] MWd/mtU fuel rod burnup.

2.3.4 CREEP COLLAPSE

Creep collapse was first observed in unpressurized fuel rod designs containing highly densifying fuel pellets. However, as a result of industry programs to better understand and control fuel pellet densification, and with the advent of fuel rod internal pressurization, cladding creep collapse has not been observed. In addition, extensive poolside and hot cell examinations by FCF and other fuel rod vendors have established that no significant gaps form in the fuel rod column that cannot be accounted for by thermal contraction during cooldown. Creep collapse analyses, which have evaluated the collapse of the cladding into hypothetical axial gaps in the fuel column were overly conservative and have been replaced with more realistic criteria. Currently, the effects of pellet support beyond the point of pellet-to clad contact are included in the analyses by the use of [b,c,d,e] included in the latest version of CROV, where [b,c,d,e] reduce conservatism. Also, fuel rod pre-pressurization (which can be adjusted) allows for additional margin for beginning-of-life (BOL) LOCA limits, and end-of-life (EOL) rod internal pressure limits. The analysis is performed with CROV version 8.0⁽²⁵⁾ utilizing a conservative power history. TACO3⁽²¹⁾ is used to generate fuel rod internal pressures and temperatures at various time steps. These are input to CROV in addition to cladding geometry. Conservatively, fission gas release is not included in the analysis. Included in CROV is an axial gap model to account for cladding support due to finite length gaps in the fuel column. An analysis performed on fuel stack axial gap data (obtained in the cold condition) showed that, for current FCF high density fuel, a [b,c,d] probability existed that any axial gap was [c,d,e] inches or less.⁽²⁶⁾ In the CROV version 8 methodology, the minimum axial gap used is [c,d] inches.

The analysis demonstrates that the fuel rod cladding will not experience creep collapse in extended burnup. This includes operation at significantly lower fill gas pressures than currently used. Analyses using TACO3 and CROV were performed on Mark-B fuel rod designs using fill gas pressures as low as []psia. The results show that cladding creep collapse will not occur at burnups up to []MWd/mtU.

2.3.5 FUEL ROD BOWING

The effects of fuel rod bowing on core design and operation are evaluated in terms of three design criteria.

1. Thermal-Hydraulic design (DNBR).
2. Local power changes due to rod bowing.
3. Fuel cladding mechanical design.

The effect of fuel rod bowing on each of these criteria has been addressed in the B&W Topical Report BAW-10147P-A.⁽²⁷⁾ Each of these design criteria is discussed in terms of extended burnup in the following sections.

2.3.5.1 THERMAL-HYDRAULIC EVALUATION

The effect of fuel rod bowing on DNBR was evaluated in Section 7 of BAW-10147P-A⁽²⁷⁾. A B&W program established to obtain rod bow (gap closure) measurements provided an extensive data base on the magnitude of fuel rod bowing. The magnitude of the rod bow was assessed as being a function of fuel assembly burnup. Correlations relating rod bow (gap closure) to burnup were developed from a statistical analysis of the rod bow measured data. These correlations (developed in BAW-10147P-A) conservatively predicted the increase in rod bow with burnup for the B&W fuel designs to a data limited exposure of [c,d,e] MWd/mtU.

In this initial evaluation, a statistical analysis of the measured rod bow and CHF test data provided a DNBR penalty equation as a function of fuel assembly burnup. The

penalty equation was based on rod bow measurements from fuel assemblies with burnups to [c,d,e] MWd/mtU. The penalty varied from [c] at [c,d,e] MWd/mtU to [c,d] DNBR for the Mark-B and [c,d] for the original Mark-C fuel assemblies at [c,d,e] MWd/mtU. Note, however, that FCF is redesigning its Mark-C fuel assembly and none of the original design assemblies are currently being irradiated.

Since BAW-10147P-A was issued, additional rod bow data have been obtained for Mark-B, Mark-BEB, Mark-B (gadolinia) and Mark-BW fuel assembly designs at fuel assembly burnups up to [c,d,e] MWd/mtU. The rod bow data (gap closure), combined with the data base, and in the original format style of Figure 5-1 of BAW-10147P-A, are shown in Figure 2.3.5-1.

Figure 2.3.5-1 shows that the Mark-B database consisting of the original data contained in BAW-10147P-A, and data obtained subsequent to BAW-10147P-A, bounds all of the later data. The Mark-B fuel design from which the highest rod bow measurements were obtained is expected to produce more bowing than the current FCF Mark-B design. The earlier fuel design had Inconel intermediate spacer grids and fuel pellets that exhibited higher levels of densification, larger fuel to clad gaps and higher percentages of tin in the Zircaloy cladding than is used in current Mark-B designs. The data for the Mark-BEB, Mark-B (gadolinia) and Mark-BW are representative of current FCF fuel designs. These data, shown as open, or unfilled symbols in Figure 2.3.5-1, show much lower levels of rod bow but still indicate saturation at [b,c,d,e] MWd/mtU assembly average burnup.

The representation of the bounding rod bow behavior, Figure 5-1 of BAW-10147P-A, is not consistent with the data. As shown in Figure 2.3.5-1, rod bow measurements obtained subsequent to BAW-10147P-A show a saturation at assembly average burnups of [c,d,e] MWd/mtU for both the older Mark-B and current FCF assembly designs in the data base. Using the 95% tolerance limit of the Mark-B data from BAW-10147P-A Figure 5-1 as an example, bounding rod bow behavior is depicted by the 95% tolerance limit to a burnup of [c,d,e] MWd/mtU and by a [b,c,d,e] for burnups beyond the saturation limit in

Figure 2.3.5-1. The [b,c,d,e], denoted as the "Observed Limit", bounds rod bow measurements to assembly average burnups of [c,d,e] MWd/mtU and will be applied to FCF Licensing analyses for reload fuel. The 95% tolerance limit curve for the current fuel designs, although not shown, would exhibit the same trend, but be much lower than the "Observed Limit" shown in Figure 2.3.5-1.

The DNBR penalty model presented in BAW-10147P-A bounded the results of CHF tests performed for gap closure values of [c,d] and [c,d]. The resulting model produces a penalty of zero for gap closure values up to [c,d]. Figure 2.3.5-2 replots the data of Figure 2.3.5-1 in terms of gap closure. It can be seen from this figure that none of the measurements indicated gap closures of greater than [c,d]. Therefore, no DNBR penalty is necessary.

The gap closure data base contains thousands of measurements that encompass the wide spectrum of fuel design parameters. Included were measurements on a range of fuel assembly designs, manufacturing variations and operational and irradiation histories. The applicability of the BAW-10147P-A analysis to extended burnup for future fuel assembly designs that may have design parameters different from those in the database will be assessed on a case by case basis. The analysis would be updated as required by the additional data.

2.3.5.2 LOCAL POWER CHANGES DUE TO ROD BOWING

Core operating limits based on CFM and LOCA criteria incorporate a peaking uncertainty which includes the effects of fuel rod bowing on local power changes. The local power peaking changes due to local neutron moderation variations resulting from rod bow were evaluated in BAW-10147P-A. It was reported in BAW-10153P-A, section 2.3.5.2, that the peaking uncertainty used to accommodate the effects of rod bow was established to be bounding for any gap closure predicted to occur in FCF fuel design. Based on the assessment of both the BAW-10147P-A data base and the more recent rod

bow data discussed above, the peaking uncertainty used to accommodate rod bow effects (BAW-10147P-A) will be based on a gap measurement standard deviation that equals or bounds the 95% tolerance limit of Figure 2.3.5-1 from 0 to [c,d,e] MWd/mtU and the "Observed Limit" for assembly average burnups greater than [c,d,e] MWd/mtU.

2.3.5.3 MECHANICAL EVALUATION

Mechanical design considerations of rod bow are concerned with the possibility of fretting on fuel cladding surfaces at 100% gap closure. Fretting is a surface wear phenomenon resulting from small relative movements between two surfaces in contact with each other. An assessment of the effect of rod bow on fuel rod fretting is presented in Section 6 of BAW-10147P-A. The assessment included the judgement that in the unlikely event that such contact would occur, an insignificant amount of wear depth would result from the small relative motion and low contact force. Therefore, rod-to-rod related fretting wear is not a concern for FCF fuel assembly designs.

Water channel spacing measurements have been taken for FCF designs through five cycles and burnups to [c,d,e] MWd/mtU. The results are shown in Figure 2.3.5.-2. There is no appreciable increase in bow magnitude with higher burnup; therefore, no additional concerns exist about clad fretting due to rod bow for extended burnup application.

2.3.6 PELLET CLADDING INTERACTION

Zircaloy-4 fuel rod failure is postulated to occur due to stress corrosion cracking from fission products, most probably cesium and iodine. This phenomenon has not been specifically identified as a failure mechanism for FCF-designed fuel. The approach to control pellet cladding interaction (PCI) is to define and control the operating conditions which can lead to failures. For this reason, the pellet-cladding gap and fuel density are designed to minimize cladding strain during operation. Tensile tests indicate that sufficient ductility is maintained over the irradiated life of high burnup fuel. The cladding has a high hoop creep rate to accommodate PCI strains, and a pickled and grit blasted inner diameter

surface finish to minimize stress corrosion cracking (SCC) initiation sites.

Due to the decreasing fuel rod power output potential at higher burnups, maximum susceptibility to PCI would occur earlier in life. For this reason, PCI potential remains low at higher burnups because of less severe operating conditions and therefore is not considered a limiting factor for extended burnup application.

2.3.7 DEFECTS

Extended burnup operation has not resulted in increased risk of fuel rod defects or leakers, nor has it resulted in increased consequences due to defects. FCF has increased discharge batch and peak fuel assembly burnup since the submission and acceptance of BAW-10153P-A. Fuel performance since that time has improved both in a reduction in the number of leaking rods observed per year and in a decrease in the coolant fission product inventory as shown in Table 2.3.7-1.

When a fuel rod defect occurs, the cladding no longer serves as a total barrier between the fuel pellets and the primary coolant. One effect of this breach in the fuel rod is that fission products released from the fuel pellets into the gap can now escape into the primary system. From there they can be deposited around the primary system in such places as steam generator heads, or, if in a gaseous state, be eventually vented from the primary system to the atmosphere. Maximum permissible primary coolant radioisotopic activity levels are controlled by the plant's relevant technical specification. An example is the standard technical specification limit of 1.0 $\mu\text{Ci/ml}$ for dose equivalent steady state I-131.

Plant operators and fuel vendors have worked to reduce primary coolant activity to levels far below the technical specification limit. These include identification and removal of leaking fuel rods and improved fuel quality and design. Two examples of fuel design features that have reduced coolant activity are the use of reconstitution and debris protection features on fuel assemblies. FCF fuel designs are now all reconstitutable and

include either [b,c,d,e

].

These and other efforts have resulted in lower coolant activity levels.

The effect of any single leaking fuel rod on primary system activity is, for the most part, a function of the type of defect and the rod power. Rod power affects the release of fission products from the fuel pellet into the gap. Rod power also affects the temperature of the steam/gas mixture in the gap of a leaking fuel rod. The net result is an increasing fission product release rate with increasing rod power. A second effect is that leaking fuel rods at high enough power levels can develop secondary defects due to internal hydriding. The release rate for a fuel rod with secondary defects is higher than for a rod with a single defect. Secondary defects from internal hydriding of leaking fuel rods usually occur in first cycle fuel and tend to be a function of time and power. The rod power level needed for secondary defects to occur within a single fuel cycle is generally greater than the operating power level of high burnup fuel.

Extended burnup operation results in increasing inventories of long half-life fission products such as Cs-137. There should then be more of these fission products available for release in high burnup fuel. However, due to rod power levels, the actual fission product spiking and steady state release from leaking fuel rods have shown that first cycle fuel rods contribute the most to primary coolant activity levels.

**Table 2.3.7-1
Average Steady State Coolant Iodine Activity
For B&W Designed Plants**

| <u>Date</u> | <u>I-131 Activity, uci/gm.</u> |
|-------------|--------------------------------|
| 1980 | |
| 1981 | |
| 1982 | |
| 1983 | |
| 1984 | |
| 1985 | [b,c,d,e] |
| 1986 | |
| 1987 | |
| 1988 | |
| 1989 | |
| 1990 | |
| 1991 | |

2.3.8 DNBR

The current FCF position with regard to DNBR has not changed from that stated in BAW-10153P-A. For convenience, this position is repeated below.

A major thermal-hydraulic design criterion for PWR's is the prevention of DNB during normal operation and during incidents of moderate frequency, classified as Condition I or Condition II events. For any of these events, the reactor core is assured of meeting the design criteria by demonstrating that the predicted minimum DNBR is greater than the corresponding design limit DNBR.

The core power distribution is the only DNBR calculational input affected by burnup. Core power distributions are defined for the steady state by fuel cycle design, and limited during operation by technical specifications to power distributions which maintain initial condition DNBR limits. Extended burnup has no impact on DNBR. Accident related aspects of DNBR are addressed in Section 4.0 (of BAW-10153P-A).

2.4 FUEL ROD THERMAL PERFORMANCE

The design for safe operation of nuclear cores requires the establishment of heat rates to preclude fuel melting. In addition, bounding values of stored energy are required

input for the LOCA analyses. The buildup of pressure within the fuel rod from noble gases produced and released during irradiation also requires bounding value analyses performed with accurate models and prediction methods.

The approved TACO3⁽²¹⁾ fuel pin analysis code and applications methodology will be used to analyze these phenomena. TACO3 has previously been approved for use in licensing applications up to rod average burnups of [c,d,e] MWd/mtU. TACO3 has also been shown⁽³³⁾ to be acceptable for the analysis of fuel rods whose internal pressures exceed the reactor coolant system pressure, independent of burnup. The following paragraphs discuss the TACO3 models that are important in analyzing extended burnup fuel rods. Based upon this evaluation, TACO3 is acceptable for the analysis of FCF fuel rods up to rod average burnups of [c,d,e] MWd/mtU.

2.4.1 DENSIFICATION AND SWELLING

An important contributor to changes in fuel diameter and end-of-life rod internal void volume is the phenomenon of fuel densification. Densification has been observed to occur early in life and results in a decrease in fuel diameter, increase in fuel-clad gap, and, consequently, an increase in fuel temperature. Densification effectively postpones fuel swelling and, therefore, increases extended burnup internal void volume and decreases internal gas pressure.

Fuel swelling is also an important phenomenon. Fuel swelling is produced from the products of nuclear fission. Fuel swelling reduces the rod internal void volume available for fission gas release storage.

The best-estimate fuel densification and swelling model in the current fuel pin analysis code (TACO3) is based on the work of Marlowe⁽²⁸⁾. A detailed description of this model is provided in Appendix F of the TACO3 topical report⁽²¹⁾. The model accurately predicts the densification and swelling behavior of fuel with characteristics that range from very stable non-densifying to highly densifying. A single 1700°C 24 hour resinter point is

the required input for this model. The option for using two resinter points (1700°C, 6 and 24 hours), however, is provided. Both options provide accurate predictions. The densification and swelling portions of the model have been successfully benchmarked using the EEI/EPRI data base⁽²⁹⁾ and FCF fuel density data. The FCF data includes measured fuel densities from pellets with burnups that exceed [c,d,e] MWd/mtU. No unusual fuel densification and swelling effects occur at extended burnups that would preclude using this model to analyze fuel with [c,d,e] MWd/mtU and higher rod average burnups.

2.4.2 GAP CLOSURE

Radial temperature gradients present within fuel pellets during operation cause thermal stresses to develop that cause the pellets to crack and break up. The pellet fragments remaining following the break up process relocate toward the cladding inner surface. The relocation process closes the fuel-clad gap and reduces the fuel temperature. Pellet cracking and relocation begins during the first ramp to power and continues during the early life of the rod.

Gap closure has the greatest effect on fuel with low to moderate burnups. At extended burnups the fuel-clad gap will have closed due to clad creep down and fuel swelling. At extended burnups, therefore, gap closure will no longer directly impact fuel temperatures. It does, however, have an indirect effect on extended burnup parameters, such as fission gas release, which are dependent on fuel history effects. The ability to correctly predict fuel temperatures at low to moderate burnups will impact the ability to correctly predict extended burnup parameters such as fission gas release.

The gap closure model in the current fuel pin analysis code (TACO3) is a function of [b,c,d,e]. The approach used in developing the model consisted of matching predicted centerline fuel temperatures with measured data. The data base included over [] points and extended across the following ranges:

Measured Centerline Temperatures
Linear Heat Rates
Burnups
Fuel-Cladding Diametral Gaps [b,c,d,e]
Fill Gases
Fill Gas Pressures

A statistical evaluation of the TACO3 temperature predictions indicated that no burnup, linear heat rate, or temperature bias exists through a burnup of [c,d,e] MWd/mtU. Since the fuel-clad gap has the greatest influence on the precision of the code predictions, as discussed above, and the gap has essentially closed at [c,d,e] MWd/mtU burnup, the code will, therefore, reliably predict conditions at burnups of [c,d,e] MWd/mtU and beyond.

2.4.3 GAP CONDUCTANCE

The largest resistance to heat flow from the pellet is the fuel-clad gap. At the beginning of life, this gap contains helium and may contain a trace of residual air. During irradiation, the helium becomes diluted with the fission gas that has been released. The thermal conductivity of the xenon and krypton fission gas isotopes is substantially less than helium. Fission gas release, therefore, decreases the fuel-clad gap conductance and increases the fuel temperature. An accurate gaseous gap conductance model in a fuel performance code will reflect this behavior. When fuel-clad contact occurs, the heat flow from the pellet also travels through regions of solid-solid, fuel-clad contact. Contact conductance models have been included in fuel performance codes to account for this behavior. Thermal radiation also contributes to the total gap conductance but is not a strong effect. Thermal radiation between the fuel and cladding, under normal operating conditions, is typically less than [b,c,d,e] of the total gap conductance.

The gaseous gap conductance model of the current fuel performance code (TACO3) was derived from purely analytical considerations. The predictions from this model agree very well with measurements. Although the TACO3 contact conductance

model was derived with the aid of experimental data, the fuel centerline temperature predictions from this model also agree well with measured data. The TACO3 gaseous and contact conductance models are described in detail in Appendix D of the TACO3 topical report. A statistical evaluation performed with measured centerline fuel temperatures and TACO3 predictions yielded the following:

Entire Data Base

[b,c,d,e]

High Temperature Regime

[b,c,d,e]

Operating Regime

[b,c,d,e]

The measured-to-predicted mean and standard deviation of the high temperature and operating regimes are nearly equal. Furthermore, these quantities are nearly equal to the respective quantities of the entire data base. This confirms that there is no temperature dependent bias in the TACO3 fuel temperature predictions. A histogram of the measured-to-predicted temperatures and plots of the measured-to-predicted temperatures versus burnup and LHR indicate that the distribution is approximately normal and there is no bias with respect to burnup or LHR (see Ref. 21, Figures I-5, 6, 7, & 8). Note that the measured-to-predicted means of the entire data base, high temperature regime, and operating regime are all approximately unity, which confirms that the TACO3 temperatures represent best-estimate predictions. These statistical results add confidence to the TACO3 extended burnup fuel temperature predictions.

Post-irradiation examinations of extended burnup fuel indicate that fuel-clad bonding, as distinct from hard fuel-clad contact, begins to occur during extended burnup operation. Bonding eliminates the small gas filled voids that would normally be present during hard fuel-clad contact. These voids are taken into account in the TACO3 contact conductance model. The noble gases that occupy the voids have a much lower thermal conductivity than the solid material that fills these voids during fuel-clad bonding. The current model claims no benefit at extended burnups for the bonding effect in the thermal calculations, therefore, it is conservative and produces fuel temperature predictions that are greater than actual. This bonding effect becomes significant at rod average burnups that exceed [c,d,e] MWd/mtU where hard fuel-clad contact has existed for a substantial period of time. It may be desirable in later models to quantify the additional margin available when credit is taken for [b,c,d,e].

2.4.4 FISSION GAS RELEASE

During the irradiation of nuclear fuel, stable and long-lived noble gas atoms (xenon and krypton) are produced. The solubility of these atoms is small and, therefore, precipitation of the gas occurs within the fuel matrix. The process of resolution acts against

precipitation and an equilibrium process between precipitation and resolution is established. The gas atoms, being in dynamic solution, diffuse to the grain boundaries. The primary driving force for this diffusion is the concentration gradient. The gas atoms coalesce and form gas bubbles on the grain boundaries that grow and eventually become interlinked, forming a network of escape tunnels.

In addition to steady-state fission gas release, additional amounts of fission gas can be released during and shortly after power transients. Grain boundary separation (microcracking) has been observed after transients and correlations have been found between the transient fission gas release and the increase in surface area. Post test microstructure examinations have indicated that grain boundary separations can be produced by the growth and coalescence of fission gas bubbles. At temperatures where significant grain growth occurs, grain boundary movement is able to sweep up fission gas atoms. This causes a rapid growth of the grain boundary bubbles, producing microcracking.

The steady-state fission gas release model in the current fuel performance code (TACO3) is based on the work of Hering⁽³⁰⁾ and is described in detail in Appendix H of the TACO3 topical report. It is not practical to model in great detail all of the mechanisms described previously, but the TACO3 steady-state model accounts, as far as possible, for the physical processes of fission gas release. The model is strongly temperature and burnup dependent and, at extended burnups, predicts a markedly greater fission gas release from the rim region of the fuel. This release is consistent with local fission gas release measurements. Transient fission gas release is [b,c,d,e

].

The TACO3 fission gas release model was benchmarked to fission gas release data from a number of sources. This data included fission gas release from Westinghouse rods irradiated in the Zorita⁽³¹⁾ and BR-3⁽³²⁾ reactors. These rods operated at comparatively high power levels and the measured fission gas release from these rods was, consequently,

also comparatively high. The TACO3 code accurately predicts the fission gas release from these rods. The maximum rod average burnup of these rods was [c,d,e] MWd/mtU. A comparison of steady-state fission gas release measurements and predictions indicates that the TACO3 steady-state fission gas release model predicts measured data remarkably well.

There is no current evidence to suggest that fission gas release from nuclear fuel increases abruptly at a specific burnup. However, the fission gas release rate does increase non-linearly as a function of burnup. This burnup enhancement is included in the TACO3 model. The TACO3 model accurately predicts the gas release from the Westinghouse BR-3 rod with 61,500 MWd/mtU rod average burnup and is expected to perform equally well in predicting the gas release from rods with [c,d,e] MWd/mtU burnups.

2.4.5 FUEL ROD INTERNAL PRESSURE

The internal pressure of a fuel rod is a function of several variables: Initial helium pressure, fission gas release, total internal void volume, and the absolute temperature of the gas occupying the various void volumes. The pressure within a fuel rod may be calculated with the ideal equation of state by applying it to each of the interconnected void volumes within a rod. This approach was used in the current TACO3 fuel performance code. The accuracy of the internal pressure predictions calculated with this approach is limited to the individual accuracies of the temperature, fission gas release, and internal void volume predictions. The accuracy of the TACO3 temperature and fission gas release predictions was addressed above. The TACO3 internal void volumes were also compared with measured extended burnup data. The predicted volumes were slightly conservative (by approximately [] percent). The accuracy of these predictions combined with the accuracy of the TACO3 temperature and fission gas release predictions adds assurance as to the accuracy of the TACO3 internal pressure predictions at extended burnups.

Conservatism is added to the TACO3 internal pressure predictions by including

several limiting Condition 1 transients to the power history. These transients are included at nominally [c,d,e] MWd/mtU rod average burnup intervals. Additional conservatism is added to the pressure predictions by adding pressure penalties to the TACO3 best-estimate predictions. These penalties correspond to the TACO3 code, fuel rod manufacturing, and the predicted power history uncertainties.

The addition of a limiting Condition 1 transient at nominally [c,d,e] MWd/mtU burnup intervals is, perhaps, an overly conservative practice that compensates for the possibility of an unplanned reactor event as well as the increasing uncertainty in the internal pressure predictions with burnup. The increasing uncertainty is primarily due to the lack of extended burnup fuel temperature data. [c,d] transients are included in an internal pressure analysis of a [c] GWd/mtU burnup rod. The last several transients coupled with the nonlinear burnup dependence of the TACO3 fission gas release model substantially increases the EOL best-estimate and bounding predicted pressures. The bounding EOL pressure is compared to the fuel rod internal gas pressure criterion that limits the internal pressure to be less than the value which would cause the fuel-clad gap to increase due to cladding creep during steady-state operation, as presented in the topical report entitled Fuel Rod Gas Pressure Criterion.⁽³³⁾ This criterion will be applied to justify operation with internal pressures that exceed the nominal reactor coolant pressure.

2.4.6 STORED ENERGY

The predicted energy stored within fuel pellets is used in the Emergency Core Cooling System (ECCS) safety analyses. LOCA initialization analyses are performed with the current fuel performance code (TACO3) in the following manner. TACO3 is used to generate best-estimate volumetric average fuel temperatures as a function of linear heat rate and burnup, internal rod gas pressure and composition, and rod dimensions and characteristics.

A conservative factor is applied to the TACO3 best-estimate volumetric average fuel temperature predictions. A $T_{95/95}$ volumetric average fuel temperature is used to initialize

the stored energy in the LOCA analysis. This temperature is defined as

$$T_{95/95} = (\mu + K\sigma) = [b, c, d, e]$$

where

$T_{95/95}$ = 95%/95% one-sided upper tolerance limit temperature, °C,

T = TACO3 best-estimate temperature, °C,

μ = mean meas./pred. = [c, d, e],

K = 95/95 one-sided tolerance factor based on a sample of [c, d] from a normal population = [c, d, e]

σ = std. dev. meas./pred. = [c, d, e].

The $T_{95/95}$ volumetric average fuel temperature is used to initialize the stored energy in LOCA analyses. Manufacturing (fuel-clad gap) uncertainties and cladding oxide formation are not explicitly considered in this analysis. The $T_{95/95}$ temperature is sufficiently conservative to account for these effects as well as TACO3 code uncertainties.

The stored energy within fuel pellets is typically a maximum near the beginning of life. This is due to the initially large fuel-clad gaps and the energy available from non-depleted fresh fuel. At extended burnups, the fuel rod internal pressure becomes an ECCS analysis issue. This issue has been addressed by extending the TACO3 EOL fuel rod internal pressure criterion to the ECCS analysis. This criterion limits the internal pressure to be less than that which would cause the fuel-clad gap to increase due to cladding creep during steady-state operation. This methodology provides a conservative approach for establishing the fuel rod LOCA initialization parameters at rod average burnups up to and exceeding [c, d, e] MWd/mtU.

2.4.7 FUEL MELT

The TACO3 fuel performance code is used to calculate the linear heat rate to melt (LHRM), which is an input to reactor protection system limits. The criterion addressed by this analysis is that the predicted maximum fuel temperature at a given burnup value must be less than the melting temperature of UO₂.

The analysis method used with TACO3 is described in BAW-10162P-A; a best-estimate temperature prediction is compared to a melt-limit temperature, T_L, that has been reduced from the UO₂ melting temperature to account for prediction uncertainties, such that when the predicted temperature equals T_L, there will be a 95% probability at the 95% confidence level that fuel melting will not occur. Although recent data⁽³⁴⁾ indicates that the melting temperature is constant up to a burnup of about [c,d,e] MWd/mtU, TACO3 assumes a reduction with burnup as follows:

$$T_L = [b, c, d, e \quad]$$

Where Bu = burnup in MWd/mtU

Even with the burnup-dependent reduction in melt temperature, low-burnup fuel is most limiting, to burnups of at least [c,d,e] MWd/mtU. This is because the fuel-clad gap is largest at beginning-of-life and this effect dominates.

2.4.8 FUEL THERMAL CONDUCTIVITY

There are two on-going international research programs investigating the premise that fuel thermal conductivity decreases with burnup. The basis for this premise is that the stoichiometry of the fuel changes due to the fission products produced during depletion. The thermal conductivity of the fuel in the current fuel performance code (TACO3) is not burnup dependent. The TACO3 fuel temperature predictions, however, agree well with measurements across the entire range of available data. The fuel temperature measurements⁽³⁵⁾ from IFA-432 rod 3 are currently recognized as representing the highest

burnup data; 40,000 MWd/mtU. The TACO3 predictions match this data well. It appears, therefore, that if the fuel thermal conductivity is changing with burnup, the TACO3 gap conductance models effectively account for these changes such that the TACO3 predicted temperatures agree well with extended burnup measured data. FCF belongs to both international programs examining this phenomenon and should the results from these programs indicate that a change is needed, steps will be taken to enact these changes.

2.5 NEUTRONICS

A detailed evaluation of extended burnup effects on core physics parameters was performed in BAW-10153P-A. That evaluation provided justification for FCF-designed fuel assembly burnups up to [c,d,e] MWd/mtU. The conclusion drawn in section 2.6.5 of BAW-10153P-A was that physics predictions for extended burnup cores were within existing uncertainties. The current FCF neutronics methods have been shown to be sufficient for design and licensing analyses of extended burnup fuel cycles. The calculational methods referenced by BAW-10153P-A have been extended to include approved revisions³⁶ to the standard methods, methods documented in the Safety Criteria and Methodology topical report^{37,38}, and those developed for application to the Mark-BW fuel assembly³⁹. A revised calculational uncertainty was developed and verified for application with an advanced nodal code, NEMO⁴⁰, that will be implemented for design and analysis of all fuel cycles, including cycles with extended burnup fuel. Benchmark comparisons of NEMO calculations with operating plant data indicate that burnup has negligible effects on the accuracy of power distribution and core reactivity predictions. The implementation of NEMO, including its revised calculational uncertainty, will provide margins to safety-related design criteria for fuel cycles with high burnup fuel that are essentially the same as those provided with the currently accepted design codes and calculational uncertainty.

Since the completion of BAW-10153P-A, a FCF fuel assembly has achieved a burnup greater than [c,d,e] MWd/mtU. This occurred during the eleventh cycle of Oconee 1. Comparisons of measured to predicted nuclear parameters for that assembly, and the reactor core, show good agreement between calculations and measurements for the entire cycle, thus confirming the capability of the physics methods to evaluate performance of extended burnup fuel. Relative power comparisons, which are a good indication of the ability to predict overall behavior of a fuel assembly, were made between the predictions and measured data, and the maximum difference was less than [c,d]. Therefore, the conclusions in BAW-10153P-A remain valid for extended burnup goals of [c,d,e] MWd/mtU for a fuel assembly and [c,d,e] MWd/mtU for a fuel rod. FCF will continue to monitor fuel cycles with extended burnup fuel and will inform the NRC of any significant deviation between predictions and measurements of the various physics parameters.

2.6 MATERIALS QUALIFICATION

The demands of high burnup operation have increased efforts to produce improved or advanced materials for fuel rod and assembly construction. These new materials are selected to give superior performance in such areas as corrosion and growth. Such materials must be qualified before their use in full batch implementation.

As part of a qualification, materials are first tested ex-reactor and then in-reactor. Ex-reactor assessments include data evaluation taken from the general literature, testing of materials by the component vendor, and specific FCF contracted testing. In-reactor testing includes poolside and selective hot cell examination of irradiated components. Results are verified by literature reviews. The products of such testing are models which predict strength, strain capabilities, strain rates, and corrosion rates for the material.

The materials utilized in current fuel assembly designs have been qualified by the above methods. Initial test results were presented in BAW-10153P-A. Additional data at higher burnups is provided in this report. From the behavioral models, the material conditions at extended burnups can be predicted and decisions made as to the acceptability of existing fuel assembly designs at the extended burnups. In some cases, for example fuel rod growth, predictions may indicate that an assembly design change is required to provide further clearance between end fittings at extended burnups. In other cases, for example clad corrosion, changes in the cladding composition, either within the Zircaloy-4 compositional range or outside of the range, are indicated as the best means to achieve extended burnup. Low corrosion rates have been demonstrated on low tin Zircaloy-4 samples in high temperature environments and cladding approaching this composition is currently specified by FCF for its fuel. Other alloy compositions are under continued testing to determine whether additional benefits can be obtained for extended burnup use and recommendations for further improvements may be made as more data becomes available.

The qualification of future fuel materials and models used by FCF will likely include data from non-US reactors and laboratories. Some data will come from industry participatory programs such as NFIR. Other data will come from joint development programs with FCF partner companies. An example of the latter is the current program by FCF to qualify advanced claddings.⁽⁴²⁾ In this program, twelve advanced cladding alloys are being irradiated in reactors in Europe. Poolside PIE data will be compared between US and European plants. Hot cell work for material properties will use fuel rods from European reactors.

Figure 2.2.1-1

[b,c,d,e]

Figure 2.2.1-2

[b,c,d,e]

Figure 2.3.1-1

[

b,c,d,e

]

Figure 2.3.2-1

[b,c,d,e]

Figure 2.3.3-1

[b,c,d,e]

Figure 2.3.3-2

[b,c,d,e]

Figure 2.3.3-3

[b,c,d,e]

Figure 2.3.3-4

[

b,c,d,e

]

Figure 2.3.3-5

[b,c,d,e]

Figure 2.3.5-1

[b,c,d,e]

Figure 2.3.5-2

[

b,c,d,e

]

3.0 FUEL ASSEMBLY BURNUP CAPABILITIES

3.1 INTRODUCTION

The preceding section evaluated the impact of extended burnup on the fuel system design and core neutronics. The conclusions of these evaluations are summarized in the following two sub-sections.

3.2 FUEL SYSTEM EVALUATION SUMMARY

The overall conclusion of the fuel system evaluation is that there is no inherent limitation in licensing fuel assembly burnups to a value of [c,d,e] MWd/mtU.

[

b,c,d,e

].

The following design upgrades to FCF fuel assemblies have been made to achieve high fuel system burnup levels:

- Conversion to annealed guide tubes.
- Revision of holddown spring material and designs.
- Use of lower tin content fuel rod cladding.
- Optimization of cladding annealing parameters.
- Use of lower back-fill pressures in fuel rods.
- Increased space between the fuel rods and the upper grillage to accommodate fuel rod growth.

These changes have been incorporated on a continuing basis and are based on results from data taken in various demonstration and test programs.

In summary, FCF-designed fuel systems can be safely and reliably operated to assembly average burnups of at least [c,d,e] MWd/mtU. Feedback from demonstration and test assembly programs will continue.

3.3 NEUTRONIC EVALUATION SUMMARY

The neutronic evaluation concludes that standard methods are satisfactory for design of extended burnup fuel cycles and that reactor operation with these cycles will be similar to current cycles. The impact of changes in kinetic parameters on system response to transients is evaluated in Section 4.

4.0 SAFETY ASPECTS OF EXTENDED BURNUP

4.1 INTRODUCTION

The underlying conclusion in section 4.2.6 of BAW-10153P-A relative to safety analysis is that extended burnup has a minor effect on transient results. It was pointed out that the moderator temperature coefficient can influence the outcome of the steam line break event and would be addressed on a cycle by cycle basis.

In general, cycle by cycle reload safety evaluation analyses are performed to verify that the core specific parameters are bounded by the values used in the safety analyses. Parameters such as peaking, shutdown margin, reactivity coefficients, and radiological consequences are checked on a cycle by cycle basis. If the parameters for the designed core are bounded by the values used in the safety analyses, then the core design is acceptable. However, if the parameters for an extended burnup core were to exceed the

bounds of the values used in the safety analyses, then either the core design would be changed or the safety analysis value for that parameter would be revised to bound the cycle specific value. This could entail either a limited evaluation of the transients sensitive to the particular parameter to demonstrate acceptable consequences, or a complete reanalysis of one or more transients.

Therefore, extending the assembly burnup limit is acceptable relative to physics parameters and safety analyses as long as the core designs are verified to be within the appropriate bounds on a cycle by cycle basis.

4.2 RADIOLOGICAL EVALUATION

As discussed in BAW-10153P-A, high burnup fuels have different mixtures of fission product nuclides than reference burnup fuel. These differences generally result in slightly higher thyroid doses and slightly lower whole body doses, but have very little impact on the overall radiological consequences. Radiological consequences of fuel cycles achieving extended burnup levels will continue to be evaluated on a cycle specific basis.

4.3 ECCS EVALUATION

The ECCS evaluation for fuel licensing (10CFR50.46) is conducted or reviewed on a cycle specific basis. As part of these studies a determination of the most severe burnup conditions for LOCA calculations is made. For the licensing of extended burnup cores, the burnup studies will be extended using appropriate parameters to cover the maximum exposure to be licensed. Because these studies are highly plant dependent, they will be conducted at the time of the core reload safety evaluation.

To assure that the ECCS methods and base data are adequate to conduct extended

burnup evaluations, the models have been reviewed for dependencies. Extended burnup affects LOCA calculations through higher internal pin pressures, thicker initial fuel pin oxide layers, adjustments to pellet materials properties, differing neutronics coefficients, and altered pellet power profiles. All of these parameters are input determinable within the model. Therefore, although the values will differ for extended burnup conditions, there is no limit on the applicability of the LOCA models. Similarly, the range of applicability of fixed models within the LOCA techniques was reviewed and determined to encompass the conditions of extended burnup. Of particular interest was the fuel pin rupture modelling. The NUREG-0630 model, used by B&W Nuclear Technologies (BWNT), provides stress rupture criteria up to stress values substantially in excess of those expected for extended burnup conditions.

The expected results of LOCA evaluations at extended burnup are that local power peaking will be limited with burnup such that BOL will remain the most severe LOCA evaluation conditions. The limiting of local power for extended burnup fuel is not expected to be of consequence because fuel with these high burnup levels will not produce high linear heat rates.

4.4 DECAY HEAT

The current FCF position with regard to Decay Heat has not changed from that stated in BAW-10153P-A. For convenience, this position is repeated below:

The amount of heat generated by the decay of fission products in irradiated fuel must be calculated when evaluating spent fuel storage, emergency core cooling systems, and when shipping radioactive fuel. The heat load used in designing storage racks, spent fuel pools, and core cooling systems is calculated based on relatively short or no cooling times, i.e., immediately after shutdown, because this is the condition of maximum heat load. The thermal power at this time is largely a function of short-lived fission products which tend to saturate at relatively low burnups. Therefore, the design of these systems is not appreciably affected by extended-burnup. The maximum allowable thermal power of fuel which is to be transported is determined by the design of the shipping cask. Extended-burnup fuel will have a higher heat rate than a comparable fuel assembly with less burnup

after the same cooling time. The practical effect of this is to increase the amount of cooling time necessary before the extended-burnup assembly can be shipped or to decrease the amount of fuel which can be shipped in a cask.

The methodology used to evaluate the decay heat generation in irradiated fuel is in accordance with ANSI/ANS-5.1-1979, the American National Standard for Decay Heat Power in Light Water Reactors. No modifications to those methods are necessary due to the increase in fuel burnup associated with extended-burnup fuel cycles.

4.5 SEISMIC AND LOCA EVALUATION

Extending the fuel assembly burnup affects certain mechanical characteristics used in the structural evaluation for seismic and LOCA events. These include the fuel rod-to-upper end fitting interface gap, spacer grid relaxation and its associated effect of assembly frequency, holddown spring relaxation and changes in material properties. Methods and procedures used in the seismic and LOCA analysis are described in Topical Report BAW-10133.⁽¹⁸⁾

The fuel rod-to-upper end fitting gap limits the amount of possible fuel rod slippage through the spacer grids. Changes in the gap size are a function of the growth differential between the fuel assembly and the fuel rods, both of which are burnup dependent. As discussed in section 2.2.1, the gap size can be predicted for a given burnup and is incorporated directly into the dynamic response analysis.

Spacer grid relaxation affects both the fuel rod slip forces and fuel assembly response frequencies. Irradiation-induced grid relaxation, discussed in Section 2.2.2, reduces the grip force on the fuel rods and the associated force required to slip the rods through the grids. A large percentage of this relaxation occurs early in assembly life and with insignificant changes in the extended burnup range. The limiting case of a fully relaxed intermediate grid is one of the model parameters used in the vertical seismic and LOCA analysis studies. PIE data indicate that the fuel assembly's natural frequencies decrease slightly with increasing burnup and resulting grid relaxation. This reduction has an insignificant effect on the spacer grid impact loads.

Irradiation-induced relaxation of the holddown springs decreases the holddown spring force on the fuel assembly. As discussed in Section 2.2.1, the spring rate is not affected, only preload changes. Parameter studies show that decreasing preload does not significantly affect the dynamic fuel assembly response. The energy absorbed during the event is dependent only on the spring rate.

To be conservative, the material properties for beginning-of-life conditions are used in the structural and load analyses, since the effects of irradiation would be to increase yield strength. In all cases, the calculated loads are well within elastic load limits.

5.0 CONCLUSION

The extended burnup capabilities of FCF fuel designs have been evaluated based on peak rod burnups of [c,d,e] MWd/mtU and peak assembly burnups of [c,d,e] MWd/mtU. The methods and data described or referenced in this report support plant specific licensing to these burnups or higher.

The criteria examined include material properties, reactor environments, and the ability of codes to predict the behavior of the components throughout life. Some criteria are limiting early in life, for example the LOCA condition, while others are critical at end of life, for example the cladding corrosion condition. All relevant criteria have been examined.

No unexpected or abrupt changes in fuel rod performance have been identified that would preclude continued safe, reliable operation to the above defined burnups. This statement is based on the present fuel performance data base that includes fuel irradiated to approximately [c,d,e] MWd/mtU.

As stated in the original 1986 report, BAW-10153P-A, there is no inherent limitation in licensing FCF designed fuel up to a maximum fuel assembly burnup of [c,d,e] MWd/mtU. This report, BAW-10186P, requests limits of [c,d,e] MWd/mtU for a maximum fuel assembly burnup and [c,d,e] MWd/mtU for a maximum fuel rod burnup. These values are still lower than those indicated in BAW-10153P-A as being supported. Demonstration and test assembly programs have provided and are continuing to provide verification of acceptability of fuel performance at these exposures.

6.0 REFERENCES

1. BAW-10153P-A, Extended-Burnup Evaluation, April 1986.
2. Letter, H.N. Berkow, NRC to J.H. Taylor, Licensing B&W, Acceptance for Licensing Topical Report BAW-10153P, "EXTENDED BURNUP EVALUATION", December 3, 1985.
3. BAW-10172P "Mark-BW Mechanical Design Report." July 1988.
4. Letter, A.C. Thadani, NRC to J.H. Taylor, Licensing B&W, Acceptance for Referencing Babcock & Wilcox Topical Report BAW-10172P, "Mark-BW Mechanical Design Report" (TAC NO. 68873)", December 19, 1989.
5. Standard Review Plan, Section 4.2, NUREG-0800, Rev 2, U.S. Nuclear Regulatory Commission, July 1981.
6. BAW-1781P, " Rancho Seco Cycle 7 Reload Report - Volume 1- Mark-BZ Fuel Assembly Design Report ", April 1983.
7. BAW-2132, Irradiation of Mark-B10 Lead Assemblies in Oconee 1 Cycle 14 - Design Report. March 1991.
8. B&W Document, "Mark-C Design Report, Rev. 1," P.C. Childress, W.R. Eisenhauer, J.T. Willse, W.T. Brunson, R.S. Hoskins, W.J. West, and R.A. Copeland, August 1978.
9. NUSCO-173 Connecticut Yankee Atomic Power Company Haddam Neck Plant, Technical Report Supporting Cycle 17 Operations. June 1991.
10. ASME Code Section III," Nuclear Power Plant Components ", 1983 Edition.
11. RDD:88:5431-02:01, PIE Results on Mark BZ Zircaloy Grids After Three Cycles. J.T. Mayer and T.D. Pyecha, December 10, 1987.
12. RDD:87:2675-01:01, PIE Results on Oconee-1 Mark BZ Assemblies After Three Cycles. J.T. Mayer, T.D. Pyecha and T.G. Pitts, November 15, 1987.
13. T.D. Pyecha, et al. 1985. "Waterside Corrosion of PWR Fuel Rods Through Burnups of 50,000 MWd/mtU." Presented at the LWR Fuel Performance Meeting, April 21-24, 1985, Orlando, Florida.
14. EPRI NP-5132, Zirconium Alloy Oxidation and Hydriding Under Irradiation: Review of Pacific Northwest Laboratories Test Program Results. Project 1250-4 Final Report. April 1987.

15. BAW-1623, "Control Rod Guide Tube Measurement Program," June 1980.
16. LRC 4733-4 "Hot Cell Examination of Creep Collapse and Irradiation Growth Specimens - End of Cycle 1." July 1977
17. F. Garzarolli, P. Dewes, G. Maussner, and H. Basso. "Effects of High Neutron Fluences on Microstructure and Growth of Zircaloy-4", ASTM STP 1023, Zirconium in the Nuclear Industry, pages 641-657, November 1989.
18. BAW-10133P, Rev-1, Mark-C Fuel Assembly LOCA-Seismic Analyses Topical Report, Babcock & Wilcox, Lynchburg, Virginia, June, 1986.
19. NPGD-TM-176, STARS- Structural Analysis of a Reactor System, Babcock & Wilcox, Lynchburg, Virginia, April 1972.
20. BAW-10132P-A, Supp. 1, Analytical Methods Description - Reactor Coolant System Hydrodynamic Loadings During a Loss-Of-Coolant-Accident- Supplement-1, Topical Report, May 1979.
21. BAW-10162P-A, D.A. Wesley and K.J. Firth, "TACO3 - Fuel Pin Thermal Analysis Code," August 1989.
22. W.J. O'Donnell and B.F. Langer, "Fatigue Design Basis for Zircaloy Components." Nuclear Science and Engineering, Volume 20, pages 1-12.
23. BAW-352 "Elevated Temperature Burst Tests on Hydrided Zircaloy-4 Tubing" December 13, 1968.
24. EPRI NP-7499-SL, Hot Cell Examination of Oconee 2 Fuel Rods. September 1991.
25. BAW-10084P-A, Rev. 3, Program to Determine In-Reactor Performance of B&W Fuels--Cladding Creep Collapse--Revision 3, submitted October 1991.
26. Letter, D.M. Crutchfield, NRC to J.W. Taylor, Licensing B&W, Acceptance for Referencing of a Special Licensing Report. Contains Safety Evaluation of Special Report JHT/86-011A, "Creep Collapse Analysis for B&W Fuel." December 5, 1986.
27. BAW-10147P-A Rev. 1, Fuel Rod Bowing in Babcock & Wilcox Fuel Designs, Babcock & Wilcox, Lynchburg, Virginia, May 1983.
28. NEDO-12440, M.O. Marlowe, "In-Reactor Densification Behavior of UO₂," General Electric Co., July 1973.

29. D.W. Brite, J.L. Daniel, et.al., "EEI/EPRI Fuel Densification Program Final Report, Summary and Conclusions," BPNL, Jan. 1975.
30. W. Hering, "The KWU Fission Gas Release Model for LWR Fuel Rods," J. Nucl. Mater., Vol. 114, 1983.
31. WCAP-10180, Vols 1 and 2, M.G. Balfour, et. al., "Zorita Research and Development Program", Sept. 1982.
32. WCAP-10238, Vols 1 and 2, M.G. Balfour, et. al., "BR-3 High Burnup Fuel Rod Hot Cell Program", Nov. 1982.
33. BAW-10183P, D.A. Wesley, et. al., "Fuel Rod Gas Pressure Criterion (FRGPC)," July 1991.
34. J. Komatsu, T. Tachibana and K. Konashi, "The Melting Temperature of Irradiated Oxide Fuel," J. Nucl. Mat. 154, 1988.
35. NUREG/CR-4717, D.D. Lanning, "Irradiation History and Final Postirradiation Data for IFA-432", Nov. 1986.
36. BAW-10122A, Rev.1, Normal Operating Controls, Babcock & Wilcox, Lynchburg, Virginia, May 1984.
37. BAW-10179P, Safety Criteria and Methodology for Acceptable Cycle Reload Analysis, B&W Fuel Company, Lynchburg, Virginia, February 1991.
38. BAW-10163P-A, Core Operating Limit Methodology for Westinghouse-Designed PWRs, Babcock & Wilcox, Lynchburg, Virginia, June 1989.
39. BAW-10152-A, NOODLE - A Multi-Dimensional Two-Group Reactor Simulator, Babcock and Wilcox, Lynchburg, Virginia, June 1985.
40. BAW-10180, Rev.1, NEMO - Nodal Expansion Method Optimized, B&W Fuel Company, Lynchburg, Virginia, May 1992.38, Vol.s 1 and 2, Nov.6
41. BAW-1385, Rev. 5, Water Chemistry Manual for 177 FA Plants, January 1990.
42. BAW-2133P MARK-BW Advanced Claddings Fuel Rod Evaluation. March 1991.

ATTACHMENT 1

Appendix A to BAW-10186P

Responses to Questions 1,4,5,6,7,9,10,13,14,15,16,17,18

Question 1.

FCF's methodology in the application of its TACO3 fuel performance code, for licensing submittals, is to treat the code predictions as best-estimates, and to add to these predictions certain factors or penalties designed to account for model uncertainties and to bound the available data. These factors or penalties are then combined with bounding input assumptions to achieve bounding calculations of fuel performance.

However, the data bases for all the key code predictive parameters (e.g., fuel temperatures, fuel thermal properties, cladding mechanical properties, fission gas release, and cladding corrosion) thin out or become non-existent at high burnups (greater than 40 MWd/kgU rod-average). When this happens, conventional statistics fitting theory clearly indicates that the confidence and tolerance levels for estimated parameters and models will increase within regimes where little or no data exist.

When applying TACO3 for predicting bounding performance calculations for rod-average burnups exceeding 60 MWd/kgU, does FCF have an overall plan for increasing current confidence/tolerance limits used in the application of TACO3, and/or validating existing ones where no data currently exists? This question will be repeated below for individual performance parameters.

Response 1.

The revised burnup and power biased fuel temperature uncertainty factors for the TACO3⁽¹⁾ LOCA initialization and heat-rate-to-melt analyses that will be applied at rod average burnups exceeding 40 MWd/kgU are presented in Figures 13.3, 13.5, and 13.7. Mark-B and Mark-BW17, in these figures, designate typical fuel rod designs for B&W (15 x 15) and Westinghouse (17 x 17) reactors, respectively. Biased uncertainty factors for different fuel rod designs will be obtained using the methodology that was presented in the response to Question 13 and used to obtain those factors illustrated in Figures 13.3, 13.5, and 13.7.

The [c,d] power history uncertainty, approved for the TACO3 EOL internal gas pressure analyses, will be reduced to [c,d,e] for all uranium-dioxide fuel analyses. This reduction in power history uncertainty is based upon the uncertainty in the NEMO⁽²⁾ power history predictions. Even with this power history uncertainty reduction, it is shown in the responses to Questions 14 and 15 that the TACO3 best-estimate fission gas release and bounding EOL

internal gas pressure predictions are conservative, perhaps overly conservative, and no additional penalties are warranted at rod average burnups up to [c]MWd/kgU. In addition, the fuel temperature, fission gas release, and internal gas pressure issues addressed in Questions 13, 14, and 15 will not significantly affect the TACO3 creep collapse initialization and clad strain analyses. Therefore, no additional uncertainties are necessary for either the TACO3 creep collapse initialization or the clad strain analyses.

Question 4.

Because the rod-average linear heat generation rate (LHGR) tends to decrease with burnup, the operating time required to achieve a given increment of burnup increases. The correlation between fast neutron fluence and burnup may also change at high burnup. However, performance outcomes such as cladding oxidation and hydriding are more dependent on operating time-at-temperature than on burnup per se.

Please give typical values for the incremental additions to operating time and to fast neutron fluence that correspond to the requested extensions of assembly-average and rod-average burnups. What will be the maximum in-reactor residence times and fluences for this burnup extension? How do the maximum in-reactor residence times for current FCF fuel designs compare with the upper limits of the current data sets for cladding oxidation, hydriding, and growth?

Response 4.

There is very little addition to the maximum operating time for Mark-B fuel assemblies going to the requested burnup extension in B&W designed cores. Present Mark-B fuel designs have operated to [c,d]EFPD. In terms of fast fluence, the maximum assembly and fuel rod exposures to date are [b,c,d,e] and [b,c,d,e] n/cm², E>1MeV, respectively. For the requested burnup extension, the maximum reactor residence time is projected to be [c,d]EFPD and the maximum fast neutron fluence is projected to be [b,c,d,e] and [b,c,d,e], E>1MeV for fuel assembly and fuel rod burnups of [c] and [c] MWD/kgU respectively. The same maximum residence times and fast fluence would apply to the Mark-BW fuel design. To date the maximum residence time for the Mark-BW fuel assembly is [c,d]EFPD. The in-reactor residence times (exposure), and burnups are compared for the various FCF programs in Table 4.1.

For a graphical representation of the changes requested, the burnup and exposure times for the FCF database are shown in Figures 4.1 and 4.2. The figures show burnup on the "y" axis and exposure, in EFPD, on the "x" axis. Also plotted on the figures are the operational envelopes. Each operational envelope is enclosed by three curves. These are, 1) the peak pin power envelope, 2) the maximum fuel rod burnup limit, and 3) the maximum exposure limit. The envelopes will be adjusted as new information is obtained and codes are benchmarked against new data. Also shown are the points representing recent and near future discharge fuel assemblies. The

discharge fuel assembly points represent the average burnups for a fuel assembly. In Figure 4.1 for the Mark-B experience, the near future data points that will be examined at a planned poolside post irradiation examination (PIE) at TMI-1 in November 1995 are indicated. These additional data points will allow corrosion and growth models to be benchmarked for very long in-core exposures ([b,c,d,e]). With this additional data, FCF will be able to benchmark cladding corrosion and growth models for both high burnup and long exposures. Figure 4.2 for the Mark-BW17 shows the present data as well as the projected fourth cycle SCA PIE at [c,d]MWD/kgU in January 1997.

Future high burnup fuel is expected to fall into either of two distributions based on current design studies. The first distribution represents fuel assemblies discharged after two 2-year cycles, or after three 18-month cycles, reaching [c]to[c]MWD/kgU peak pin in [c,d]to [c,d]EFPD. The second distribution represents fuel assemblies discharged after three 2-year cycles, or four 18-month cycles, reaching [c]to [c]MWD/kgU peak pin in [c,d]to [c,d]EFPD. These zones are plotted in Figure 4.1 Current design studies show only a small effect on fast fluence due to residence time with fast fluence tending to decrease slightly at longer operating times.

The maximum discharge burnup for the two fuel designs will progress over the next six to seven years to approach the limits requested. Starting in 1997/1998 time period, fresh fuel with the higher enrichments needed to provide the reactivity to reach the requested burnups will be introduced in-core. The presently planned fuel cycles for both Mark-B and Mark-BW17 will result in a gradual progression in operational exposure. The planned progression of discharge burnups and exposures over the next four years is listed in Table 4.2.

Table 4.1
Exposure and Burnup for FCF Fuel Database

| Design | Exposure EFPD | Burnup MWd/kgU | Oxidation Data | Hydriding Data | Growth Data |
|----------------------|---------------|----------------|----------------|----------------|-------------|
| Mark-B PIE-Nov 95 | [b,c,d,e] | | | | |
| Mark-B | | | | | |
| Mark-GdB | | | | | |
| Mark-BEB | | | | | |
| Mark-BEB | | | | | |
| Mark-BW | | | | | |
| Limits | | | | | |

Burnups are given as Fuel Assembly average values.

* A rod segment from a segmented rod with a segment average burnup of [c,d]MWd/kgU was examined.

Table 4.2
Expected Discharge Burnups by Design and Year

| Year of Discharge | Mark-BW17 Design | | Mark-B Design | |
|-------------------|------------------|---------------|----------------|---------------|
| | Burnup MWd/kgU | Exposure EFPD | Burnup MWd/kgU | Exposure EFPD |
| 1995 | [b,c,d,e] | | | |
| 1996 | | | | |
| 1997 | | | | |
| 1998 | | | | |

Burnups shown are the maximum fuel assembly values

FIGURE 4.1 Mark-B Database, Burnup vs Residence Time.

[b,c,d,e]

FIGURE 4.2 Mark-BW17 Database, Burnup vs Residence Time.

[b,c,d,e]

Question 5.

In figure 2.2.1-1, fuel rod axial growth is plotted against fast neutron fluence. What burnups do the peak fluence values correspond to? Are the fluence values calculated or measured, and what are the growth uncertainty limits at the burnups requested?

Response 5.

The fast fluence and burnup relationship for Figure 2.2.1-1 is given in Table 5.1. At a burnup of [c] calculated to be [b,c,d,e] n/cm², E>1MeV. At that fluence the difference between the one sided 95/95 UTL and the best estimate growth for all fuel rods (the growth uncertainty) is [c,d,e] for the model shown in Figure 2.2.1-1. Revised values for the growth uncertainty will be determined as the data set expands and such new values used as appropriate. The overall relationship between the fast fluence and burnup is shown in Figure 5.1. This relationship is essentially identical for both the Mark-B and Mark-BW17 designs as both have nearly the same ratio of fuel mass to fuel assembly volume. The fluence is a function of the total number of fissions that occur within a given volume. As burnup increases there is an accumulation of fission products that act as neutron absorbers, thus neutron flux levels increase for a given power production with burnup. Also the fissile inventory falls so the neutron flux has to increase to maintain the same power density. This means that the fluence increases slightly faster than burnup and can be described in the form of:

$$[b,c,d,e] \quad] \quad \text{where } A = [b,c,d,e] \text{ and } B = [b,c,d,e], \quad x$$

is burnup in MWd/kgU and Φ is fluence in n/cm², E>1MeV.

Since the fission product poisons generally have long half lives, there is very little difference between the fluence with [c] MWd/kgU at [b,c] EFPD and the fluence with [c] MWd/kgU at [c,d] EFPD. Fluences for the high burnup assemblies from the PIE database are slightly below the fluence to burnup curve at higher burnups. The high burnup assemblies typically run with cooler moderator temperatures than the CASMO3 simulation assumes. The cooler moderator results in better thermalization of the neutron spectrum and results in a lower fast to thermal flux ratio. Over time this

integrates into a lower fast fluence for the lower moderator temperature. Therefore, the impact of extended cycle lengths would be a slight decrease in fast fluence from that predicted by CASMO3.

Thus the fluence from the [b,c,d,e] model is accurate or slightly conservative for burnups to [c] MWd/kgU.

The effect of the different U/H ratios for the Mark-B and Mark-BW17 designs is so slight that the one curve can be used.

Burnup values have been verified by chemical analysis of hotcell fuel specimens. The uncertainty for fluence is [b,c,d]. The uncertainty for burnup is [b,c,d]. Most of the burnups and fast neutron fluences in the database were calculated with PDQ7 and FLAME^(3,4). Later the burnups and fluences were calculated using NEMO⁽²⁾ with cross section data obtained from single-assembly CASMO3⁽⁵⁾ calculations. Since fuel rod and fuel assembly growth databases are built using best estimate calculated values for fluence, the UTL accounts for the [b,c,d] uncertainty in the fluence. Therefore, growth models statistically derived from the growth database against fluence can be used with confidence to [c] MWd/kgU.

Table 5.1
Fast Fluence to Burnup for Figure 2.2.1-1

| Program | Fluence, N/cm ² , E > 1MeV, x 1.0E+21 | Burnup, MWd/kgU |
|--------------------|--|-----------------|
| Mark-GdB | | |
| Mark-GdB | | |
| Mark-GdB | | |
| Mark-GdB - Hotcell | | |
| Mark-GdB - Hotcell | | |
| Mark-BEB 1 Cycle | | |
| Mark-BEB | | |
| Mark-BEB | | |
| Mark-BEB | | [b,c,d,e] |
| Mark-BEB | | |
| Mark-BEB - Hotcell | | |
| Mark-B | | |

FIGURE 5.1 Fast Fluence vs Burnup

[b,c,d,e]

Question 6.

The conservatism of growth and oxidation model application relative to RXA cladding and guide tube materials is emphasized in Sections 2.2.1 and 2.2.3. If authorized, will extended burnup be applied only to cores having all-RXA assembly components? If not, are there applicable data for SRA components, or will the uncertainty limits be expanded to their case for extended-burnup applications?

Response 6.

Early FCF fuel designs used SRA structural components. A transition to RXA material was made to take advantage of the lower irradiation growth associated with the RXA condition. FCF does not anticipate the use of SRA components for extended burnup application without sufficient justification to demonstrate equivalent or superior properties. In addition, the lower initial enrichments used in the early fuel designs did not provide sufficient reactivity to achieve high batch burnups.

Question 7.

On page 13, it is stated the RXA guide tube growth rate can be accommodated by the hold down springs of current designs. Please demonstrate how this conclusion was determined for each FCF fuel design.

Response 7.

Earlier Mark-B fuel designs, using alloy 718 helical holddown springs, used SRA guide tube material which had a significantly higher growth rate than the RXA material now used. A significant number of these fuel assemblies have experienced, without failure, the same holddown spring compression and stress at burnups of [c] Mwd/kgU that future fuel assemblies with RXA guide tubes will experience at [c] Mwd/kgU. Mark-BEB Irradiated holddown springs have been tested for spring force and compression to a burnup of [c,d] Mwd/kgU.

The FCF fuel designs with the Mark-B cruciform spring , Mark-BW leaf spring, and future holddown spring designs achieving the burnup goal of [c] Mwd/kgU shall meet the following design requirement:

The fuel assembly shall not become solid between core plates at the limiting condition which is cold shutdown. The analyses showing compliance to this criteria use the UTL fuel assembly growth and SRSS of the fuel assembly and core plate spacing tolerances.

Conformance to the criteria will be based on analyses and PIE examinations as data at the higher burnups can be obtained. The PIE examinations will provide additional fuel assembly growth data resulting in a reduction in the uncertainty of the growth model, and/or force compression testing of the holddown spring design(s).

The Mark-B Cruciform spring irradiated to a burnup of [c] Mwd/kgU will be tested the last quarter of 1995.

Further, the fuel designs will optimize fuel assembly length, fuel assembly growth, and holddown spring performance. The holddown springs will be able to operate to burnups of [c] Mwd/kgU based on testing which has shown:

1. The holddown springs can achieve maximum compression without cracking or fracture. The springs are tested [b,c,d,e] during design.
2. The holddown spring alloy 718 has been exposed to higher fluences than the holddown spring will receive at [c] MWd/kgU in other applications. No sudden falloff in spring force or embrittlement has been observed. These applications where alloy 718 has been used as springs include the spring stops in spacer grids and the holddown springs in orifice rod assemblies.
3. The increase in fuel assembly burnup will not increase the holddown spring fatigue usage factor. This is due to the fact that the main transients which impact the holddown spring are a function of total exposure time and the number of cycles of exposure. That is the number of shutdowns and startups is the same, or less as modern plants generally have experienced fewer mid cycle SCRAMS and shutdowns. Current holddown springs have experienced over [c,d] EFPD exposure.
4. Guide tube growth for RXA GTs in the Mark-GdB LTA has been obtained to [c,d] GWd/mtU with good experience.

Question 9.

On page 15, it is implied that fretting due to spacer grid spring relaxation is not expected for FCF fuel designs. However, recent fuel failures in Three Mile Island-1 appear to be due to grid fretting and the NRC staff are aware of grid fretting failures from other vendors at extended burnups and residence times.

Please provide further justification why each FCF fuel design will not experience fretting failures due to grid spring relaxation at the burnup level requested.

Response 9.

The recent grid fretting fuel failures observed at TMI-1 occurred in lead assemblies supplied by another vendor. Although FCF has experienced some failures from grid fretting problems, all but two of these failures were associated with a now-discontinued Alloy 718 (Inconel) intermediate spacer grid design. The two Zircaloy grid fretting failures are believed to be associated with setting of the spring stop in the spacer grid cells during manufacture. However, for failure to occur additional driving forces appear to be required, such as flow excitation (cross-flow vibration) associated with LOCA equalization holes present in B&W reactor designs. In both cases the failures have been observed in third burn assemblies and the failed rods were either in the first or second row adjacent to the reactor core barrel. No Zircaloy grid fretting failures have been observed in FCF fuel assemblies located in interior locations, unlike the TMI-1 situation referenced above.

Setting of the spring stop may occur by oversizing the cell, or by handling, which pushes the fuel rod against the spring stop. Undersized cells in peripheral grid locations could also occasionally occur when the fuel assemblies were loaded with fuel rods. The set of these cells combined with fuel diametral creepdown could then result in the rod becoming loose in the cell when it is operating under cross flow conditions.

In all cases the grid fretting damage appears to be the result of manufacturing or handling set of the spacer grid cell combined with fuel assembly residence in a location of higher crossflow. No factor has been found which suggests residence time would affect assemblies built and handled to specifications. Cell size increases due to spacer spring relaxation tend to be self limiting

as the spring stress driving the relaxation is reduced with relaxation. In current fuel rod designs the reduction in fuel rod diameter due to cladding creep is stopped by pellet support at burnups within the current base of experience. Thus some contact force is expected between the fuel rod and the spring stop up to the requested fuel rod burnup limit of [c] MWD/kgU. Mark-B fuel assemblies with Zircaloy-4 spacer grids have operated to fluences near the requested limits, and are now operating near the maximum projected residence time without any evidence of increasing fretting failures. The Mark-BW17 fuel assembly spacer grids are similar in design and operate with similar stress levels and are expected to perform in the same manner. Should any such trends start, normal radiochemistry monitoring and follow on fuel inspection would identify the location of the failed rods and determine if spacer grid fretting was responsible. Although spacer grid fretting with increasing burnup is not expected to occur, should some additional failures from this mode occur, the impact on coolant radiochemistry would be slight. Experience with spacer grid fretting failures has shown these rods to have some of the lowest release rates of any type of fuel rod defect. Spacer grid fretting will not restrict operation at the requested fuel assembly burnup limit of [c] MWD/kgU.

Question 10.

Is cladding stress due to cladding creepdown and fuel swelling accounted for in TACO3? Could the hoop stress from this source be expected to increase to levels of concern at extended burnup? If not, what prevents this from being a problem?

Response 10.

The information presented in Section 2.3.3 of the TACO3 topical report⁽¹⁾ indicates that the TACO3 total cladding strain is composed of creep, irradiation growth, thermal, and elastic strains. Furthermore, the cladding stresses are a function of the pressure exerted on the cladding surfaces and the cladding inside, mean, and outside radii which are determined from the total strain. Cladding creepdown and fuel swelling effects are reflected in the internal gas and fuel-clad contact pressure as well as the cladding strain predictions. The TACO3 predicted stresses, therefore, are clearly a function of cladding creepdown and fuel swelling. The TACO3 cladding stress and strain equations function in either a compressive or tensile mode. When fuel-clad contact occurs and the contact pressure exerted on the inside surface of the cladding from fuel swelling attains a sufficient level, a stress reversal occurs and the cladding begins to creep in an outward direction. This reduces or relaxes the cladding stresses; extended burnup cladding hoop stresses are typically less than [c]ksi. Cladding relaxation and strain hardening⁽⁶⁾ effects [b,c,c,d]. The TACO3 stress predictions are, therefore, conservative. This conservatism, however, has not placed excessive limitations or restrictions on the operation of nuclear fuel at extended burnups.

Question 13.

In Section 2.4.8, it is stated that the TACO3 code currently accounts (through the gap conductance) for whatever slight degradation has been found to-date in fuel thermal conductivity. However, there is growing evidence (References 4 and 5), that at temperatures below 1200°C, the fuel thermal conductivity is significantly degraded by advancing burnup. Please quantify these effects on power-to-melt and PCT in LOCA as a function of burnup up to the proposed burnup limit.

Response 13.

The TACO3⁽¹⁾ fuel thermal conductivity is not burnup dependent and does not degrade with advancing burnup. Incorporating a burnup dependent thermal conductivity relationship such as SIMFUEL^(5,6) into TACO3, however, produces overly conservative fuel temperature predictions. The TACO3 fuel temperature predictions were successfully benchmarked to measured data up to rod average burnups of [c] MWd/kgU. This indicates that the method used for calculating extended burnup fuel temperatures in TACO3 contains conservatism that offsets the effects of not treating burnup in the TACO3 fuel thermal conductivity relationship up to rod average burnups of [c] MWd/kgU. This conservatism must be subtracted from the TACO3 fuel temperature predictions before the impact of including burnup dependency in the fuel thermal conductivity can be assessed. The manner in which the TACO3 fuel temperature predictions were corrected for the conservatism in the TACO3 fuel temperature calculational method and including burnup dependency in the fuel thermal conductivity is highlighted below.

The TACO3 code exhibits conservatism in both extended burnup gap conductance and the radial power distribution within the pellet. The TACO3 radial power profiles (Appendix E, Reference 1) produce peak burnups that exceed recent extended burnup Neodymium EPMA data⁽⁷⁾. This data indicates that the peak burnup near the pellet surface is approximately twice the pellet average burnup. A [c,d] reduction in the TACO3 peak power is required to produce peak burnups that agree with these measurements. High peak powers near the pellet surface produce conservative LOCA initialization volumetric average pellet temperature predictions.

Two special versions of the TACO3 code were produced to investigate burnup dependent fuel thermal conductivity and radial power profile

effects. The fuel thermal conductivity in the first special version was replaced with the SIMFUEL^(8,9) thermal conductivities shown plotted in Figure 13.1. The radial power profiles in the second special version were changed to reduce the peak by [c,d] and produce local radial burnup profiles that more nearly match measured Neodymium EPMA data. The changes in the volumetric average fuel temperatures due to the fuel thermal conductivity and radial power profile effects were evaluated with these two special versions and added to the volumetric average temperatures generated with the TACO3 LOCA initialization methodology described in Appendix-I⁽¹⁾. These predictions were generated with the Mark-B and Mark-BW17 fuel rod characteristics and power histories shown in Appendix-I⁽¹⁾. The bounding volumetric average fuel temperatures and corresponding fuel temperature uncertainties obtained from these calculations exceeded those obtained with the TACO3 methodology at a [c] MWd/kgU rod average burnup. This difference was not acceptable because the TACO3 code was successfully benchmarked to measured fuel temperature data up to [c] MWd/kgU. The fuel temperature uncertainties were corrected, therefore, by [b,c,d,e]

]TACO3 fuel temperature uncertainty. These uncertainty differences were [b,c,d,e]

]burnups where the TACO3 fuel temperature predictions are not benchmarked. The bounding volumetric average fuel temperatures obtained from these calculations are compared with those obtained with the TACO3 methodology in Figures 13.2 and 13.4. The combined effect of not treating burnup dependent fuel thermal conductivity and the conservatism due to radial power profile and gap conductance effects does not exceed [c,d] at a [c] MWd/kgU rod average burnup. The corresponding multiplicative uncertainty factors obtained from these calculations are shown plotted in Figures 13.3 and 13.5.

The TACO3 code was benchmarked to measured centerline fuel temperature data with the radial power profiles described in Appendix-E⁽¹⁾. Although the conservatism in the TACO3 radial power profiles will affect the fuel volumetric average temperature predictions, it will not affect the centerline fuel temperature predictions or the heat-rate-to-melt analyses. Only the effects of not treating burnup in the TACO3 fuel thermal conductivity will affect the heat-rate-to-melt analyses. The special version of TACO3 containing the SIMFUEL thermal conductivities was again used

to estimate the effect of burnup dependent thermal conductivity on the TACO3 Appendix-I⁽¹⁾ heat-rate-to-melt methodology. These melt temperature calculations were performed in a manner identical with those performed for the volumetric average temperatures except that radial power profile effects were not included. That is, the melt temperature uncertainties calculated for the Appendix-I⁽¹⁾ Mark-B and Mark-BW17 fuel rod designs at a 40 MWd/kgU rod average burnup were again found to exceed the TACO3 uncertainty. The differences between these uncertainties and the [b,c,d] TACO3 uncertainty, therefore, were [b,c,d,e

]. Clearly, a reduction in fuel thermal conductivity will produce a decrease in the predicted linear heat rate where melting occurs. The melt temperature reductions shown in Figure 13.6 represent the difference between the limiting melt temperature predictions obtained from these calculations and the TACO3 methodology. The corresponding melt temperature uncertainty factors are shown in Figure 13.7.

It is clear from Figures 13.3, 13.5, and 13.7 that it is necessary to increase the uncertainties in the present TACO3 LOCA and heat-rate-to-melt analyses at extended burnups to address the additional uncertainties associated with the apparent existence of burnup dependent fuel thermal conductivity effects. Therefore, the methods described in the response to this question will be used to determine revised burnup and power biased fuel temperature uncertainty factors that will be applied to the TACO3⁽¹⁾ fuel temperature predictions obtained for LOCA initialization and heat-rate-to-melt analyses at rod average burnups exceeding [c]Mwd/kgU.

Figure 13.1 Burnup Dependent Thermal Conductivity

[b,c,d,e]

Figure 13.2 95/95 Vol. Ave. Fuel Temp. Comparison

[b,c,d,e]

Figure 13.3 Vol. Ave. Fuel Temp. Uncertainty

[b,c,d,e]

Figure 13.4 95/95 Vol. Ave. Fuel Temp. Comparison

[b,c,d,e]

Figure 13.5 Vol. Ave. Fuel Temp. Uncertainty

[b,c,d,e]

Figure 13.6 Fuel Melt Temperature Reduction

[b,c,d,e]

Figure 13.7 Melt Temperature Uncertainty

[b,c,d,e]

Question 14.

It is speculative to assert (page 46) that the TACO3 fission gas release model will either predict or bound the release from extended-burnup rods, without code-data comparisons over the full temperature and burnup ranges of interest. There is the potential for a thermal release from the ultra-high burnup rim region. There is also potentially enhanced diffusional release in the 500 to 850°C temperature range, as indicated in Reference 6.

Please compare TACO3 fission gas release predictions to data for FCF rods that have operated above 6 kW/ft at rod-average burnups above 55 MWd/kgU, if possible. Also, please show predicted fission gas release for the high burnup, low temperature HBEP BR-3 test PWR rods BK-365, 3-128, and 01-7-A. The data for these three rods are reported in Reference 7.

Response 14.

Three well-characterized rodlets, identified as R1, R2, and R3, were ramp tested in the Studsvik R2 experimental reactor⁽¹⁰⁾. These rodlets, which were part of the DOE/B&W extended burnup program⁽¹¹⁾, had burnups slightly greater than [c] MWd/kgU. During the tests, rodlets R1, R2, and R3 were subjected to peak power levels of [c,d], [c,d], and [c,d] kW/m [b,c,d,e], respectively. All rodlets were held at the peak power conditions for [c] hours. No failures were experienced. The measured and predicted fission gas release for rodlets R1 and R3 are listed in Table 14.1. Fission gas release measurements were not conducted for rodlet R2. The transient fission gas release predictions presented in this table were generated with the approved methodology⁽¹⁾ [b,c,d,e

].

A comparison of the measured and TACO3 predicted steady-state fission gas release for HBEP BR-3 rods BK-365, 3-128, and 01-7-A is presented in Table 14.2. It can be seen from the measured-to-predicted ratios presented in Tables 14.1 and 14.2 that the TACO3 best-estimate transient and steady-state fission gas release predictions [b,c,d,e] for all of the above rodlets and rods. Therefore, the TACO3 fission gas release predictions bound the available data with rod average burnups that exceed [c] MWd/kgU and the application of the TACO3

code and associated methodology to rod average burnups of [c]
MWd/kgU is acceptable.

Table 14.1

Transient Fission Gas Release Comparison

| <u>Rodlet</u> <u>I.D.</u> <u>_____</u> | <u>EOL</u> <u>Burnup</u> <u>GWd/tU</u> | <u>Meas.</u> <u>FGR**</u> <u>(%)</u> | <u>Pred.</u> <u>FGR</u> <u>(%)</u> | <u>Ratio</u> <u>Meas./Pred.</u> |
|--|--|--|--|------------------------------------|
| R1 | [| b,c,d,e | |] |
| R3 | [| b,c,d,e | |] |

** Xenon Release

Table 14.2

Steady-State Fission Gas Release Comparison

| <u>Rod</u> <u>I.D.</u> <u>_____</u> | <u>EOL</u> <u>Burnup</u> <u>GWd/tU</u> | <u>Meas.</u> <u>FGR</u> <u>(%)</u> | <u>Pred.</u> <u>FGR</u> <u>(%)</u> | <u>Ratio</u> <u>Meas./Pred.</u> |
|---|--|--|--|------------------------------------|
| BK 365 | [| b,c,d,e | |] |
| 3-128 | [| b,c,d,e | |] |
| 01-7-A | [| b,c,d,e | |] |

Question 15.

Please provide for each FCF fuel type predicted fission gas release and rod internal gas pressure up to extended burnups requested, using a typical (license-application) power history and methodology. Also show the corresponding best-estimate calculations. Please provide the code input for these calculations, including the power histories.

Response 15.

The B&W Fuel Company is presently manufacturing nuclear fuel for B&W (15 x 15) and Westinghouse (17 x 17) plant types and the internal gas pressure and fission gas release predictions presented in response to this question are representative of these two different plant types. The predictions also serve as examples of the methodology that would be used to generate bounding EOL internal gas pressure predictions for other fuel designs and plant types such as Westinghouse (15 x 15) or B&W (17 x 17). The fuel for B&W (15 x 15) and Westinghouse (17 x 17) plant types is referred to as Mark-B and Mark-BW17, respectively.

The best-estimate and bounding internal gas pressures for typical Mark-B and Mark-BW17 fuel designs and power history envelopes are shown in Figures 15.1 and 15.2, respectively. These predictions were generated with the approved TACO3 licensing methodology⁽¹⁾ except that [b,c,d,e

]. This [b,c,d,e] reflects the present uncertainty in the NEMO nuclear code⁽²⁾ predictions and was approved for GDTACO licensing methodology⁽¹²⁾. The [c,d,e] value will be used for all TACO3 bounding pressure licensing analyses in the future. Best-estimate internal gas pressures without the [c,d] transients, that are part of the approved licensing methodology, were included in these figures to demonstrate the conservatism in this approach. The predictions for these figures were generated with the typical rod characteristics, power history envelopes, and oxide conditions presented in Tables 15.1 through 15.8. Note that the bounding pressures for these rod designs exceed the fuel-clad lift-off criteria⁽¹³⁾ before attaining the [c] MWD/kgU rod average requested burnup limit. Either the rod designs and/or the power history envelopes would be expected to change for [c] MWD/kgU rod average burnup fuel. These figures demonstrate that the bounding internal gas pressures are

conservative, perhaps overly conservative, even with the reduction in the power history uncertainty. The EOL predicted bounding pressures are approximately [c,d] and [c,d] times the best-estimate predicted pressures for the Mark-B case with and without the transients, respectively, and even greater for the Mark-BW17 case.

The best-estimate fission gas release predictions corresponding to the above internal pressure predictions are presented in Figures 15.3 and 15.4. Bounding fission gas release predictions are not explicitly calculated as part of the TACO3 Monte Carlo bounding internal gas pressure methodology⁽¹⁾. Best-estimate fission gas releases without the [c,d] transients are again included to demonstrate the conservatism in the approved licensing methodology.

A special version of the TACO3 code was produced to investigate burnup dependent fuel conductivity effects on internal rod pressure; see the response to question 13. The fuel thermal conductivity in this version was replaced with the SIMFUEL^(8,9) thermal conductivities shown plotted in Figure 13.1. The change to the SIMFUEL burnup dependent fuel thermal conductivities increased the Mark-B and Mark-BW17 best-estimate predicted pressures by [c,d] and [c,d] psi, respectively. These increases, which appear to be primarily due to the temperature increase of the gas within the pellet dish volumes, are small in comparison with the conservatism added with the bounding internal gas pressure methodology⁽¹⁾. Note that the typical fuel rod designs analyzed would not be operated at rod average burnups above approximately [c] MWd/kgU without design changes or reductions in the operating power levels. An objective in presenting the above examples was to demonstrate the analysis methods that would be used to rod average burnups of [c] MWd/kgU.

Table 15.1

Typical Mark-B and Mark-BW17 Fuel Characteristics

| | <u>Mark-B</u> | | | <u>Mark-BW17</u> | | |
|---------------------------------|---------------|-----|-----|------------------|-----|-----|
| | Nom. | UML | LML | Nom. | UML | LML |
| Outside Dia. (inch) | | | | | | |
| Inside Dia. (inch) | | | | | | |
| RMS Rough. (μ inch) | | | | | | |
| Dish Fraction | | | | | | |
| Dish Radius (inch) [| | | | b,c,d,e | |] |
| Enrichment (%) | | | | | | |
| Chamfer Vol. (in ³) | | | | | | |
| Open Pore Fraction | | | | | | |
| Density (%) | | | | | | |
| Density Change (%) | | | | | | |

Table 15.2

Typical Mark-B and Mark-BW17 Cladding Characteristics

| | <u>Mark-B</u> | | | <u>Mark-BW17</u> | | |
|----------------------------|---------------|-----|-----|------------------|-----|-----|
| | Nom. | UML | LML | Nom. | UML | LML |
| Outside Dia. (inch) | | | | | | |
| Inside Dia. (inch) | | | | | | |
| RMS Rough. (μ inch) [| | | | b,c,d,e | |] |
| Length (inch) | | | | | | |

Table 15.3

Typical Mark-B and Mark-BW17 Rod Characteristics

| | <u>Mark-B</u> | | | <u>Mark-BW17</u> | | |
|----------------------------------|---------------|-----|-----|------------------|-----|-----|
| | Nom. | UML | LML | Nom. | UML | LML |
| Fuel Col. Len. (in) | | | | | | |
| System Pres. (psia) | | | | | | |
| Back. Pres. (psia) [| | | | b,c,d,e | |] |
| Resid. Pres. (psia) | | | | | | |
| Sorbed Gas (cm ³ /gm) | | | | | | |
| Plenum Vol. (in ³) | | | | | | |

Table 15.4

Typical Mark-B and Mark-BW Thermal-Hydraulic Conditions

| | <u>Mark-B</u> | <u>Mark-BW17</u> |
|------------------------------------|---------------|------------------|
| Subchannel Flow Rate (lb/hr) | | |
| Subchannel Hydra. Dia. (inch.) | | |
| Coolant Inlet Temperature (°F) [| b, c, d, e |] |
| Subchannel Area (in ²) | | |
| Enthalpy Rise Factor | | |

Table 15.5

Typical Mark-B and Mark-BW Power History Envelopes

| | <u>Mark-B</u> | | <u>Mark-BW17</u> | |
|---------------------------|-----------------------------------|--|---------------------------|-----------------------------------|
| Rod Avg. Burnup (GWd/mtU) | Rod Avg. Linear Heat Rate (kw/ft) | | Rod Avg. Burnup (GWd/mtU) | Rod Avg. Linear Heat Rate (kw/ft) |

[b, c, d, e]

Table 15.6

Typical Steady-State Normalized Axial Power Profiles

Axial Elev. ----- Mark-B
(inches) Burnup (GWd/mtU)

[b, c, d, e]

Axial Elev. ----- Mark-BW17
(inches) Burnup (GWd/mtU)

[

b,c,d,e

]

Table 15.6 (continued)

Typical Steady-State Normalized Axial Power Profiles

| Axial Elev. (inches) | <u>Mark-B</u> Burnup (GWd/mtU) | |
|-------------------------|-----------------------------------|------------|
| | [| b, c, d, e |

| Axial Elev. (inches) | <u>Mark-BW17</u> Burnup (GWd/mtU) | |
|-------------------------|--------------------------------------|------------|
| | [| b, c, d, e |

Table 15.6 (continued)

Typical Steady-State Normalized Axial Power Profiles

Axial Elev. ————— Mark-B
(inches) Burnup (GWd/mtU)

[b, c, d, e]

Axial Elev. ————— Mark-BW17
(inches) Burnup (GWd/mtU)

[b, c, d, e]

Table 15.7

Typical Transient Normalized Axial Power Profiles

| Axial Elev. (inches) | <u>Mark-B</u> Burnup (GWd/mtU) |
|-------------------------|-----------------------------------|
|-------------------------|-----------------------------------|

[b,c,d,e]

| Axial Elev. (inches) | <u>Mark-BW17</u> Burnup (GWd/mtU) |
|-------------------------|--------------------------------------|
|-------------------------|--------------------------------------|

[

b,c,d,e

]

Table 15.8

Typical Mark-B and Mark-BW17 Cladding Oxide Input

| <u>Mark-B</u> | | <u>Mark-BW17</u> | |
|---------------------------------|----------------------------------|---------------------------------|----------------------------------|
| Rod Avg. Burnup (GWd/mtU) | Rod Avg. Thickness (inch.) | Rod Avg. Burnup (GWd/mtU) | Rod Avg. Thickness (inch.) |

[b,c,d,e]

Oxide Thermal Conductivity =[c,d]Btu/hrft°F

Table 15.9

Typical Normalized Cladding Oxide Axial Profiles

Axial Elev. Mark-B
(inches) Burnup (GWd/mtU)

[b,c,d,e]

Axial Elev. Mark-BW17
(inches) Burnup (GWd/mtU)

[b,c,d,e]

Table 15.9 (continued)

Typical Normalized Cladding Oxide Axial Profiles

Axial Elev. Mark-B
(inches) Burnup (GWd/mtU)

[b, c, d, e]

Axial Elev. Mark-BW17
(inches) Burnup (GWd/mtU)



[

b,c,d,e

]



Table 15.9 (continued)

Typical Normalized Cladding Oxide Axial Profiles

Axial Elev. Mark-B
(inches) Burnup (GWd/mtU)

[b,c,d,e]

Axial Elev. Mark-BW17
(inches) Burnup (GWd/mtU)

[b,c,d,e]

Figure 15.1 Typical Mark-B Internal Pressure

[b,c,d,e]

Figure 15.2 Typical Mark-BW17 Internal Pressure

[b,c,d,e]

Figure 15.3 Typical Mark-B Fission Gas Release

[b,c,d,e]

Figure 15.4 Typical Mark-BW17 Fission Gas Release

[b,c,d,e]

Question 16.

In Section 4.4 it is stated that no change in methodology is warranted with respect to decay heat calculation (for LOCA analysis) at extended burnups. However, are not the confidence limits on ORIGEN code calculations for short-lived fission product concentrations at the requested extended burnups larger than for lower-burnup applications of the code, due to the greater uncertainty on fission yields for plutonium isotopes vs. uranium isotopes? What is the corresponding increase in uncertainty for decay heat, and should this be accounted for in the methodology for the calculation of decay heat input for LOCA analyses?

Response 16.

The decay heats used for LOCA analyses are independent of ORIGEN calculations. They are defined and controlled by the BWNT ECCS evaluation model to meet the requirements for calculation of decay heat defined by 10CFR50.46, Appendix K. The fission product decay, as required by Appendix K, is based on the proposed ANS standard, "Decay Energy Release Rates Following Shutdown of Uranium Fueled Thermal Reactors" (approved by subcommittee ANS-5 in October 1971, for infinite operation times a factor of 1.2). The BWNT ECCS evaluation model has been reviewed and approved by the NRC. It is widely accepted that decay heat using the ANS 1971 methodology is conservative for LOCA applications.

Question 17.

Are there any accident analyses which are affected by the shift in radial distribution of the thermal resistance and the volumetric heat generation rate at extended burnup? If so, which ones, and how sensitive are they?

Response 17.

The shift in radial distribution of the thermal resistance and the volumetric heat generation rate (radial power profile) causes a corresponding shift in radial temperature distribution within the fuel pellet and changes the pellet volumetric average temperature.

For most accident analyses these effects are not significant because of the reduced power production capability of extended burnup fuel. This includes, in particular, condition 2 events that are limited by DNBR and/or centerline fuel melt criteria because reactor trip occurs based on safety limits established for the higher power fresh fuel. Accident analyses that could potentially be affected include the LOCA, in which fuel initial volumetric average temperature (stored energy) is important, and the reactivity insertion accident (RIA), in which the fuel response to a rapid energy input must be evaluated. For PWR cores the limiting RIA event is the ejection of a control rod assembly.

Accident analyses for FCF fuel are performed with codes that are initialized to TACO3 fuel thermal predictions. As discussed in response to question 13, TACO3 provides a conservative representation of both gap conductance and radial power distribution (volumetric heat generation rate) at extended burnup conditions. A shift in radial distribution of thermal resistance is not modeled explicitly but the effect of this shift on fuel temperature is bounded by a combination of modelling conservatisms and revised burnup and power biased fuel temperature uncertainty factors.

LOCA analyses for FCF fuel are performed with either of two evaluation model code packages^(14,15). Both of these methods initialize the fuel hot spot radial power profile and fuel volumetric average fuel temperature to TACO3 predictions. The maximum local power (Fq) limit is reduced for extended burnup fuel to ensure that 10CFR50.46 limits are met. Thus extended burnup

effects, including the shift in volumetric heat generation rate, are represented.

Two methods of performing ejected rod analyses for FCF fuel are approved. BAW-10081-A, which is referenced in FSARs of currently operating B&W reactors, uses point kinetics coupled with a conservative fuel rod heatup analysis method to calculate peak fuel enthalpy. The peak enthalpy calculation applies the maximum energy insertion to the highest power fuel rod (assuming that this rod is at the design $F_{\Delta H}$ limit). This method ensures a conservative enthalpy calculation but does not include any burnup-dependent materials properties.

BAW-10150-A presents an updated, but still conservative method for performing rod ejection analyses. This method uses a point kinetics system response with a Doppler reactivity weighting factor developed from a 3-D spatial kinetics analysis. A detailed fuel thermal-hydraulics analysis (LYNXT) provides a conservative evaluation of the transient fuel and cladding temperature in the determination of fuel enthalpy and departure from nucleate boiling ratios (DNBR). The neutronics prediction in this method is dependent on core neutronics characteristics and is not sensitive to localized changes in fuel or cladding materials properties. The DNBR analysis is primarily dependent on surface heat flux, which is also insensitive to these effects, and applies the incremental power due to the ejected rod to the hot fuel rod (assuming that this rod is at the design $F_{\Delta H}$ limit), using a design power distribution. The fuel rod thermal model is initialized to TACO2 (TACO3 would be used for future applications). This method ensures a conservative enthalpy calculation but, again, does not include any burnup-dependent materials properties.

Both of the RIA prediction methods overpredict energy insertion and expected fuel failures. Thus, the currently licensed methods remain valid. Neither method includes the models that would be necessary to explicitly model extended burnup fuel thermal response, however, these models are not considered to be necessary since the overall analysis is very conservative.

Initial evaluations of the REP Na-1 RIA test performed at the French CABRI test reactor and presented at the Twentieth Water Reactor Safety Information Meeting on October 26, 1994 were that the rod failure which occurred in that test might be related to a high exposure rim formed on the outer edge of the fuel pellet.

This rim has a very fine grain structure, high porosity, and high fission gas content. The high local power (2.5 to 3 times power at the center of the pellet) imposed on this region of low density and conductivity was postulated to cause very high local temperatures at the pellet surface, causing swelling, interaction with the cladding, and a resulting rupture of the cladding. Later evaluations (such as that presented by C. M. Allison at the May 3, 1995 ACRS subcommittee meeting) indicate that sensitivity of the fuel response to the rim region power and porosity effects is significantly reduced when a realistic pulse width is considered for the energy insertion (i.e. 100 msec, typical of a PWR, rather than 10 msec as used in the test). Thus it is not expected that this effect will be a significant actor in future accident analyses.

FCF is currently developing a three-dimensional transient core neutronics code that will be capable of performing realistic 3-D ejected rod calculations. This code is expected to be submitted for NRC review by the end of 1995. It is anticipated that the use of the 3-D calculations will demonstrate that energy insertion levels for extended burnup fuel are low enough such that detailed fuel rod transient calculations for extended burnup fuel will not be necessary.

Question 18.

In the reference list of the subject document there appears to be a typographical error in the identification of BAW-10084P-A as an NRC approved document. This document has not been approved by NRC as of 5/1/95.

Response 18.

The acceptance letter and accompanying safety evaluation report (SER) for BAW-10084P-A were issued by the NRC on April 20, 1995. FCF has incorporated the acceptance letter and SER into the accepted version of the report. The accepted version of BAW-10084P, Rev. 3 was submitted to the NRC on July 18, 1995.

References

1. D. A. Wesley and K. J. Firth, "TACO3 -- Fuel Pin Thermal Analysis Computer Code," BAW-10162P-A, B&W Fuel Co., Lynchburg, Va., October 1989.
2. G. H. Hobson, et al., "NEMO -- Nodal Expansion Method Optimized," BAW-10180P-A. Rev 1., March 1993
3. H. A. Hassan, et. al., Babcock & Wilcox`s version of PDQ7 - User`s Manual, BAW-10117A, Babcock & Wilcox, February 1977.
4. C. W. Mays, "FLAME3 -- Computer Code for Calculating Core Reactivity and Power Distribution," BAW-10124A, August 1976.
5. M. Edenius, et. al., "CASMO3 -- A Fuel Assembly Burnup Program," Studsvik/NFA-89/3, Studsvik AB, Nykoping, Sweden, November 1989.
6. Y. Matsuo, "Creep Behavior of Zircaloy Cladding under Variable Conditions" ASTM-STP-1023, 1988.
7. K. Malen and S. Bengtsson, "PIE on ANO-1 High Burnup Fuel, Final Report," Studsvik/N(H)-93/15 Rev., Appendix C5, August 31, 1993.
8. P. G. Lucuta, et. al., "Thermal Conductivity of SIMFUEL," J. Nucl. Mater. 188, 1992, pp. 198-204.
9. P. G. Lucuta, et. al., "Task 1.4 Thermal Properties of UO₂ - Based SIMFUEL," Belgonucleaire High Burnup Chemistry Report, HBC 92/43, Nov. 1992.
10. D. A. Wesley, et. al., "Mark-BEB Ramp Testing Program," ANS 1994 International Topical Meeting on LWR Fuel Performance, West Palm Beach, Florida, April 19, 1994.
11. L. W. Newman, et. al., "Development of an Extended Burnup Mark-B Design Thirteen Progress Report: July 1987 - December 1990 and Project Summary," DOE/ET/34213-16, BAW-1532-13, 1990.
12. D. A. Wesley, et. al., "GDTACO - Urania Gadolinia Fuel Pin Thermal Analysis Code," BAW-10184-A, B&W Fuel Co., Lynchburg, Va., June 1994.

13. D. A. Wesley, et. al., "Fuel Rod Gas Pressure Criterion (FRGPC)," BAW-10183P-A, B&W Fuel Co., Lynchburg, Va., March 1994.
14. B.M. Dunn, et al, "B&W's ECCS Evaluation Model," BAW-10104PA, Revision 5, Babcock & Wilcox, Lynchburg, Virginia, November 1986
15. "RSG LOCA - BWNT Loss of Coolant Accident Evaluation Model for Recirculating Steam Generator Plants," BAW-10168P Revision 2, B&W Nuclear Technologies, Lynchburg, Virginia, October 1992

ATTACHMENT 1

Appendix B to BAW-10186P
Responses to Questions 2, 3, 8, 11, 12

QUESTION 2: The Mark B fuel designs appear to be the only FCF design that has been irradiated to rod-average burnups near 60 MWd/kgU with the remaining FCF designs irradiated to burnup levels only 60% or less of the burnup limit requested. There are several phenomena of concern that are fuel/plant design specific, such as corrosion, grid spacer spring relaxation, assembly and fuel rod growth, and crud buildup. What lead test programs (LTAs) or other testing programs are planned to demonstrate that these design specific phenomena are satisfactory for the Marks BW and Mark C designs?

RESPONSE 2: FCF has several test programs in place coordinated with those of our parent company Framatome. One of these programs which is in its third cycle will calibrate FCF models to Framatome data by irradiating both FCF and Framatome fuel rod claddings in the McGuire 1 reactor. This will allow better use of the extensive Framatome high burnup database for 17x17 fuel designs for the Westinghouse reactor plant design. Framatome has completed fuel assembly irradiations to 58 MWd/kgU with peak fuel rod burnups of 60 MWd/kgU, and will complete irradiation of a 65 MWd/kgU fuel rod in 1995.

Post-irradiation examination (PIE) programs have been made and are planned to gather data on lead-burnup assemblies of both the Mark-B and Mark-BW designs. The U.S. programs are described in Table 2.1. Details on the current PIE database are given in the response to question 4. Since the Bellefonte reactor plant is in a delay status, there is no testing currently planned for the Mark-C fuel design. The near term PIEs will provide a means to match predicted performance with actual performance to provide sufficient confidence to commit fuel designs for higher burnups. Starting in 1997, core designs will begin the transition to fuel with sufficient enrichment to achieve maximum fuel rod burnups of 65 MWd/kgU. FCF will perform fuel inspections on the first Mark-B batch to have maximum fuel rod burnups exceeding 64 MWd/kgU and the first Mark-BW17 batch to have maximum fuel rod burnups exceed 60 MWd/kgU. Also the first Mark-BW17 batch to have maximum fuel rod burnups exceed 64 MWd/kgU will be examined.

Table 2.1 shows the various performance attributes to be inspected at each planned PIE. Crud thickness and spacer grid spring relaxation are not listed. Crud thickness measurements are sometimes taken during cladding oxide measurements. Crud thickness is determined by performing oxide measurements before and after crud removal. These measurements to date have not shown any burnup effect on crud thickness. There are no plans to directly measure spacer grid spring relaxation. No evidence has been observed to indicate that spacer grid spring relaxation is a problem as explained in the response to question 9.

TABLE 2.1 Near Term High burnup PIEs Planned

| PLANT | DESIGN | BURNUPS MWd/kgU | MEASUREMENTS |
|-----------------|--|--------------------|--------------|
| TMI-1 | Mark-B [Extended Cycles] | | |
| McGuire 1 12/95 | Mark-BW17- SCA [Advanced Claddings & FCF & French Claddings] | [b,c,d,e] | |
| McGuire 1, 1/96 | Mark-BW17 | | |
| McGuire 2, 7/96 | Mark-BW17 | | |
| McGuire 1, 4/97 | Mark-BW17 - SCA [Advanced Claddings & FCF & French Claddings] | | |

Key to Measurements

[b,c,d,e]

QUESTION 3: Several discussions in the subject document state that mechanical analyses have been performed up to the burnups levels requested and that these analyses demonstrate adequate margin for all FCF designs. Please provide design specific calculational results for the following analyses: cladding fatigue, cladding stress and strain, creep collapse, cladding corrosion and centerline melting. If the analysis results are already in the subject document, please refer to the appropriate page number. Also provide the power histories used to perform these calculations.

RESPONSE 3: Each of the FCF fuel rod designs is evolving with time, to meet customer needs (with the exception of the Mark-C design, which is currently on hold due to a delay in the construction schedule for the Bellefonte reactors). Each of the design evolutions is analyzed with the models and evaluation methods presented in BAW-10186P to determine burnup capability and margins to the various design criteria. When these evaluation methods and criteria are applied to specific fuel rod designs and power histories, some applications will be limited to burnup values that are less than [c] MWd/kgU. FCF is requesting approval for the methods that are used to determine the burnup capability of the specific designs, for application at fuel rod average burnup values up to [c] MWd/kgU.

The following tables and figures present results of the requested analyses for two specific fuel rod designs, one Mark-B and one Mark-BW17, both of which are currently in service. For these analyses, power histories were chosen to illustrate the effects of operation to [c] MWd/kgU. The power histories selected are not necessarily bounding; for reload cycle designs, the process used is to [b,c,d,e

]. This approach permits the use of a given fuel rod design for different customers having different reload cycle needs (e.g. cycle lengths, feed batch size, enrichment). Table 3.1 summarizes the analyses performed and lists the tables (3.4 and 3.5) and figures (3.2 through 3.6) where individual results are provided. Table 3.2 provides design details for the two fuel rods analyzed, while Table 3.3 and Figure 3.1 show the power histories assumed.

TABLE 3.1 Summary of Fuel Rod Analyses

| ANALYSIS | LIMITING CRITERIA | RESULTS | DETAILED RESULTS PRESENTED IN |
|--------------------|---|---|---|
| Cladding Fatigue | Fatigue Usage Factor $\leq [c]$ | Fatigue Usage Factor Mark-BW = [c,d] Mark-B = [c,d] | Mark-BW17 in Table 3.4 Mark-B in Table 3.5 |
| Rod Pressure | Peak Rod Pressure $\leq [c,d]$ psi above nominal system pressure: Mark-B $\leq [c,d]$ psia Mark-BW17 $\leq [c,d]$ psia and $\epsilon_{\text{cladding}} / \epsilon_{\text{shelllet}} \leq [c,d]$ | At [c] MWd/kgU, Peak Rod Pressure is: Mark-BW = [c,d,e]psi Mark-B = [c,d] psi | Mark-B and Mark-BW17 pin pressures are shown in Figure 3.2 |
| Cladding Stress | Cladding stress intensity less than limits based on ASME criteria. | Stress Intensities less than limits, minimum margins are Mark-BW = [b,c,d,e] Mark-B = [b,c,d,e] | Mark-BW17 in Table 3.4 Mark-B in Table 3.5 |
| Cladding Strain | Cladding transient strain $\leq [c,d]$ | LHGR limits to preclude exceeding 1% cladding transient strain were determined. | LHGR limits shown vs burnup are shown for: Mark-BW17 in Figure 3.3 Mark-B in Figure 3.4 |
| Creep Collapse | No predicted creep collapse | No creep collapse predicted | Cladding ovality vs burnup shown in Figure 3.5, note 1. |
| Cladding Corrosion | Peak Oxide thickness $\leq [c,d]$ μm . | Maximum oxide thickness at [c] MWd/kgU is: Mark-BW = [b,c,d,e] Mark-B = [b,c,d,e] | Maximum oxide thickness shown in Figure 3.6 |

TABLE 3.1 Summary of Fuel Rod Analyses

| ANALYSIS | LIMITING CRITERIA | RESULTS | DETAILED RESULTS PRESENTED IN |
|--------------------|------------------------------------|--|--|
| Centerline Melting | No predicted centerline fuel melt. | LHGR limits to preclude centerline fuel melting were determined. | LHGR limits shown vs burnup are shown in: Mark-BW17 in Figure 3.3 Mark-B in Figure 3.4 |

Notes:

1. The shape of the cladding ovality vs burnup curve for the Mark-BW17 and Mark-B differs due to differences in the ratio of cladding thickness to diameter and power histories. [b,c,d,e

].

TABLE 3.2 Fuel Design Description

| PARAMETER | MARK-B | MARK-BW17 |
|--|--------|-----------|
| Fuel Rod Length, in. | | |
| Cladding OD, in. | | |
| Cladding ID, in. | | |
| Fuel Stack Length, in. | | |
| Fuel Pellet Diameter, in. | | |
| Pellet - Cladding Gap, in. | | |
| Fuel Pellet Density, %TD. | [| b,c,d,e] |
| Fuel Dish Radius, in. | | |
| Volume Fraction in Pellet Dishes | | |
| Fuel Stack Chamfer Volume, in ³ . | | |
| Plenum Volume, in ³ . | | |
| Fill Gas Pressure, psig | | |

TABLE 3.3 Steady State Power History

| Mark-B Avg LHGR = 5.72 kw/ft | | Mark-BW17 Avg LHGR = 5.58 kw/ft | |
|---------------------------------|-----|------------------------------------|-----|
| Burnup, MWd/kgU | RPD | Burnup, MWd/kgU | RPD |
| [b,c,d,e] | | | |

TABLE 3.4 Mark-BW17 Cladding Stress Results

| STRESS CONDITION | LIMIT (psi) | MAXIMUM STRESS (psi) | MARGIN |
|---|-------------|----------------------|--------|
| Primary Membrane (Pm) | [b,c,d,e] | | |
| Primary Membrane + Bending (Pm + Pb) | | | |
| Primary Membrane + Bending + Local (Pm + Pb + Pl) | | | |
| Primary Membrane + Bending + Local + Secondary (Pm + Pb + Pl + Q) | | | |
| | LIMIT | MAXIMUM | MARGIN |
| FATIGUE USAGE FACTOR | [b,c,d,e] | | |

| TABLE 3.5 Mark-B Cladding Stress Results | | | |
|---|-------------|----------------------|--------|
| STRESS CONDITION | LIMIT (psi) | MAXIMUM STRESS (psi) | MARGIN |
| Primary Membrane (Pm) | [b,c,d,e] | | |
| Primary Membrane + Bending (Pm + Pb) | | | |
| Primary Membrane + Bending + Local (Pm + Pb + Pl) | | | |
| Primary Membrane + Bending + Local + Secondary (Pm + Pb + Pl + Q) | | | |
| | LIMIT | MAXIMUM | MARGIN |
| FATIGUE USAGE FACTOR | [b,c,d,e] | | |

Figure 3.1 Fuel Rod Power History

[b,c,d,e]

Figure 3.2 Peak Pin Pressure vs Burnup

[b,c,d,e]

Figure 3.3 LHGR Limits for Mark-BW17 Fuel Rod

[b,c,d,e]

Figure 3.4 LHGR Limits for Mark-B Fuel Rod

[b,c,d,e]

Figure 3.5 Cladding Ovality vs Burnup

[b,c,d,e]

Figure 3.6 Maximum Cladding Oxide Thickness vs Burnup

[

b,c,d,e

]

QUESTION 8: There are other data (Reference 1) ($> 11 \times 10^{21}$ n/cm²) and high corrosion (≥ 50 μ m and hydrogen levels ≥ 400 ppm) that suggests that cladding ductility at high fluence will degrade significantly, such that the 1% strain limit and fatigue strength curves may not be applicable. Discuss the reference 1 data relative to fatigue strength and cladding strain requirements. Does FCF have ductility and fatigue strength data for FCF cladding up to the burnup level requested? If not how can FCF be assured that the cladding can withstand normal operation and anticipated operational occurrences (AOOs) for this burnup extension, particularly if cladding ductility is degraded.

RESPONSE 8: The reference 1 data are restricted by EPRI and are not available to FCF for a reasonable price. Therefore, FCF cannot readily comment on that data. FCF does not have fatigue data on irradiated cladding. However, FCF has tensile data (yield strength, UTS and ductility) on cladding from fuel rods up to an average burnup of [c,d] MWd/kgU and a local burnup of [c,d] MWd/kgU. The corresponding fast fluences ($E > 1$ MeV) are [b,c,d,e] n/cm², rod average and [b,c,d,e] n/cm², local. A rod average burnup of [c,d] MWd/kgU would correspond to a fast fluence of approximately [b,c,d,e] n/cm², $E > 1$ MeV.

Evaluations by FCF indicate that the test method used to determine cladding ductility is of prime importance. The expanding mandrel test (ring) used by FCF approximates the conditions experienced by a high burnup fuel rod undergoing a power transient or an AOO. Both axial and ring tensile testing by FCF shows good ductility on high burnup cladding. A summary of ductility data is given in Table 8.1. The good FCF high burnup ductility performance is also borne out by the results of ramp testing on Mark-BEB segmented fuel rods irradiated in ANO-1 to a minimum of [c] MWd/kgU. The segments were ramped to a maximum of [c,d] kw/ft ([c,d] kw/m) and no failures were observed. These results are discussed in the response to question 14. The cladding for the Mark-BW17 would be expected to have similar performance as the cladding specification, texture and heat treatment are essentially identical.

In condition I and II events (AOOs are condition II events), the only phenomenon that results in cladding tensile stresses above yield is pellet cladding interaction (PCI), not an increase in fuel rod internal pressure. The ring or axial tensile tests are appropriate to simulate PCI and these have shown very good performance at burnups up to [c] MWd/kgU. Therefore, the cladding ductility is not degraded with burnup below the 1% strain limits that set reactor operation for condition I and II events.

Also from reviewing Table 8.1 it can be observed that there is little effect from corrosion. Specimens tested with both high fluence and high oxide thickness showed uniform ductility well above 1%. Based on the combined evidence of the FCF cladding data, and the results of ramp testing, fuel rod integrity will not be impacted by fuel rod burnups up to [c] MWd/kgU provided all of the operational criteria are met.

The cladding ductility for FCF cladding was determined by the following techniques. For all tests a segment of fuel rod was defueled and a length of cladding was cut. For the tensile tests a length of [b,c,d,e] was used. For ring tests a length of [c,d] inches was used. The samples were then

ultrasonically cleaned to remove any loose fuel debris.

In tensile tests the specimen was then mounted on an Instron machine. Extensometer gaging platforms were spring-loaded to the specimen such that the knife edges were 2 inches apart and centered on the specimen and a resistance heated split tube furnace installed around the specimen.

The temperature was increased to the test temperature and when a stable temperature was achieved, then the Instron head movement was paced to give a constant strain rate until the specimen broke.

For ring tensile tests the specimen was then mounted on a split mandrel which was connected to an Instron machine. Then a resistance heated split tube furnace was installed around the specimen. The temperature was increased to the test temperature and when a stable temperature was achieved, the Instron was moved at a constant head speed until the specimen broke.

TABLE 8.1 FCF Irradiated Uniform Ductility Data Summary

B-19

[

b,c,d,e

]

TABLE 8.1 FCF Irradiated Uniform Ductility Data Summary

[

b,c,d,e

]

Figure 8.1 FCF Cladding Irradiation Ductility

[b,c,d,e]

QUESTION 11: Calculated cladding oxidation is sensitive to both the maximum coolant temperature, and to the local heat flux and consequent cladding temperatures. However, it is clear from Table 1-2 that both the maximum coolant temperatures and the rod dimensions (hence heat flux at given LHGRs) vary between the FCF fuel rod designs. Therefore, we are not sure how to interpret the discussion in Section 2.3.2, and especially the accompanying figure 2.3.1-2. We do not understand how the single "OXIDEPC" curve in that figure can be directly compared to the data points from different designs operating in varied coolant conditions. Does the curve in the figure represent some bounding or design curve, applicable to all FCF fuel designs and expected operating conditions? How can span-average oxide thickness be considered conservative when failure due to corrosion and embrittlement is a localized event?

We also note that open-literature data on corrosion layer thicknesses for Zircaloy-4 clad PWR rods include thicknesses in excess of 100 microns, for rod average burnups as low as 45 MWd/KgU. (See, for example, References 2 and 3) Therefore, the concluding statement of Section 2.3.2, that "parameters are well within design models" needs more justification. Please compare design calculations for oxide layer thickness as a function of burnup (tailored to appropriate rod dimensions and operating conditions) to data, for each of the FCF fuel designs separately. Discuss the maximum cladding temperature of the corrosion data sets relative to the maximum calculated temperatures for each of the FCF fuel designs. What are maximum possible coolant outlet temperatures for plants with FCF fuel?

RESPONSE 11: The oxide vs burnup curve shown in Figure 2.3.1-2. used a [b,c,d,e] rod power history as input into OXIDEPC along with design parameters for the Mark-B fuel rod. It was used to show the expected progression of oxide thickness with burnup for the cycle designs then existing. Separate calculations would be performed for each design and for specific limiting power histories in the future. Note that FCF is now using a new oxide code COROS02 which is described in the response to question 12. The response to question 3 shows both the power histories and resulting oxide thickness as calculated by COROS02 for the Mark-B and Mark-BW designs. New power histories will be evaluated as future fuel cycle designs evolve.

Span average oxide thickness will no longer be used as a criterion. FCF agrees that the local maximum oxide is important in preventing failure due to corrosion. The span average oxide thickness was used as a criterion as it permits correlation between the oxide code and measured data from poolside exams. Due to bounce of the eddy current probes used to measure oxide thickness, local oxide maximums are considered unreliable, but the span average values show good consistency between poolside and hotcell measurements. In the future, FCF will use the maximum local predicted value of oxide as a criterion, but will benchmark the oxide code predicted span average values to the measured span average values. Details on the use of COROS02 in predicting the maximum local oxide value are given in the response to question 12.

With respect to the reference 2 and 3 data, a review showed one graph, Figure 1 in reference 2 where the oxide thickness at [c] MWd/kgU exceeded [c,d,e]. This data represents 4 cycles of operation in the Ringhals 3 reactor with type 3a cladding. The reported operating conditions with the exception of lithium levels (3.5 ppm BOC) are not particularly severe, so FCF cannot explain the high oxide thickness at [c] MWd/kgU. If FCF were irradiating fuel under different operating conditions for the first time, FCF would require a PIE program or other supporting data to follow cladding corrosion for the first use of elevated lithium at levels such as those used in Ringhals 3. Other industry data supports the use of modern cladding to rod average burnups of [c] MWd/kgU. In reference 3, figure 1 showed the oxide thickness vs burnup for typical Westinghouse cladding. Only one high burnup data point at > 60 MWd/kgU exceeded the [c,d] μm criterion used by FCF. That high datapoint was 136 μm. Although spalling was reported, no fuel failures were observed. It is assumed that the cladding was standard Zircaloy-4 with around 1.5 wt% Sn given the manufacturing date of 1982. With the improvement of > 30% in corrosion observed with low tin optimized annealed cladding, burnups of [c] MWd/kgU can be achieved with reasonable power histories as shown in the response to question 3. Hence FCF requests permission to go to the requested burnup provided that the specified criteria are met. High burnup fuel cycles will be evaluated using the particular features of each fuel cycle in terms of fuel design and operating conditions.

The cladding temperatures of the FCF corrosion data set are below those used in the most limiting analyses. The high burnup data available now represents fuel that was pushed with long residence times compared to future fuel cycles in which the fuel will achieve higher burnups in shorter residence times. The PIE just completed at TMI will benchmark the oxide code to a variety of conditions and represents the highest long term cladding temperatures observed to date ([c,d]MWd/kgU in [c,d] JEPD). The current benchmarking of the oxide code provides confidence that the code will properly predict cladding corrosion under future operating conditions. Preliminary results from TMI show good correlation between COROS02 predictions and measured values for low tin zircaloy-4 cladding. Two assemblies were inspected which had reached [c,d] MWd/kgU in [c,d] JEPD (2 cycles). The results were:

| Assembly | Number of Fuel Rods Examined | Span 2 Average Oxide Thickness Range, μm. | COROS02 Span 2 Average Prediction, μm. |
|----------|------------------------------|---|--|
| NJ05YU | 15 | [b,c,d,e] | |
| NJ05YM | 15 | | |

FCF is now using the oxide code COROS02 as described in the response to question 12. A description of the use of COROS02 in predicting fuel rod cladding oxide is also provided in the response to question 12.

The maximum possible outlet temperature is T_{sat} for the nominal operating conditions. However, typical coolant outlet temperatures are significantly less, and tend to decrease with burnup. As an example, for the three and four loop Westinghouse designed plants that the Mark-BW17 was designed for the typical maximum core outlet temperature is 625 °F. Only for the highest powered fuel rods does the effective maximum coolant temperature reach T_{sat} (654.6 °F @ 2280 psia). A comparison of the Mark-B and Mark-BW operating conditions shows:

| DESIGN | TYPICAL MAXIMUM CORE EXIT TEMPERATURE, °F | T_{sat} , °F |
|-----------|---|----------------|
| Mark-BW17 | [c,d] | 654.6 |
| Mark-B | [c,d] | 649.4 |

A significant portion of the FCF corrosion database is poolside data on peripheral fuel rods and all of the planned exams are for poolside exams of peripheral rods. As current and future fuel design burnups increase, the oxide predictions from COROS02 will be compared to this data. The reliability of peripheral oxide data as a benchmark for COROS02 for FCF use is considered to be excellent, based on data that shows that the peripheral line scan oxide measurements give a good indication of fuel rod oxide thickness. Figure 11.1 shows the limiting span 2 (second span from top) average oxide values for the 4 cycle Mark-GdB fuel assembly as a function of position within the fuel assembly. The peripheral rod scans were all obtained poolside. The interior rod scans were all obtained in the hotcell. The values for the corner rods were the average of the two scans from both faces. The interior scans were the average of two or three linear scans with the fuel rod rotated between scans. The maximum poolside value is [c,d]µm while the maximum interior value is [c,d]µm. This represents a good agreement.

Also a comparison was made between hotcell and poolside oxide measurements that were obtained from the Mark-BEB 3 cycle LTAs at [c,d] MWd/kgU. The limiting span 2 oxide values were compared between two fuel assemblies operated symmetrically, one with the fuel rods examined poolside, the other with the fuel rod examined in the hotcell. The comparison shows:

| | | | | |
|--------|----------|---------------|----------|---|
| NJ023Q | Hotcell | Average Oxide | [b,c,d,e |] |
| | | Maximum Oxide | [b,c,d,e |] |
| NJ023P | Poolside | Average Oxide | [b,c,d,e |] |
| | | Maximum Oxide | [b,c,d,e |] |

Hotcell measurements have also compared oxide thickness from the eddy current oxide probe to that obtained by metallography. On five fuel rods, the oxide thickness was determined at four points 90 deg apart, both by eddy current probe, then by sectioning the fuel rod and examining the oxide layer by metallography. These results are shown in Figure 11.2 which shows a slight over prediction by the oxide probe at higher oxide thicknesses. Overall, a comparison can be made between the oxide code prediction of the span average and the maximum rod average span determined by peripheral eddy current scans. This allows benchmarking of the code for new fuel types and reactor environments.

FIGURE 11.4

Cycle Mark-GdB Span 2 Average Oxide, um vs Fuel Rod Position

[

b,c,d,e

]

Figure 11.2 Comparison of Eddy Current and Metallographic Oxide Thickness Results

[b,c,d,e]

QUESTION 12: Describe or reference the OXIDEPC code mentioned in Figure 2.3.2-1. Does this code utilize the Garzarolli model shown on page 16 and described in reference 13 of BAW-10186P, or some other model? How is the model applied? For example, is it evaluated at the temperature of the oxide-water interface or that of the metal-oxide interface? If the latter, how is the heat flux effect accounted for? And, how is the differential form integrated through time, given that the powers and temperatures at a given axial node may vary significantly through the power history?

RESPONSE 12: The code OXIDEPC uses the Garzarolli model shown on page 16. The model is evaluated at the metal-oxide interface. The rise in temperature across the oxide layer is accounted for using a constant thermal conductivity for the oxide of [c,d,e]w/cm °K. The fuel rod is divided into a series of axial nodes similar to those used in a fuel performance code and the coolant temperature, cladding temperature and corrosion rate are calculated at each node. Then the corrosion rate is integrated for the time step to determine the increase in oxide thickness, and then the process starts again at the next time step using the new oxide thickness.

For future use the OXIDEPC code has been replaced by the Framatome code COROS02 described in references 1 and 2, attached. At the end of this response is a written description on the planned use of COROS02 in predicting fuel rod cladding oxide. The COROS02 code uses similar fuel rod design and operational inputs as those used by TACO3. In the COROS02 code the oxide is calculated by the formula:

Pre Transition, for oxide layer growth up to the transition thickness in the range of 2 to 3 μm:

[b,c,d,e]

Post Transition, for oxide layer growth once the transition oxide thickness has been reached:

[b,c,d,e]

[b,c,d,e]

The benchmarking for COROS02 is shown in Figure 12.1 for standard tin cladding and in Figure 12.2 for low tin cladding.

COROS02 OXIDE PREDICTION

COROS02 uses input similar to a standard fuel performance code such as TACO3. The inputs used are:

[b,c,d,e]

FIGURE 12.1

Standard Tin Cladding Predicted vs Measured Oxide Thickness

[b,c,d,e]

FIGURE 12.2

Low Tin Cladding Predicted vs Measured Oxide Thickness

[

b,c,d,e

]

REFERENCES

- 1 P.H. Billot, et. al., Comparison of Zircaloy Corrosion Models from the Evaluation of In-Reactor and Out-of Pile Loop Performance, Ninth International Symposium on Zirconium in the Nuclear Industry, ASTM STP 1132, Philadelphia, 1991, p. 539.
- 2 M. Morel, et. al., Technique and Method for Upgrading Corrosion Performance through Framema Fuel Experience Feedback, Proceedings of the 1994 International Topical Meeting on Light Water Reactor Fuel Performance, April 17-21, 1994, West Palm Beach, Fl. p 296.

Appendix C to BAW-10186P

**Additional information provided as a result of the
telephone conference of February 29, 1996**

Following are the responses to questions raised during a telephone conference held on February 29, 1996 between FCF personnel, E. Kendrick of NRC/NRR, and C. Beyer, of PNL. All of the questions address responses to NRC review questions provided in references 1 and 2. In order to avoid confusion with the earlier responses, these responses are numbered sequentially, starting with "C-1." Each question includes a reference to the previous response (from references 1 and 2) that is being supplemented.

Question C-1. In response # 3 on page B-9 (reference 2), table 3.4 shows a fatigue usage factor of 0.55 and a margin of 15.4%. Which is correct?

Response: The fatigue usage factor is [c,d] and the margin should be [c,d,e]. Table 3.4 will be corrected as shown on the attachment.

Question C-2. Regarding responses #4 and #8 (references 1 and 2, respectively), provide additional information and clarification for the Mark-GdB and Mark-BEB assemblies discussed in Table 4.1. Also, in the response to question 8, Framatome Cogema Fuels has burnup experience listed at 57.3 and 58.3 MWd/kgU. What programs are these data points from and what is the operating history? What oxide and hydrogen levels are associated with these data points? Response #8 lists cladding from a fuel rod with a burnup of 59.7 MWd/kgU, but table 8.1 does not show data for that burnup. What do the reported test values from Figure 8.1 mean?

Response: The [c,d] MWd/kgU data is from the Mark-BEB program. The assembly was irradiated for four cycles in ANO-1, for a discharge burnup of [c,d] MWd/kgU. Examination of the Mark-BEB assembly was sponsored through three cycles by the DOE (Reference 3). Two of the segmented rods, from locations N3 and C13, were removed from the assembly and shipped to STUDSVIK for non-destructive inspection and ramping of selected segments. Additional data for these rod segments and discussion of the ramp tests is provided in response to question C-6, below.

The [c,d] MWd/kgU data points are from the Mark-GdB assembly (References 4 and 5). The Mark-GdB was a fuel assembly with selected fuel rods containing UO₂ pellets and others containing a mixture of UO₂ and UO₂ - Gd₂O₃ pellets with 8 wt% Gd. Fuel rods with only UO₂ pellets had either solid or annular fuel pellets. The Mark-GdB assembly had RXA Zircaloy-4 intermediate spacer grids and guide tubes. It was irradiated for four cycles in Oconee 1. A poolside examination was conducted. Later a rod # 12530 (All UO₂ - annular pellets) from location H9 with a rod burnup of [c,d] MWd/kgU was extracted from the assembly and sent to the hotcell for evaluation. That rod was sectioned and cladding segments tested for ductility using both axial and ring tensile tests. The fuel assembly operating history is shown in Table C-2.1. Additional design details are provided in references 4 and 5. Poolside exam data is shown in Table C-2.2 and Hotcell data is shown in Table C-2.3. Tables C-2.4 and C-2.5 provide a summary of the cladding tensile tests. Because cladding tensile specimens are taken from many different elevations, the fuel assembly average burnup and fast

fluence were assigned to those test results when plotted. The uniform ductility is the strain (elastic + plastic) at which necking occurs. The total ductility is the strain after the specimen breaks.

| Table C-2.1 Mark-GdB Operating History | | | |
|---|---------------------------|-------------------------------|----------------------|
| Oconee 1 Cycle | Cycle Exposure EFPD | FA total Burnup MWd/kgU | Operating Conditions |
| 8 | [b,c,d,e] | | |
| 9 | | | |
| 10 | | | |
| 11 | | | |
| Annular UO2 fuel enrichment Cladding OD/ID: Pellet OD/ID: [b,c,d,e] Density: Fill Gas Pressure: | | | |

| Table C-2.2 Mark-GdB Poolside Exam After Four Cycles | |
|--|-------------|
| Measurement | Value |
| Fuel Assembly Growth | [b,c,d,e] |
| Assembly Average Fuel Rod Growth | |
| Peripheral Fuel Rod Oxide Scans. (16 rods totals) | |
| Span average and maximum values, μm by eddy current line scan. Span 1 is at top of assembly. | |

Table C-2.3
Mark-GdB Hotcell Exam After Four Cycles

| Measurement | Value |
|--|-------------|
| Interior Rod H9 (12530) UO ₂ Fuel Rod Oxide Scans. | Span |
| | 1 |
| | 2 |
| Span Average Values, μm by eddy current coil on line scan. Value is average of three scans with rod rotated between scans. | 3 |
| Scans were at 90, 170 and 340° of rotation. | 4 [b,c,d,e] |
| | 5 |
| | 6 |
| | 7 |
| Span 1 is at top of assembly | |

Table C-2.4
Mark-GdB Tensile Specimen Summary (4 Cycle Fuel Rods)
Axial Tensile Tests

| Sample | Axial Location ⁽¹⁾ | Oxide | Hydrogen | Temp | Yield Strength | Ultimate Strength | Uniform Strain | Total Strain |
|----------|-------------------------------|-------|------------------------------|-------|----------------|-------------------|----------------|--------------|
| | | μm | ppm | deg F | ksi | ksi | % | % |
| 12530-2A | [b,c,d,e] | | | | | | | |
| 12530-6E | | | | | | | | |
| 12530-2F | | | | | | | | |
| 12530-6A | | | | | | | | |
| | | * | Specimen Was Lost in Testing | | | | | |

(1) Location = Distance from bottom of rod, inches

(2) The specimen broke outside the extensometer, so the actual elongation is higher than that indicated

Table C-2.5

Mark-GdB Tensile Specimen Summary (4 Cycle Fuel Rods)

Ring Tensile Tests

| Sample | Axial Location ⁽¹⁾ | Oxid e | Hydrogen | Temp | Ultimate Strength | Uniform Strain | Total Strain |
|--|-------------------------------|--------|----------|-------|-------------------|----------------|--------------|
| | | μm | ppm | deg F | ksi | % | % |
| 6TN | [b,c,d,e] | | | | | | |
| 7TN | | | | | | | |
| 8TN | | | | | | | |
| 6TK | | | | | | | |
| 7TK | | | | | | | |
| 8TK | | | | | | | |
| 9TN | | | | | | | |
| 10TN | | | | | | | |
| 11TN | | | | | | | |
| 9TK | | | | | | | |
| 10TK | | | | | | | |
| 11TK | | | | | | | |
| (1) Location = Distance from bottom of rod, inches | | | | | | | |
| (2) Yield strength not available | | | | | | | |

Question C-3. Regarding response #7, page A-13, please provide the guide tube growth data for the Mark-GdB LTA.

Response: The Mark-GdB fuel assembly had an assembly average fast fluence of [b,c,d,e] n/cm², E > 1 MeV. The measured growth was [b,c,d,e]d/l. The limits based on the current growth model for this fluence are an LTL of [c,d,]d/l and a UTL of [c,d,]d/l.

Question C-4. Regarding the response to question #11, what are the corrosion constants in COROS02 and what is the method of integration? What is the matchup between COROS02 prediction and measured data for both span average and peak oxide (such as moving average?)

Response: The corrosion equation is:

$$[b,c,d,e] \quad] \quad \text{For pretransition}$$

$$[b,c,d,e] \quad] \quad \text{For post Transition Corrosion}$$

$$[b,c,d,e] \quad]$$

Where T is the oxide/metal interface temperature (K), t_{trans} is the transition time in seconds, and S is oxide thickness in meters.

The constants are :

| Constants | Standard Tin Zircaloy-4 | Low Tin Zircaloy-4 |
|---------------------------|-------------------------|--------------------|
| K pre (m ² /s) | [b,d,c,e] | |
| Q pre (J/mol K) | | |
| K post (m/s) | | |
| Q post (J/mol K) | | |

The oxide thickness is determined by explicitly integrating through the time steps functions of the independent variables.

The rate equation is in the form of:

$$[b,c,d,e] \quad]$$

This is algebraically manipulated to form a series of independent equations:

$$[\quad \quad \quad b,c,d,e \quad \quad \quad]$$

Where ΔS : Change in oxide thickness, meters

[b,c,d,e]

ΔS is chosen such that [b,c,d,e]

In addition the time steps must also satisfy the requirement that:

[b,c,d,e]

The COROS02 corrosion code was benchmarked to French reactor data as shown in Figures 12.1 and 12.2 in the response to question #12 (reference 2). The comparison shown on page B23 compared the COROS02 prediction to US reactor data. In Table C-4.1 the COROS02 prediction vs measured values for both span average and peak value are listed. The peak value consists of [b,c,d,e] data points. A typical [c] inch scan consists of around 460 to 630 data points [b,c,d,e]. This comparison shows that the COROS02 model, which was benchmarked to European data, does a good job of predicting the US reactor data and indicates that all of the low-tin zircaloy-4 data can be considered to be part of the same population.

| Table C-4.1 COROS02 Measured vs Predicted | | | | | |
|--|------------------------------|---|---|--|---|
| Assembly ID | Number of Fuel Rods Examined | COROS02 Span 2 Average Value, μm | COROS02 Span 2 Maximum Value, μm | Measured Span 2 Average Value, μm | Measured Span 2 Max Value, μm (Moving Average) |
| NJ05YU Mark-B | 15 | [b,c,d,e] | | | |
| NJ05YM Mark-B | 15 | | | | |
| NJ0K45 Mark-BW17 | 8 | | | | |
| NJ0K46 Mark-BW17 | 12 | | | | |

Question C-5. Regarding Figure 13.1, page A-20 (reference 1), please correct the references.

Response: A revised copy of the figure is attached, with the references corrected. This figure will replace page A-20 when the Acceptance version of BAW-10186P is published.

Question C-6. Regarding response # 14 (reference 1), please provide the base irradiation power history plus the ramped axial power profile for the rods tested at Studsvik. Also, what were the clad strains on rodlets R1 and R3?

Response: The segmented rods shipped to STUDSVIK for non-destructive inspection and ramp testing each had five segments. Table C-6.1 provides the burnup conditions for the Mark-BEB assembly. Table C-6.2 provides the data for the segmented rods. Axial power distribution and power history are tabulated in Tables C-6.3 and C-6.4 for the base irradiation. The Unit EFPD in these tables are the equivalent full power days accumulated from the first cycle of LTA operation (ANO-1, cycle 5) to the discharge of the LTA at the end of its fourth cycle (cycle 8). Spiral profilometry and ramped power profiles are provided on figures excerpted from references 6 and 7 (attachment). This information can be used to determine clad strain. Also, since the rodlets in this test program have acquired different designations in different publications, the nomenclature used in each is provided below:

| Rod Number (Assembly location) | Ref 6 & 7 Rodlet Number | Ref 8 Rodlet Number |
|-----------------------------------|----------------------------|------------------------|
| [| b,c,d,e |] |

Peak axial oxide and corresponding hydrogen by ceramography is:

Segment 2: [b,c,d,e]with[b,c,d,e]hydrogen
 [b,c,d,e]with[b,c,d,e]hydrogen
 Segment 4: [b,c,d,e]with[b,c,d,e]hydrogen
 [c,d]- not measured

| Table C-6.1 Mark-BEB Operating History | | | |
|---|---------------------------|-------------------------------|----------------------|
| ANO-1 Cycle | Cycle Exposure EFPD | FA total Burnup MWd/kgU | Operating Conditions |
| 5 | [b,c,d,e] | | |
| 6 | | | |
| 7 | | | |
| 8 | | | |

| Table C-6.2 Segmented Rod Description | | | | | |
|--|-----------------------|-----------------------------|---|--|---|
| Segment Number | Description | Segment Length inches | Segment Fuel Stack Length inches | Segment Average Fast Fluence n/cm ² x 10 ²¹ E > 1 MeV | Segment Average Burnup MWd/kgU |
| 65-# (C13) or 66-# (N3) | | | | | |
| 1 | Lower End Segment | [b,c,d,e] | | | |
| 2 | Lower Long Segment | | | | |
| 3 | Short Segment | | | | |
| 4 | Upper Long Segment | | | | |
| 5 | Upper End Segment | | | | |
| [b,c,d,e] | | | | | |

Table C-6.3
Rod 14333L (C13) Segment Power History (Kw/Ft)

| | Axial Segment Number |
|-------------|----------------------|
| Unit EFPD | |
| [b,c,d,e] | |

Table C-6.3
 Rod 14333L (C13) Segment Power History (Kw/Ft)

| | Axial Segment Number |
|-----------------------------|----------------------|
| Unit EFPD | |
| | |
| [] [] [] [] [] [] [] | |
| [] [] [] [] [] [] [] | |

Table C-6.3
 Rod 14333L (C13) Segment Power History (Kw/Ft)

| | Axial Segment Number |
|-----------|----------------------|
| Unit EFPD | |
| [|][][][][][] |
| [|][][][][][] |

| | Axial Segment Number |
|-------------|----------------------|
| Unit EFPD | |
| [b,c,d,e] | |

Table C-6.4
Rod 14334L (N3) Segment Power History (Kw/Ft)

| | Axial Segment Number |
|--------------------|----------------------|
| Unit EFPD | |
| | |
| [][][][][][] | |

Table C-6.4
Rod 14334L (N3) Segment Power History (Kw/Ft)

| | Axial Segment Number |
|-----------|---------------------------|
| Unit EFPD | |
| [|] [] [] [] [] [] [] |
| [|] [] [] [] [] [] [] |
| [|] [] [] [] [] [] [] |

Table C-6.4
 Rod 14334L (N3) Segment Power History (Kw/Ft)

| | Axial Segment Number |
|-----------|----------------------|
| Unit EFPD | |
| [|][][][][][] |
| [|][][][][][] |

Table C-6.4
Rod 14334L (N3) Segment Power History (Kw/Ft)

| | Axial Segment Number |
|-----------|----------------------|
| Unit EFPD | |
| [|][][][][][] |
| [|][][][][][] |

| Table C-6.4 Rod 14334L (N3) Segment Power History (Kw/Ft) | |
|--|----------------------|
| | Axial Segment Number |
| Unit EFPD | |
| [| [[[[[[[[[[] |
| [| [[[[[[[[[[] |

REFERENCES:

1. Attachment 1 to letter, J.H. Taylor to R.C. Jones, August 22, 1995, JHT/95-88
2. Attachment 1 to letter, J.H. Taylor to R.C. Jones, December 6, 1995, JHT/95-119

3. L.W. Newman, et al., Development of An Extended Burnup Mark B Design, Thirteenth Progress Report, July 1987 -- December 1989 and Project Summary. BAW-1532-13, Babcock & Wilcox, Lynchburg, VA , (DOE/ET/34213-16), December 1990.
4. L.W. Newman, et. al., Development of an Advanced Extended-Burnup Fuel Assembly Design Incorporating Urania-Gadolinia, Project Summary Report, BAW-1681-10, Babcock & Wilcox, Lynchburg, VA, (DOE/ET/34212-56), August 1988.
5. L.W. Newman, et. al., Development of an Advanced Extended-Burnup Fuel Assembly Design Incorporating Urania-Gadolinia, Project Summary Report, BAW-1681-11, Babcock & Wilcox, Lynchburg, VA, (DOE/ET/34212-58), February 1991.
6. EXP R2-F139R, 9139, NF(P)-92/19, "STUDSVIK/BW Mk-BEB Ramp Test Program. Rod Segmentation and non-destructive Examinations," K. Malen, Sept. 30, 1992.
7. EXP R2-F139, 9139, NF(R)-92/52 Revised), "Power Ramp Irradiation of BWFC Test Fuel Rodlets in the R2 Reactor at STUDSVIK," S. Djurle, Sept. 9, 1993.
8. D.A. Wesley, et. al., "Mark-BEB Ramp Testing Program," Paper presented at the ANS Light Water Reactor Fuel Performance Meeting, West palm Beach, Florida, April 17-21, 1994.

Figure 6.8
Ramp Test of Rod 65-2 (R2 No. 2323)
Axial Distribution of Test Fuel Rod Power
During Holding at the Ramp Terminal Level

[

b,c,d,e

]

Figure 6.1
Ramp Test of Rod 65-4 (R2 no. 2324)
Axial Distribution of Test Fuel Rod Power
During Holding at the Ramp Terminal Level

[b,c,d,e]

Figure 6.15
Ramp Test of Rod 66-2 (R2 No. 2325)
Axial Distribution of Test Fuel Rod Power
During Holding at the Ramp Terminal

[

b,c,d,e

]

Appendix D7

[

b,c,d,e

]

Appendix D8

[

b,c,d,e

]

Appendix D9

[b,c,d,e]



APPENDIX D

October 28, 1997
JHT/97-39

Document Control Desk
U. S. Nuclear Regulatory Commission
Washington, DC 20555-001

Subject: Application of BAW-10186P-A, Extended Burnup Evaluation

Gentlemen:

The safety evaluation report (SER) for FCF's Extended Burnup Topical report, BAW-10186P, was issued in April and contained limitations on the predicted cladding corrosion levels. Some items related to these limitations were not explicitly addressed, allowing some interpretation by FCF. As a result, FCF and the NRC, including its contract reviewer at PNNL, held several telephone conferences to reach agreement on these interpretations. The purpose of this letter is to document the agreements reached in these conferences and to facilitate immediate application of BAW-10186P based on current understandings. Following are the agreements reached in these conferences:

The SER for BAW-10186P characterizes the COROS02 corrosion model as "best estimate or slightly conservative." The NRC has agreed that the model may be used as a true best estimate predictor. FCF will use available high burnup data for FCF fuel designs to quantify the amount of conservatism in the model at the NRC imposed 100 micron limit. The prediction will then be adjusted by this amount and used as a best estimate predictor for oxide thickness calculations as appropriate.

FCF evaluates its fuel for oxide thickness on a sub-batch rather than on a core-wide basis. For each cycle, a sub-batch is defined as fuel that is inserted and discharged from the core at the same time so the fuel assembly residence times are identical. FCF will use the maximum burnup rod in each sub-batch as the rod with maximum oxide thickness for the purpose of evaluating the maximum oxide limit.

The maximum acceptable predicted oxide thickness limit imposed by the NRC is 100 microns. In order to gather more data for fuel with oxide layers in this range, FCF will allow a small number of fuel rods to have predicted values greater than 100 microns. The fuel assemblies containing these rods will be designated as lead assemblies. Eight fuel assemblies may be designated as lead corrosion assemblies for each fuel cycle. The eight assemblies may come from different sub-batches.

These assemblies will be placed in non-limiting core locations with respect to relative power distribution during the cycle that the predicted oxide thickness exceeds the NRC imposed 100 micron limit. Corrosion measurements will be taken on the lead corrosion assemblies after they are discharged from the core to verify the best estimate nature of the COROS02 code. These measurements will be taken to continue to refine the quantification of the best-estimate conservatism. The total number of lead corrosion assemblies in a given fuel cycle will not exceed eight; the total number of lead assemblies in a given fuel cycle, for any reason, will not exceed twelve.

To summarize, FCF and its utility customers will take the following steps in future fuel cycle designs:

1. The conservatism in the COROS02 corrosion model will be quantified; COROS02 will be used as a best estimate predictor,
2. The peak burnup fuel rod in each sub-batch will be used in determining the maximum oxide for that sub-batch,
3. Up to eight fuel assemblies from different sub-batches in each fuel cycle may have fuel rods with predicted oxide layers greater than 100 microns and will be designated as lead corrosion assemblies; corrosion measurements will be taken on the lead corrosion assemblies after they are discharged from the core; and the total number of lead assemblies in any fuel cycle will not exceed twelve.

The information included with this letter is for information only. No action is required on the part of the NRC.

The agreements documented in his letter provide an interim solution to the ongoing concern with cladding corrosion. The NRC has indicated that one solution to the problem is improved cladding materials. FCF has a program underway to license an advanced cladding alloy with a topical report (BAW-10227P) that was submitted to the NRC in September 1997. The topical contains all the safety evaluations necessary to support a rule change to include this material in the appropriate sections of 10 CFR 50. The NRC's timely review of BAW-10227P will be needed to support implementation of the advanced alloy as a long term solution to the cladding corrosion concern.

Very truly yours,

C. J. McPhatter for

J. H. Taylor, Manager
Licensing Services

cc: L.E. Phillips, NRC
S. L. Wu, NRC
J. L. Birmingham, NRC
C. E. Beyer, PNNL
R. B. Borsum

Attachment 2

Appendix E to BAW-10186

Supplement 1 to BAW-10186 Revision 1

**Supplement 1 to
BAW-10186 Revision 1
(43-10186-02)
Mark-BW Extended Burnup**

by

**John Strumpell
Garry Garner
John Willse**

November 19, 2001

Table of Contents

| | |
|--|----|
| 1.0 INTRODUCTION..... | 4 |
| 2.0 SUMMARY..... | 4 |
| 2.1 FUEL ROD BURNUP..... | 4 |
| 2.2 KEY UPDATED PIE MEASUREMENTS..... | 5 |
| 2.2.1 Fuel Rod Oxide..... | 6 |
| 2.2.2 Fuel Assembly Growth..... | 6 |
| 2.3 COMMITMENTS TO PLANNED EXAMINATIONS..... | 7 |
| 3.0 DATA SOURCES..... | 7 |
| 4.0 FUEL ROD AND ASSEMBLY MODELS..... | 12 |
| 4.1 FUEL ROD AND FUEL ASSEMBLY GROWTH..... | 12 |
| 4.1.1 Fuel Assembly Growth..... | 12 |
| 4.1.2 Shoulder Gap Closure..... | 13 |
| 4.2 FUEL ASSEMBLY STRUCTURE OXIDATION..... | 15 |
| SPACER GRID IRRADIATION GROWTH..... | 16 |
| 4.4 OXIDATION, CORROSION AND CRUD..... | 17 |
| 4.5 FUEL ROD BOWING..... | 18 |
| 4.6 CONTROL ROD DROP TIME..... | 18 |
| 4.7 DEFECTS..... | 21 |
| 5.0 EXAMINATIONS..... | 22 |
| 6.0 CONCLUSION..... | 23 |
| 7.0 REFERENCES..... | 23 |

List of Tables

| | |
|--|----|
| Table 2.1-1 Fuel Rod Burnup for High Burnup Mark-BW Fuel..... | 5 |
| Table 3.0-1 Major Fuel Performance Programs..... | 7 |
| Table 3.0-2 U.S. M5™ Fuel Rod Demonstrations..... | 8 |
| Table 3.0-3 Typical Framatome ANP, Inc. Fuel Assembly Parameters (B&W Reactor Systems)..... | 10 |
| Table 3.0-4 Typical Framatome ANP, Inc. Fuel Assembly Parameters (Westinghouse Reactor Systems)..... | 11 |
| Table 5.0-1 Inspection Plans..... | 22 |

List of Figures

| | |
|---|----|
| Figure 2.1-1 Pin Burnup Distribution for Mark-BW Fuel Assemblies with Greater Than 50 GWd/mtU Average Pin Burnup..... | 5 |
| Figure 2.2-1 Corrosion of Framatome ANP M5™ Cladding..... | 6 |
| Figure 2.2-2 Framatome ANP FA Growth..... | 6 |
| Figure 4.1.1-1 Framatome ANP FA Growth..... | 13 |
| Figure 4.1.2-1 Framatome ANP Combined Zr-4 Shoulder Gap Closure..... | 14 |
| Figure 4.1.2-2 Framatome ANP M5™ Shoulder Gap Closure..... | 14 |
| Figure 4.2-1 Framatome ANP Zr-4 GT Oxide..... | 16 |
| Figure 4.3-1 Framatome ANP Grid Growth..... | 16 |
| Figure 4.4-1 Corrosion of Framatome ANP Cladding..... | 17 |
| Figure 4.6-1 Time to Dashpot-Catawba 1..... | 18 |
| Figure 4.6-2 Time to Dashpot-Catawba 2..... | 19 |
| Figure 4.6-3 Time to Dashpot-McGuire 1..... | 19 |
| Figure 4.6-3 Time to Dashpot-McGuire 2..... | 20 |
| Figure 4.7-1 Framatome ANP Failure Rate For Mk-BW Fuel..... | 21 |

Acknowledgement

The authors would like to acknowledge the many contributions from Mike Aldrich, Gary Hanson, Frank McPhatter, Scott Robertson, Gary Weatherly, Gary Williams and Rick Williamson to the content of this report.

1.0 Introduction

Framatome ANP, Inc. manufactures Mark-BW and Mark-B fuel designs that are currently licensed to fuel rod burnups of 60,000 MWd/mtU and 62,000 MWd/mtU respectively (References 1 and 2). Framatome ANP, Inc. is requesting an extension of its Mark-BW product to 62,000 MWd/mtU. This document is a Supplement to Reference 1 (BAW-10186 Revision 1) for the Mark-BW designs. This document provides the justification for the use of the Mark-BW design with M5™ cladding to 62,000 MWd/mtU. The approval of this Supplement will supercede the SER restrictions on burnup in Reference 1 (BAW-10186 Revision 1) and Reference 2 (BAW-10227 Revision 0) for the Mark-BW designs.

The extension to 62,000 MWd/mtU is requested for M5™ clad in structures made from either Zr-4 or M5™. Fuel assembly structure materials may be Zr-4 or M5™; i.e., guide tubes, instrument tube, spacer grids and other applicable components. However, since the Mark-BW fuel has a higher operating temperature than Mark-B fuel leading to an increased clad corrosion rate, fuel rod cladding fabricated in Zr-4 is excluded from this extension request.

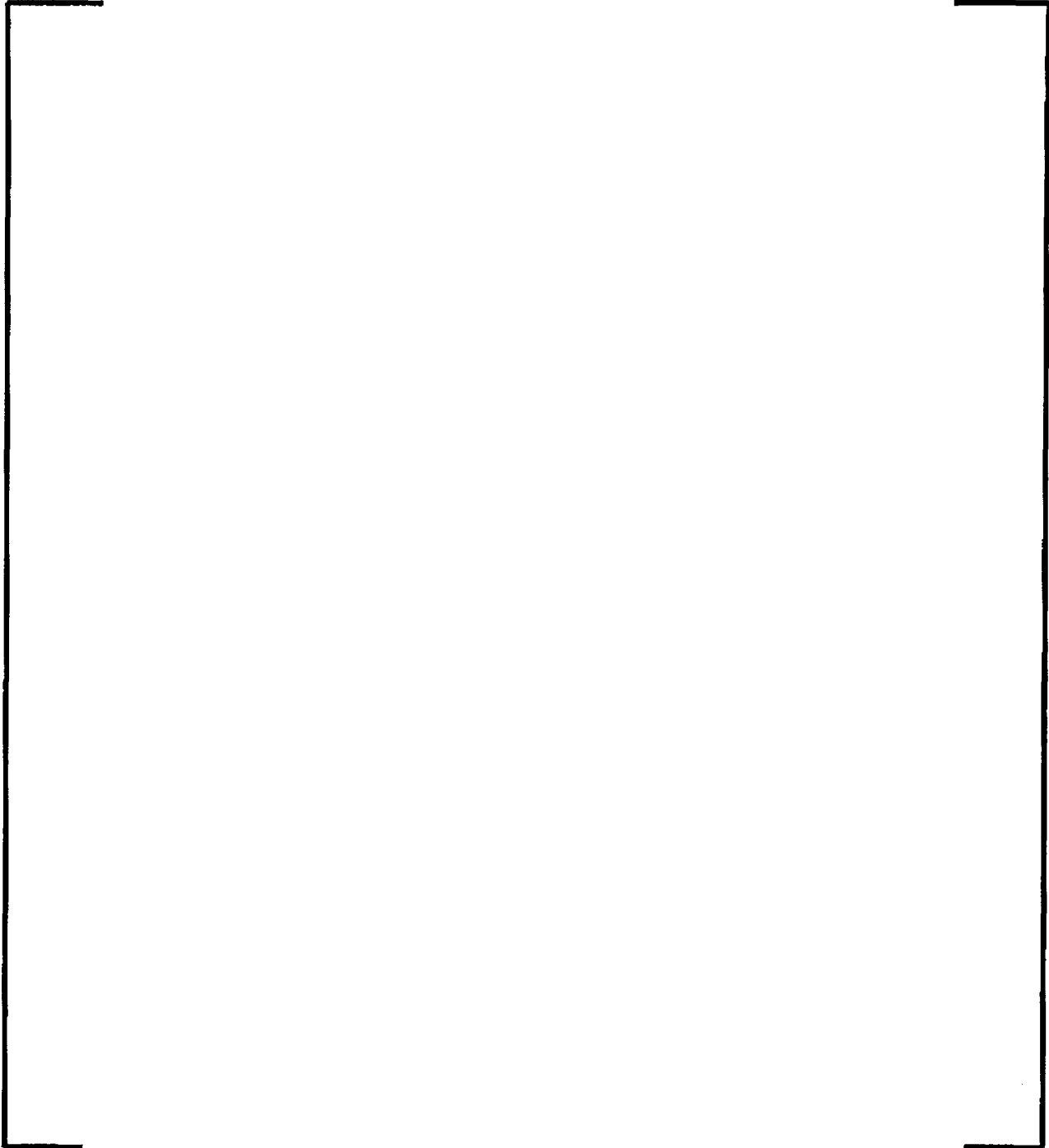
2.0 Summary

The justification for this extension of the Mark-BW fuel rod burnups to 62,000 MWd/mtU is based on the similarity to the Mark-B product and the additional data available since the submittal of References 1 and 2. These two items reduce the degree of extrapolation of the models with respect to burnup. In addition, commitments to future Post Irradiation Examination (PIE) campaigns will further increase the database for both the Mark-B and Mark-BW fuel designs. The extended burnup capabilities of Framatome ANP Inc.'s Mark-BW design have been evaluated based on peak fuel rod burnups of 62,000 MWd/mtU. The methods and data described or referenced in this report support plant specific licensing to this burnup.

2.1 Fuel Rod Burnup

Table 2.1-1 summarizes fuel rod burnup for the Mark-BW fuel from the time of the original topical (1996) to the present time. In addition, Figure 2.1-1 depicts the fuel rod burnup distribution for high burnup Mark-BW fuel at the time of the original topical reports (References 1 and 2) and the present time, respectively. A significant amount of data has been gathered since the original topical reports were submitted.

Table 2.1-1
Fuel Rod Burnup for High Burnup Mark-BW Fuel

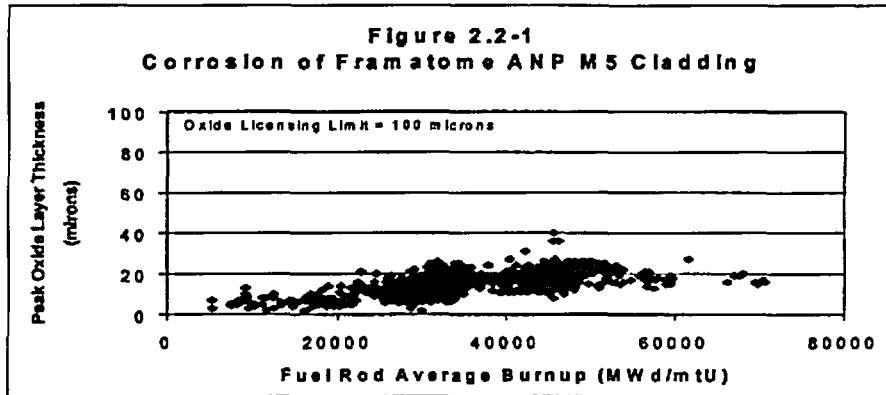


2.2 Key Updated PIE Measurements

Two key updated PIE measurements are fuel rod oxide and fuel assembly growth.

2.2.1 Fuel Rod Oxide

Figure 2.2-1 depicts the corrosion performance of alloy M5™ fuel rod cladding. As shown in the figure, the oxide thickness at 62,000 MWd/mtU is well below the 100-μm best-estimate licensing limit. See Section 4.4 for further discussion.



2.2.2 Fuel Assembly Growth

Fuel assembly growth measurements to date for both the Mark-B and Mark-BW fuel designs are plotted in Figure 2.2-2. As can be seen from this figure, a significant amount of fuel assembly growth data has been gathered since the original topical. Currently the all Zr-4 fuel assembly designs (clad and guide tubes) are limited by fuel assembly growth. As established in Reference 2, the all M5™ and the M5™ Clad upper tolerance limits (UTLs) are set as [80%] of all Zr-4. The growth data for the all M5™ design presented in Figure 2.2-2 clearly is within this UTL limit.

Figure 2.2-2
Framatome ANP FA Growth



2.3 Commitments to Planned Examinations

References 1 and 2 both have SER requirements to collect additional PIE data as a condition of approval. Two PIE campaigns are planned for the Mark-BW fuel design. These are at North Anna 1 at the end of 2001 and at North Anna 2 in 2004. Four advanced Mark-BW LTAs at North Anna 1, cycle 15 have finished their third cycle of irradiation. Following cycle 15, PIE data will be collected to verify the performance of these LTAs that contain M5™ fuel rods and guide tubes and other advanced features such as mid span mixing grids and a quick disconnect top nozzle. One of these assemblies will be reinserted into North Anna 2 for an additional cycle of irradiation beyond the current Mark-BW licensed burnup limits. The fourth cycle of irradiation for this LTA is expected to achieve rod burnups in excess of 70,000 MWd/mtU. PIE campaigns are also scheduled for Mark-B fuel at Three Mile Island-1 (2001, 2003), Davis Besse (2002, 2004, 2006), and Oconee 2 (2002). These plans are contingent on utility approval. However, the commitments in Section 5.0 remain in effect.

3.0 Data Sources

Table 3.0-1 below lists the major fuel performance inspections performed on irradiated fuel for both the Mark-B and Mark-BW fuel assembly designs in the United States. The last three rows in the table represent the inspection of a larger number of fuel assemblies experiencing typical modern fuel cycles. The assemblies measured represent the highest burnup assemblies in those cycles.

Table 3.0-1 Major Fuel Performance Programs

| Program | Plant | Completed Irradiation Cycles | Max Fuel Rod Burnup GWd/mtU | Post Irradiation Examinations |
|-------------------------|--------------|------------------------------|-----------------------------|-------------------------------|
| Mark-B | Oconee 1 | 5 ^(a) | [] | Poolside & Hotcell |
| Mark-BEB | ANO 1 | 4 ^(b) | [] | Poolside & Hotcell |
| Mark-GdB | Oconee 1 | 4 ^(c) | [] | Poolside & Hotcell |
| Mark-BZ | Oconee 1 | 3 ^(d) | [] | Poolside |
| Mark-BAB | SMUD | 3 ^(e) | [] | Poolside |
| Mark-B | Oconee 2 | 3 ^(f) | [] | Poolside & Hotcell |
| Mark-C | Oconee 2 | 3 ^(g) | [] | Poolside |
| Mark-B, Pathfinder | Oconee 1 | 3 ^(h) | [] | Poolside |
| Mark-BW15 Zircaloy LTAs | Conn Yankee | 3 ⁽ⁱ⁾ | [] | Poolside |
| Mark-BW17 Advanced Clad | McGuire 1 | 2 ^(j) | [] | Poolside |
| Mark-BW17 LAs | McGuire 1 | 3 ^(k) | [] | Poolside & Hotcell |
| Mark-BW17 Special Clad | McGuire 1 | 3 ^(l) | [] | Poolside |
| Mark-BW M5™ LTAs | North Anna 1 | 3 ^(m) | [] | Poolside |
| Mark-BW17 | Catawba 2 | 3 ⁽ⁿ⁾ | [] | Poolside |
| Mark-B | TMI 1 | 3 ^(o) | [] | Poolside |
| Mark-B | TMI 1 | 3 ^(p) | [] | Poolside |

- (a) Base FA design irradiated to high burnup for evaluation and modeling as part of a B&W/DOE/Duke Power joint program.
- (b) LTAs of an advanced, extended-burnup design.
- (c) An extended burnup fuel assembly design with selected fuel rods loaded with Gadolinia ($Gd_2O_3 - UO_2$) fuel pellets as an integral burnable poison.
- (d) LTAs utilizing Zr-4 intermediate spacer grids for low absorption.
- (e) LTAs containing axially blanketed fuel columns.
- (f) Fuel assemblies examined poolside, and selected fuel rods pulled and examined in a hotcell as part of a joint BWFC/EPRI/Duke Power fuel failure investigation.
- (g) Mark-C LTAs with 17 x 17-fuel rod array, two of these four LTAs are reconstitutable.
- (h) Pathfinder LTA with advanced Zr-4 cladding materials.
- (i) Four LTAs using Zr-4 clad fuel rods to replace stainless steel clad fuel rod assemblies.
- (j) One Lead Assembly (17x17, Mark-BW17 LA) with six different advanced cladding alloys within the Zr-4 specification.
- (k) Three Lead Assemblies (17x17, Mark-BW17 LA).
- (l) Two LAs with twelve advanced cladding alloys, six are within the Zr-4 specification, six are outside of the specification, e.g. non Zr-4 alloys.
- (m) Four Lead Assemblies (17x17, Mark-BW/M5™).
- (n) Six production Mark-BW fuel assemblies irradiated three typical cycles.
- (o) Ten production Mark-B fuel assemblies irradiated 1, 2, or 3 typical cycles.
- (p) Eleven production Mark-B fuel assemblies irradiated 1, 2, or 3 typical cycles.

The database for M5™ cladding in the U.S. is shown in Table 3.0-2 below. This data represents a small fraction of the data gathered on M5™ worldwide. The U.S. data fits well within the data gathered worldwide, which demonstrates that the cladding performs as well in U.S. cycles. This data will be discussed in greater depth in Section 4.4.

Table 3.0-2 U.S. M5™ Fuel Rod Demonstrations

| <i>Reactor</i> | <i>Fuel Assembly</i> | <i>Plant Cycles</i> |
|----------------|----------------------|---------------------|
| McGuire-1 | NJ05LC | 8, 9, 10 |
| | NJ05LD | 8, 9, 10 |
| North Anna-1 | NJ092P | 13, 14, 15 |
| | NJ092R | 13, 14, 15 |
| | NJ092T | 13, 14, 15 |
| | NJ092V | 13, 14, 15 |
| TMI-1 | NJ07VX | 11, 12, 13 |
| | NJ07VY | 11, 12, 13 |

Note: This table does not include Framatome ANP Inc.'s first full batches of M5™ clad fuel at Davis Besse and Oconee since a full first cycle of operation is not complete. A fourth irradiation cycle is planned for one of the four North-Anna assemblies. Four pins are from one of the TMI assemblies are planned for reinsert for a fourth cycle in TMI cycle 14.

The many similar features of the Mark-B and Mark-BW fuel designs allow the results of Mark-B PIE campaigns to be used to support justification for the Mark-BW burnup extension. Both designs are similarly constructed using floating grids, fuel rods seated on the bottom nozzle and like materials. The fuel rod support systems [(grid to fuel rod contact, soft stop deflection) are similar] for both designs. End grids for both designs monometallic and fabricated with Inconel 718. The intermediate grids are monometallic in Zr-4 or M5™. Tables 3.0-3 and 3.0-4 list updated fuel assembly parameters for the Mark-B and Mark-BW fuel assembly designs, respectively.

The power densities of the Mark-B and Mark-BW fuel are in the same range. The range of operating pressures and temperatures for plants using Mark-B and Mark-BW fuel are similar with the Mark-BW plants typically operating at the higher end of the temperature range. In order to minimize corrosion concerns associated with the higher temperature for the Mark-BW fuel, Framatome ANP will use only fuel with M5™ cladding in those applications. The similar metal-to-water ratios of the two designs make them equivalent from a nuclear standpoint. The mechanical, thermal-hydraulic, and nuclear similarities of the Mark-B and Mark-BW fuel designs support the use of Mark-B data to justify the Mark-BW burnup extension to 62,000 MWd/mtU. Tables 3.0-3 and 3.0-4 list updated fuel assembly parameters for the Mark-B and Mark-BW fuel assembly designs, respectively.

Table 3.0-3 Typical Framatome ANP, Inc. Fuel Assembly Parameters †
(B&W Reactor Systems)

| Assembly Designation | Mark-B |
|---|---|
| Fuel Rod Array | 15x15 |
| Holddown Spring | Helical Coil Spring or Multiple Leaf Spring |
| Cladding Material | Zr-4, M5™ |
| Guide Tube Material | Zr-4, M5™ |
| Assemblies per Core | 177 |
| Fuel Rods per Assembly | 208 |
| Control Rod/Guide Tube/Instrument Tube Locations Per Assembly | 17 |
| Debris Protection Feature | Solid Lower End Plug* |
| Rod Pitch, mm (inch) | 14.4 (0.568) |
| Fuel Rod Length, cm (inch) | []* [] |
| Active Fuel Height, cm (inch) | 360.2* (141.8) |
| Plenum Length, cm (inch) | []* [] |
| Fuel Rod O.D., mm (inch) | 10.92* (0.430) |
| Cladding I.D., mm (inch) | [] [] |
| Cladding Thickness, mm (inch) | [] [] |
| Diametrical Gap, microns (mils) | [] [] |
| Fuel Pellet O.D., mm (inch) | [] [] |
| Fuel Pellet Density, % TD | [] |
| Average LHGR, W/cm (kW/ft) | 203 (6.20) |
| System Pressure, MPa (psia) | 15.2 (2200) |
| Core Inlet Temp., °C (° F) | 292.07 (557.7) |
| Core Outlet Temp., °C (° F) | 315.7 (600.3) |

† Designs, materials and dimensions are representative of those used to date. Alternates may be used if they are demonstrated to meet the burnup requirements.

* Other Options Available.

** Design has used both densities.

Table 3.0-4 Typical Framatome ANP, Inc. Fuel Assembly Parameters †
(Westinghouse Reactor Systems)

| Assembly Designation | Mark-BW17 |
|---|---------------------------|
| Fuel Rod Array | 17x17 |
| Holddown Spring | Leaf Springs |
| Cladding Material | Zr-4, M5™ |
| Guide Tube Material | Zr-4, M5™ |
| Assemblies per Core | 193 (157) |
| Fuel Rods per Assembly | 264 |
| Control Rod/Guide Tube/Instrument Tube Locations per Assembly | 25 |
| Debris Protection Feature | Filter Lower End Fitting* |
| Rod Pitch, mm (inch) | 12.6 (0.496) |
| Fuel Rod Length, cm (inch) | [] [] |
| Active Fuel Height, cm (inch) | 365.8 (144.0)] |
| Plenum Length, cm (inch) | [] [] |
| Fuel Rod O.D., mm (inch) | 9.50 (0.374) |
| Cladding I.D., mm (inch) | [] [] |
| Cladding Thickness, mm (inch) | [] [] |
| Diametrical Gap, microns (mils) | [] [] |
| Fuel Pellet O.D., mm (inch) | [] [] |
| Fuel Pellet Density, % TD | [] |
| Average LHGR, W/cm (kW/ft) | 178 (5.43) |
| System Pressure, MPa (psia) | 15.5 (2250) |
| Core Inlet Temp., °C (° F) | 294.2 (561.6) |
| Core Outlet Temp., °C (° F) | 326.7 (620) |

† Designs, materials and dimensions are representative of those used to date. Alternates may be used if they are demonstrated to meet the burnup requirements.

* Other Options Available.

** Design has used both densities.

4.0 Fuel Rod and Assembly Models

The parameters in Chapter 4 of the SRP (Reference 3) that are significantly impacted by a burnup extension are addressed in this Section.

4.1 Fuel Rod and Fuel Assembly Growth

There are three options to consider:

- All Zr-4 - Zircaloy-4 clad and guide tubes.
- M5™ Clad - M5™ clad and Zr-4 guide tubes.
- All M5™ - M5™ clad and guide.

4.1.1 Fuel Assembly Growth

Fuel assembly (FA) growth must be controlled in order to prevent the fuel assembly structure from extending to the point of contact on the top nozzle structure and the core plate. The fuel assembly growth for both Framatome ANP Inc.'s Mark-B and Mark-BW fuel designs is plotted in Figure 4.1.1-1. A significant amount of fuel assembly growth data has been gathered since the original topical reports were submitted. Owing to the axial similarity of the fuel designs, the Mark-B and Mark-BW databases can be combined into a single database. Fuel assembly growth is highly material dependent and therefore Zr-4 and M5™ structures are plotted separately. The UTL on assembly growth for the M5™ clad and the all M5™ cases are established by [] of all Zr-4 case (Reference 2). This M5™ assembly growth UTL is clearly conservative with respect to the data presented in the graph. A margin greater than [] for closure of the fuel assembly to core plate gap exists for current FA design lengths using the conservative M5™ assembly growth UTL. Greater than [] margin exists with a conservative extrapolation of the North Anna first cycle growth value to 62,000 MWd/mtU.

Figure 4.1.1-1
Framatome ANP FA Growth



4.1.2 Shoulder Gap Closure

Framatome ANP, Inc. introduced the shoulder gap closure model in Figure 3-8 of Reference 2 as an alternative to computing it based on combined fuel assembly and fuel rod models. An updated fuel assembly shoulder gap closure curve for a Zr-4 structure is given in Figure 4.1.2-1. This model is conservative since it is based on the maximum shoulder gap closure per fuel assembly measured in the PIEs. In this instance also, owing to the axial similarity of the fuel designs, the Mark-B and Mark-BW databases can be combined into a single database. Shoulder gap is well behaved with respect to burnup and is exhibited in Figure 4.1.2-1. Framatome ANP Inc.'s existing all Zr-4 designs have more than [] inches of Beginning of Life (BOL) shoulder gap. This results in greater than [] margin for a Zr-4 design at 62,000 MWd/mtU.

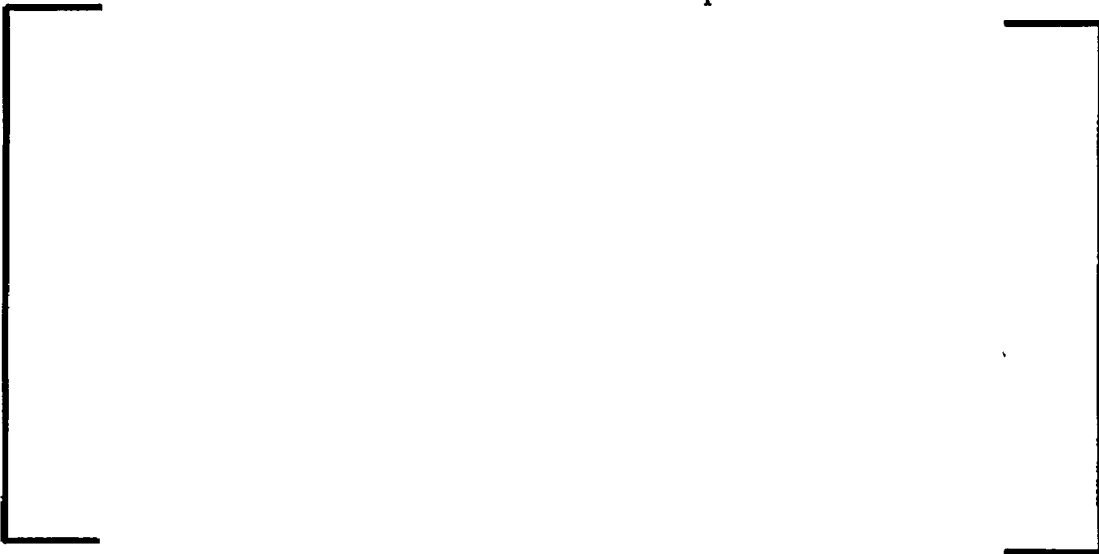
In addition, the model in Figure 4.1.2-1 is conservative for the M5™ clad case (M5™ clad and Zr-4 guide tubes) since it has been shown (Reference 2) that M5™ fuel rods have lower growth than Zr-4 which leads to a larger shoulder gap.

Figure 4.1.2-1
Framatome ANP Combined Zr-4 Shoulder Gap Closure



For the case of the all M5TM design the use of fuel rod UTLs and fuel assembly LTLs will be maintained until such time that a shoulder gap model can be developed. A shoulder gap model will be developed and used when sufficient data have been gathered. The current M5TM fuel rod model for Mark-BW is presented in Figure 4.1.2-2 along with a sample shoulder gap model developed in accordance with the concepts given in Reference 2 (fuel assembly growth is [] of that of a Zr-4 structure, fuel rod growth is per fuel rod model).

Figure 4.1.2-2
Framatome ANP M5 Shoulder Gap Closure



Actual shoulder gap measurements for Framatome ANP Inc.'s M5™ LTAs, which recently completed their 3rd cycle of irradiation at Dominion Generation's North Anna Plant are also plotted in Figure 4.1.2-2. The data here are after 2 cycles of irradiation and shows that the shoulder gap model for the M5™ design computed this way is slightly non-conservative. This is due to the fact that the fuel assemblies in North Anna are experiencing zero growth at the fuel assembly level. However, even with [], there is over [] margin at a burnup of 62,000 MWd/mtU. Ample shoulder gap margin exists for burnup extension to 62,000 MWd/mtU for the Mark-BW design. The all M5™ case is the most limiting since the use of Zr-4 guide tubes (M5™ clad or all Zr-4 cases) will lead to larger shoulder gaps due to higher FA growth.

4.2 Fuel Assembly Structure Oxidation

Although the primary concern with the oxidation rate of Zr-4 lies in its effect on fuel rods, structural tubing must also be considered as fuel assembly burnup limits are extended. Zr-4 guide tubes and instrument tubes differ from fuel rod cladding in two important ways - metallurgical structure and service environment. Concerning structure, Zr-4 fuel rod cladding is in the stress-relieved and annealed condition (SRA) whereas structural tubing is supplied in the recrystallized condition (RXA). Experience has shown that the oxidation rate of Zr-4 is strongly dependent on temperature and that the RXA material has a lower initial oxidation rate than the SRA fuel rod cladding. With respect to the service environment of structural tubing, it differs in two important ways from fuel rod cladding - temperature and exposed surface area. Structural tubing operates cooler than fuel rod cladding because it is essentially at the same temperature as that of the bulk primary coolant. Guide tubes and instrument sheaths are exposed to coolant on both the ID and OD surfaces and oxidation proceeds at approximately the same rate on each.

Guide tube oxidation data is measured in fuel assembly post irradiation examinations (PIE). The oxidation data presented in Figure 4.2-1 illustrates three important points concerning the oxidation kinetics of Zr-4 structural tubing. First, the Mark-B and Mark-BW data are seen to be similar in their evolution with burnup even though Mark-BW fuel typically operates at higher temperatures than Mark-B. Secondly, the oxidation layer thickness is on the order of one-third of that of fuel rod oxidation at higher burnup. This is because of the strong correlation of oxidation rate with temperature for Zr-4. The cooler operating structural tubing is oxidizing at a lower rate than the hotter fuel rods. Lastly, the effects of oxide thickness of the Mark-B and Mark-BW structural tubes is considered in fuel assembly structural analysis when establishing design limits and operating margins.

Many years of operational experience with Zr-4 structural tubing has resulted in no failures and the PIE data suggests that none will occur at extended burnup to 62,000 MWd/mtU. Structural margins are greater for M5™ given the lower oxidation rate for M5™ and the similar material properties of the two alloys.

Figure 4.2.1
Framatome ANP Zircaloy-4 GT Oxide



4.3 Spacer Grid Irradiation Growth

The data for Mark-B and Mark-BW grid growth can be combined due to the similarity of the designs. Grid growth is plotted in Figure 4.3-1 as a function of burnup for grid 2. Grid 2 is the top most intermediate grid, and due to the higher temperature in this region, it has been shown to have the greatest growth. The data follow a linear relation with burnup. The result of grid growth is to reduce the inter-assembly and assembly-baffle plate gaps. Framatome ANP Inc.'s evaluation of the available gap at 62,000 MWd/mtU results in sufficient margin to prevent a "solid" core condition.

Figure 4.3-1
Framatome ANP Grid Growth

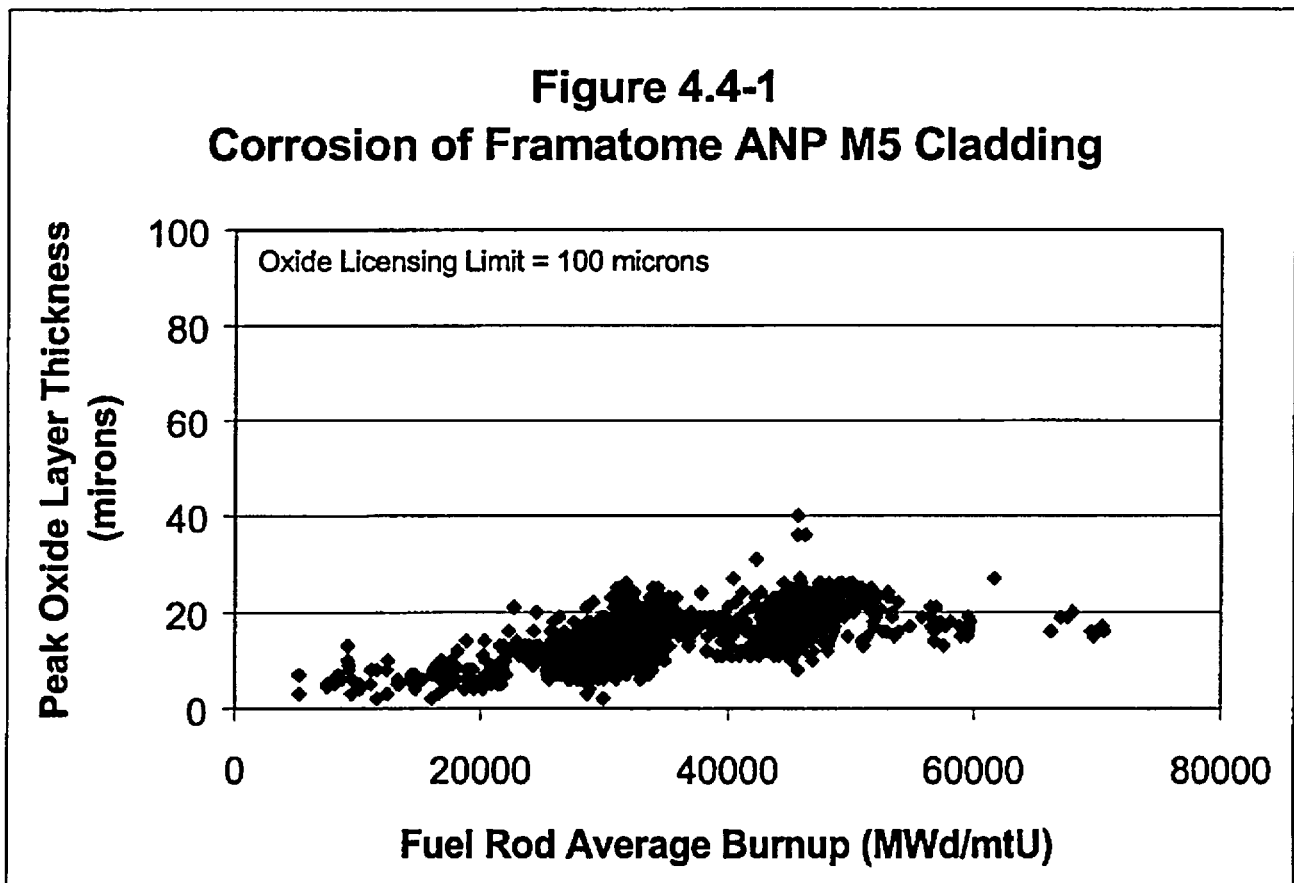


4.4 Oxidation, Corrosion and Crud

Figure 4.4-1 shows the corrosion performance of alloy M5™ fuel rod cladding. Maximum oxide thickness, measured in the highest temperature and fluence region of the fuel assembly (second spacer-grid span from the top), is plotted as a function of fuel rod burnup.

The well-known trend of increasing data scatter with burnup for Zr-4 is not observed for alloy M5™. This behavior is indicative of a lower sensitivity of the alloy's oxidation kinetics to various irradiation conditions, including reactor power histories and differences in operating conditions from one reactor to another. A reduction in maximum oxide thickness by a factor of three to four is evident at the highest achieved burnups. The margin to the 100- μm (micron) cladding licensing limit is significantly increased. Because crud formation is a result of clad oxidation, its production will be significantly reduced also.

Several years of PWR irradiation history on alloy M5™ fuel rod cladding indicates that the M5™ alloy provides the high design margins necessary for superior performance at extended burnups.

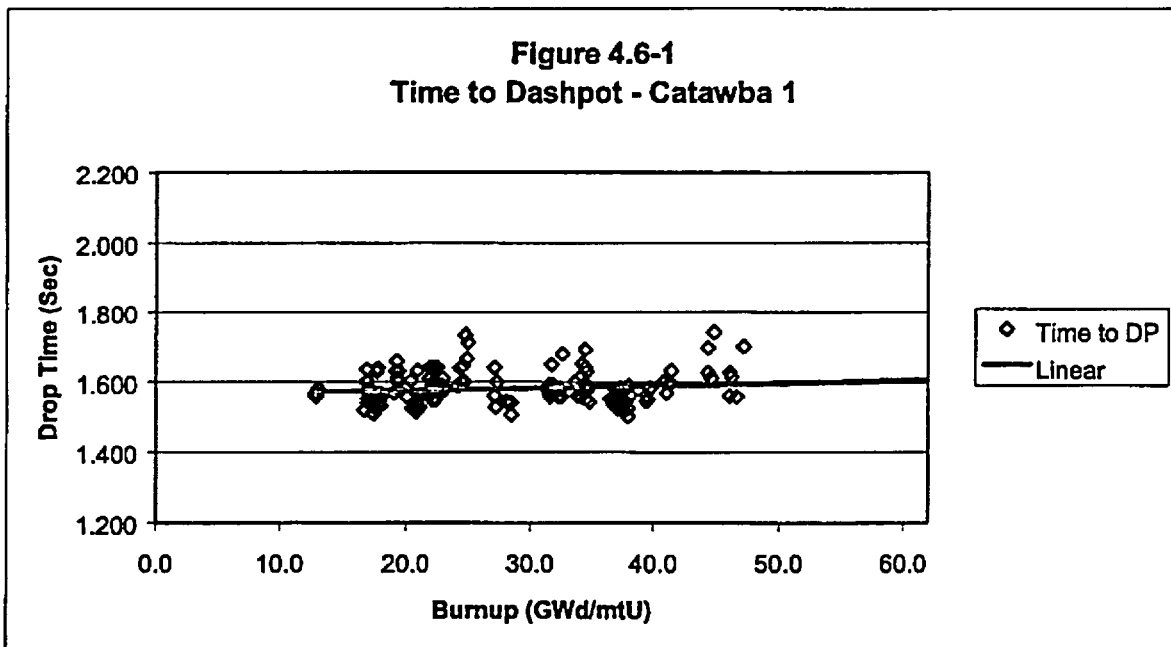


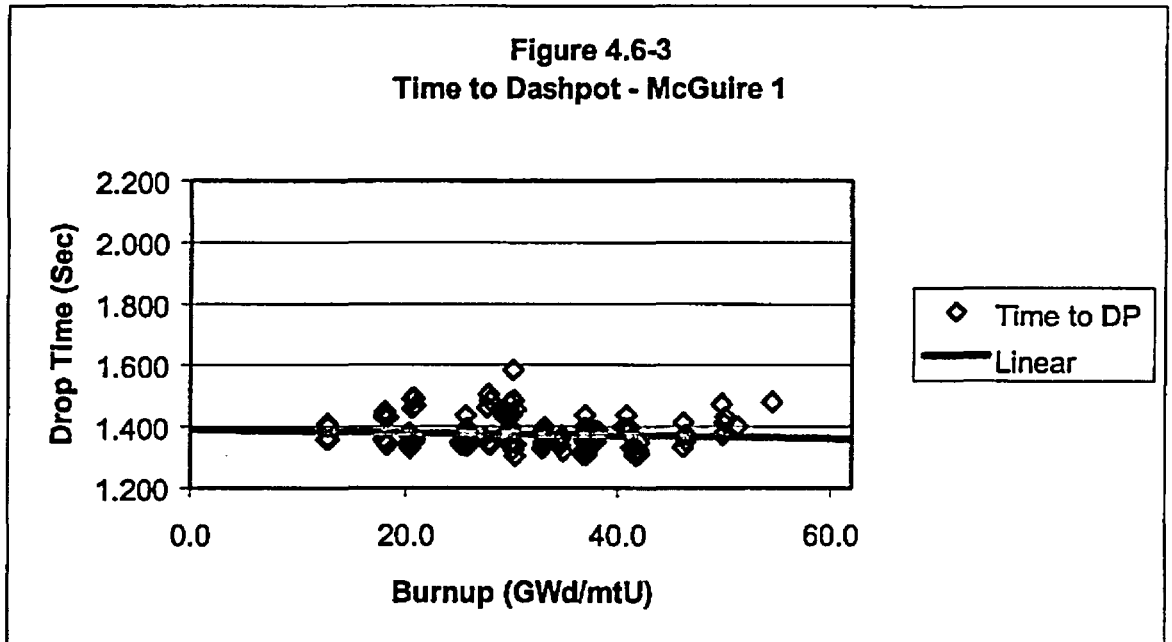
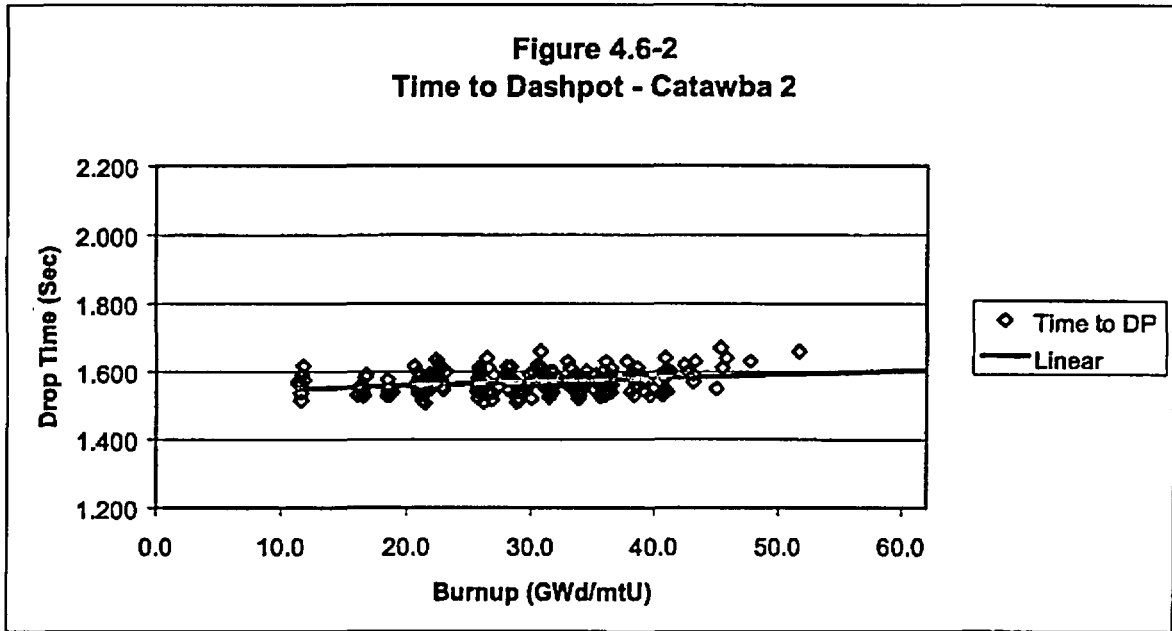
4.5 Fuel Rod Bowing

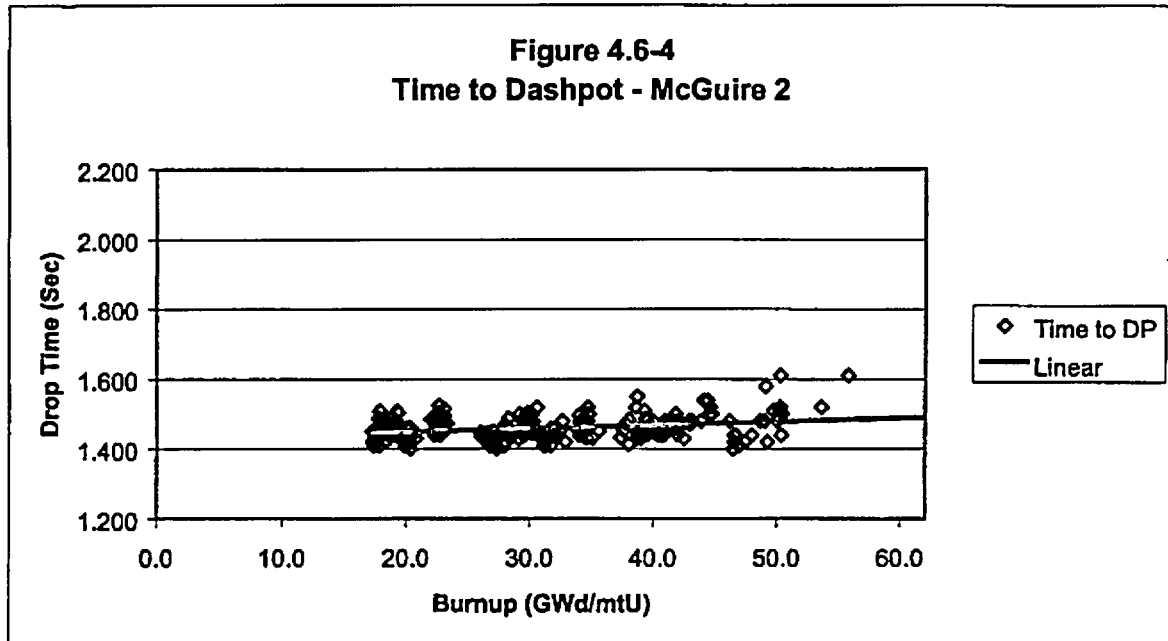
The fuel rod criteria in Reference 1 (saturation of fuel rod bow with burnup) remain applicable with the use of M5™ cladding. In addition M5™ material properties were addressed in Reference 2. Framatome ANP, Inc. restates its commitment to obtaining additional fuel rod bow data. Fuel rod bow measurements are planned for the Mark-BW M5™ LTAs that have recently completed 3 cycles of irradiation at Dominion Generation's North Anna plant.

4.6 Control Rod Drop Time

Since Framatome ANP Inc.'s Mark-BW Fuel Assembly has a dashpot integral to the guide thimbles, its design is unique relative to the Mark-B design. Therefore, only control rod drop time data from Mark-BW plants are presented. The technical specification limit for this parameter is 2.2 seconds to start of dashpot. A control rod in a position occupied by Mark-BW fuel has never exceeded this limit. Control rod drop time to start of dashpot vs. burnup is plotted for four plants fueled with Framatome ANP Inc.'s Mark-BW fuel assemblies in Figures 4.6-1 through 4.6-4 below:







The figures exhibit no appreciable correlation of drop time versus burnup as is shown by the near zero slope of the linear fits. This fact coupled with over 0.45 seconds of margin relative to the technical specification limit justifies an extrapolation to 62,000 MWd/mtU burnup. Furthermore, no Mark-BW fuel assembly has experienced an incomplete rod insertion.

4.7 Defects

The fuel reliability for the Mark-BW fuel design is excellent with over 2400 fuel assemblies delivered by year-end 2000. At the end of 2000, all plants using the Mark-BW design were operating defect free. Figure 4.7-1 below shows the failure history for the Mark-BW product since it was introduced in 1991.

Figure 4.7-1
Framatome ANP Failure Rate for Mk-BW Fuel



In the ten years the Mark-BW has been utilized there have been eight fuel rod failures identified. Four are known to be caused by debris, two failures are attributable to fuel manufacturing, and two failures have not been determined. These eight failures can be broken down into five first cycle and three third cycle failures. Mark-BW has proven to be a reliable, problem-free design with an overall failure rate of []. Changes to the manufacturing process have eliminated the third cycle failure mechanisms in future fuel for two of the three failures. Based on the burnup of the failed rods and the time of failure there is no indication that the failures are related to burnup. Increasing the burnup limit from 60,000 to 62,000 MWd/mtU will have no adverse affect on fuel reliability.

5.0 Examinations

There are currently two applicable topical reports that have Safety Evaluation Report (SER) requirements to collect additional PIE data as a condition of approval. These are the Extended Burnup Topical Report Reference 1 (BAW-10186) and the M5™ Applications Topical Report Reference 2 (BAW-10227). In summary, the requirements of these topicals are to obtain additional PIE data at burnups that exceed those presented in the report up to the current licensed limit. In some cases, the data is to be collected from LTA programs and in others the data will come from batch production assemblies. Table 5.0-1 below summarizes the specific commitments contained in these two topical reports.

Table 5.0-1
 Inspection Plans

| | BAW-10186 | BAW-10227 |
|----------------|-------------|------------------|
| PIE Data | Extended BU | M5™ Applications |
| FA Visual | LTA | LTA |
| Fuel Rod Oxide | LTA | LTA + Batch |
| GT Oxide | | LTA |
| Rod Diameter | LTA | LTA + Batch |
| Rod Growth | | LTA + Batch |
| FA Growth | | LTA + Batch |
| Shoulder Gap | | LTA + Batch |
| Rod Bow | LTA | LTA + Batch |
| FA Bow | LTA | LTA |
| CRA Drop Time | LTA | |
| CRA Drag | LTA | |
| Rod Wear | | LTA |
| HDS Height | LTA | |
| Hot Cell Work | | LTA |

6.0 Conclusion

The original Framatome ANP extended burnup topical report (BAW-10186P-A) was approved by the NRC in 1997. The NRC safety evaluation report for that document approved the Mark-BW fuel assembly design for a rod average burnup limit of 60,000 MWd/mtU. Since that approval, Framatome ANP has acquired additional higher burnup data for both the Mark-B and Mark-BW fuel designs. Framatome ANP has demonstrated the similarity of the two designs. Therefore, the additional data for the Mark-B fuel is directly applicable to the Mark-BW fuel.

The data presented in this supplement address the phenomena of fuel corrosion and growth. All the data support a burnup limit of 62,000 MWd/mtU for the Mark-BW fuel design. The other fuel damage criteria specified in Standard Review Plan 4.2 were addressed in the original submittal of BAW-10186 and provide acceptable performance up to a rod average burnup of 65,000 MWd/mtU. All analyses in BAW-10186P-A were performed with NRC approved methodology.

Framatome ANP is committed to performing additional post irradiation examinations of high burnup fuel. Data will be acquired on LTAs and full batches of fuel. In addition to oxide and growth measurements, control rod drop times will be measured to ensure continued acceptable performance. The results of these examinations will be presented to the NRC during fuel vendor fuel performance review meetings.

Based on the similarity of the Framatome ANP fuel designs, the additional data acquired since the review of BAW-10186P-A, satisfactory performance against the SRP criteria, and the commitment to acquire additional data, it is concluded that the Mark-BW fuel assembly will provide acceptable performance up to rod average burnup of 62,000 MWd/mtU.

7.0 References

1. BAW-10186P-A Revision 1, Extended Burnup Evaluation, April 2000.
2. BAW-10227P-A, Evaluation of Advanced Cladding and Structural Material (M5™) in PWR Reactor Fuel, February 2000.
3. U.S. Nuclear Regulatory Commission. July 1981. "Section 4.2, Fuel System Design." In Standard Review Plan for the Review of Safety Analysis Reports for Nuclear Power Plants--LWR Edition. NUREG-0800, Revision 2, U.S. Nuclear Regulatory Commission, Washington, D.C.